ADD66, A GENE REQUIRED FOR THE ENDOPLASMIC RETICULUM ASSOCIATED DEGRADATION (ERAD) OF ALPHA-1-ANTITRYPSIN-Z IN YEAST, FACILITATES PROTEASOME ACTIVITY AND ASSEMBLY

by

Craig McNary Scott

Bachelors of Science - Biology, State University of New York, Oneonta, 2001

Submitted to the Graduate Faculty of

Arts and Sciences in partial fulfillment

of the requirements for the degree of

Doctor of Philosophy

University of Pittsburgh

2007

UNIVERSITY OF PITTSBURGH

FACULTY OF ARTS AND SCIECNES

This dissertation was presented

by

Craig McNary Scott

It was defended on

June 29, 2007

and approved by

Dr. Gerard Apodaca, Professor, Department of Cell Biology and Physiology, University of Pittsburgh

Dr. Karen Arndt, Associate Professor, Department of Biological Sciences, University of Pittsburgh

Dr. Susan Gilbert, Professor, Department of Biological Sciences, University of Pittsburgh

Dr. Grahm Hatfull, Professor, Department of Biological Sciences, University of Pittsburgh

Dr. Jeffrey Brodsky, Professor, Department of Biological Sciences, University of Pittsburgh

ADD66, A GENE REQUIRED FOR THE ENDOPLASMIC RETICULUM ASSOCIATED DEGRADATION (ERAD) OF ALPHA-1-ANTITRYPSIN-Z IN YEAST, FACILITATES PROTEASOME ACTIVITY AND ASSEMBLY

Craig M. Scott PhD

University of Pittsburgh, 2007

Antitrypsin Deficiency is a primary cause of juvenile liver disease and arises from expression of the "Z" variant of the alpha-1 protease inhibitor (A1Pi). Whereas A1Pi is secreted from the liver, A1PiZ is retro-translocated from the endoplasmic reticulum (ER) and degraded by the proteasome, an event that may offset liver damage. To better define the mechanism of A1PiZ degradation, a yeast expression system was developed and a gene, *ADD66*, was identified that facilitates A1PiZ turn-over (Palmer *et al.,* J. Cell. Sci. *116*, 2361-2373, 2003). I report here that *ADD66* encodes an ~30 kDa soluble, cytosolic protein and that the chymotrypsin-like activity of the proteasome is reduced in *add66Δ* mutants. This reduction in activity may arise from the accumulation of 20S proteasome assembly intermediates or from qualitative differences in assembled proteasomes. Add66p also appears to be a proteasome substrate. Consistent with its role in ER associated degradation (ERAD), synthetic interactions are observed between the genes encoding Add66p and Ire1p, a transducer of the unfolded protein response, and yeast deleted for both *ADD66* and/or *IRE1* accumulate polyubiquitinated proteins. These data identify Add66p as a proteasome assembly chaperone (PAC) and provide the first link between PAC activity and ERAD.

TABLE OF CONTENTS

LIST OF TABLES

LIST OF FIGURES

LIST OF ABBREVIATIONS

15S	Half-proteasome complex
19S	Regulatory cap of the 26S proteasome
20S	Core particle of the 26S proteasome
26S	Proteasome; multi-subunit macromolecule
ADD	Antitrypsin degradation deficient
A1PiM	Antitrypsin, M allele, Wild type
A1PiZ	Antitrypsin, Z allele
ATD	Antitrypsin deficiency
CTL	Chymotrypsin-like
CP	Core particle of the 26S proteasome
DUB	De-ubiquitinating enzyme
E1	Ubiquitin activating enzyme
E2	Ubiquitin ligase
E3	Ubiquitin conjugating enzyme
ERAD	Endoplasmic reticulum associated degradation
HSP	Heat shock protein
PAC	Proteasome assembly chaperone
PGPH	Peptidylglutamyl-peptide hydrolyzing

TL	Trypsin-like
Ub	Ubiquitin
UPP	Ubiquitin proteasome pathway
UPR	Unfolded protein response
UPRE	Unfolded protein response element

PREFACE

I would like to begin and extend my most heartfelt gratitude to my advisor, Dr. Jeff Brodsky. Jeff has been a tremendous source of support, guidance, motivation, understanding, and inspiration to me during my graduate school career. Thus, I was truly fortunate to wind up with one of the best advisors and mentors one could possibly imagine. I am also thankful for being given the opportunity to join the Brodsky Lab and work under such a giant in the field of biology. Throughout my graduate school career, Jeff was a consistent force of support, making time for my work, my experiments, teaching assignments, as well as my career plans. I am extremely fortunate to have had Jeff as a role model during graduate school, allowing me to take the lessons I have learned over the years and apply them to the rest of my career.

I would also like to take a moment to thank all of the members of the Brodsky lab, past and present, that I had the opportunity to work with during my graduate school career. These brilliant and dedicated individuals were a constant bar to measure ones own work and progress against. I especially like to thank Dr. Sheara Fewell and Dr. Kunio Nakatsukasa who assisted me in various technical, theoretical, and conceptual hurdles that I have encountered over the years. I would also like to thank Jennifer Geockeler who was always there for me in any science related matter as well as many non-science related issues I might have had. Finally, I would like to thank Rob Lee and Dr. Christine Wright who not only contributed stimulating scientific

discussions, but provided friendship as well, and it was a pleasure to work with both of them in the lab.

Next, I would like to take a moment to thank my thesis committee, Dr. Gerard Apodaca, Dr. Karen Arndt, Dr. Susan Gilbert, and Dr. Graham Hatfull. These dedicated individuals provided significant contributions to my work; either in scientific guidance as well as career advice and support. Additionally, I would like to thanks all the members of the Department of Biological Sciences staff for their assistance during my quest for my doctorate. I would especially like to mention Cathy Barr for her invaluable assistance with all administrative concerns, thus allowing me to concentrate on my studies, assignments, research, presentations, and defense. I would also like to acknowledge Dr. Laurel Roberts, Dr. Valerie Oke, Carole LaFave, and Lydia Daniels for their advice, support, and mentoring in my pursuit for my teaching minor.

I would like to show my appreciation towards my friends and family that have supported my through the long journey that has lead to the completion of this degree. I want to thank my parents for all their love, support, and help in my life that has allowed me to grow into the person I am today. Only through their constant work and sacrifice have I had opportunity to pursue my goals and dreams. Without them I would not have been able to complete this stage of my life. Finally, I also want to thank my good friends; Andrew and Meryl Lotz, Steve McNamara, Abigail Ellsworth PT, DPT, and CPS, Rachel Crossman-Kepper, Dr. Lisa Sproul, and Dr. Abigail Martin, MD. These people have stayed with me during the highs and the lows of my undergraduate and graduate careers and I appreciate all their love and support.

1.0 INTRODUCTION

Cells undergo a constant flux between catabolism and anabolism. The final homeostatic state is achieved due to the choreographed relations of various proteins within the cell, themselves regulated at multiple levels. For example, the rates of protein synthesis or degradation must be precisely balanced, for even a subtle shift one way or another for prolonged periods of time will result in abnormal cell growth and/or cellular mass (Mitch and Goldberg, 1996).

An old adage states that it is easier to destroy than to create, and while that may be true in society, the process of degradation within the cell is neither simple nor easy. Protein degradation consists of a very complex set of steps that must be followed in a temporal and spatially defined manner. In brief, proteins must be recognized as being a target for degradation, transported to the site of degradation, unfolded, and then finally broken down to the proteins' basic components. It is easy to imagine that each step in the protein degradation pathway can be further delineated into multiple regulatory steps. You can then add the additional level of difficulty, in which the cell segregates select proteins into organelle structures, thus the degradation machinery must gain access to the select proteins. Therefore, it is easier to appreciate the complex nature of protein degradation.

The bulk of the work presented in this dissertation involves the role of one protein and its effect on the efficient assembly and maturation of the proteasome, a proteolytic machine that facilitates protein degradation within eukaryotic cells.

1.1 UBIQUITIN PROTEASOME PATHWAY

Unlike most regulatory mechanisms found within the eukaryotic cell, protein degradation is fundamentlly an irreversible step. Thus, elimination of a protein or protein complex abolishes the protein's function, and alters the cellular composition of proteins. All intracellular proteins are consistently being turned over by hydrolysis into their constituent amino acids. Therefore, the destruction of proteins allows efficient recycling of many proteins and the synthesis of new proteins.

In eukaryotic cells, protein degradation can be broken down into four distinct pathways. The majority of proteins destined for degradation are eliminated by the ubiquitin (Ub) proteasome pathway (UPP) (Rock *et al.*, 1994) and will be discussed in detail in this section. In contrast, many extracellular and cell surface proteins are degraded by the yeast vacuoles or lysosomes in mammals. These organelles contain proteases and hydrolyases in an acidic micro-environment that promotes uninhibited degradation of the proteins translocated into these compartments (Glickman and Ciechanover, 2002; Nandi *et al.*, 2006). A third pathway results when some cytosolic proteins are degraded by the vacuole/lysosome during cellular stress conditions via the autophagic pathway (see below). The fourth and final mechanism of protein degradation is the result of various cytosolic proteases, such as calpain or caspases. These proteases are involved in programmed cell death during development of higher eukaryotes, activated during cell injury, and play a role during apoptosis (Salvesen and Dixit, 1997; Goll *et al.*, 2003).

The destruction of a target protein by the UPP requires two discrete and successive steps: [1] selection of the target protein by tagging the substrate through covalent attachment (see below) of multiple ubiquitin molecules, and [2] the degradation of the tagged protein by the 26S

proteasome with the subsequent release of reusable ubiquitin (Bochtler *et al.*, 1999; Voges *et al.*, 1999; Glickman and Ciechanover, 2002; Soboleva and Baker, 2004; Nandi *et al.*, 2006; Reed, 2006).

The UPP begins with the choreographed actions of various enzymes that create a chain of polyubiquitin covalently attached to a substrate protein (Figure 1) (Kuhlbrodt *et al.*, 2005; Asher *et al.*, 2006; Hurley *et al.*, 2006; Lecker *et al.*, 2006; Reed, 2006; Xu and Peng, 2006). Polyubiquitination of substrates targets them for degradation by the 26S proteasome (described in detail below). Ubiquitin is a highly conserved 76 amino acid polypeptide that is abundant in all eukaryotic cells. The initial step in the ubiquitination pathway is ATP-dependent and involves the linkage of ubiquitin to a ubiquitin-activating enzyme, or E1 enzyme, via a high energy thioester bond (Ciechanover *et al.*, 1982). Ubiquitin is then transferred via a second thioester linkage to a ubiquitin conjugating enzyme (Ubc), or E2 enzyme, which in turn catalyzes the covalent transfer of ubiquitin to the substrate protein. The *C*-terminus of a glycine residue forms an isopeptide bond with a lysine residue in the substrate, though there have been reports of bond formation with cysteine residues or the *N*-terminal residue of the substrate (Ciechanover and Ben-Saadon, 2004; Cadwell and Coscoy, 2005). In some cases, substrate polyubiquitination requires another enzyme, the ubiquitin ligase, or E3 enzyme. The ubiquitin ligase can participate in the transfer of ubiquitin onto the substrate, or it can function as an adaptor to facilitate the positioning and transfer of ubiquitin from the E2 directly onto the substrate. A number of E3s have been shown to associate with select substrates (Jackson *et al.*, 2000). The consecutive addition of ubiquitin molecules to a substrate generates a polyubiquitin chain. Both E2 and E3 enzymes exist as large families and it is thought that different combinations of E2s with different E3 proteins define substrate specificity (Joazeiro and Weissman, 2000). For example, seventeen

E2s have been identified in the budding yeast, *Saccharomyces cerevisiae,* and many more exist in humans. In contrast to the E2s, whose catalytic sites are well conserved among species, only a few E3 ligases possess conserved and defined catalytic motifs (e.g., the HECT and RING domains) (Jackson *et al.*, 2000). Together, these few E2 and E3 enzymes, working in concert, can potentially target thousands of different protein substrates for proteasomal degradation.

In the last decade, a ubiquitin elongation factor was identified and termed an E4 (Hoppe, 2005). It was shown that efficient multiubiquitination was required for proteasomal targeting of the ubiquitin-fusion substrate. The first E4 protein identified, Ufd2 (Ubiquitin Fusion Degradation pathway), is involved in proteasomal targeting of chimeric degradation substrates with a stable ubiquitin moiety fused to their *N*-termini (Johnson *et al.*, 1995). In yeast, E4 binds to the ubiquitin of short Ub conjugates and catalyzes ubiquitin chain elongation in conjunction with E1, E2, and E3 enzymes. It thus renders them preferred substrates for proteasomal degradation.

1.1.1 The proteasome

The rapid and selective degradation of proteins upon conjugation with polyubiquitin is catalyzed by the 26S proteasome (Bochtler *et al.*, 1999; Gorbea *et al.*, 1999; Voges *et al.*, 1999; Heinemeyer *et al.*, 2004; Asher *et al.*, 2006; Nandi *et al.*, 2006). The 26S proteasome is an ~2.5 MDa complex that is composed of approximately 60 different subunits whose function is to selectively degrade proteins into short amino acid peptide sequences. There are two fundamental differences between the 26S proteasome and other proteases: [1] the 26S proteasome is dependent on ATP hydrolysis for protein degradation. [2] The 26S proteasome progressively

Figure 1. The ubiquitination pathway.

The ubiquitination pathway is the result of three key steps: Activation of ubiquitin, transfer of ubiquitin, and ubiquitination. Ubiquitin is activated in a two-step reaction by an E1 ubiquitin-activating enzyme in a ATP dependent manner. The initial step involves production of an ubiquitin-adenylate intermediate (not illustrated). The second step transfers ubiquitin to the E1 active site cysteine residue, with release of AMP. This results in a thioester linkage between the *C*-terminal carboxyl group of ubiquitin and the E1 cysteine sulfhydryl group. The next step transfers ubiquitin from the E1 to the active site cysteine of a ubiquitin-conjugating enzyme E2 via a trans(thio)esterification reaction. The final step of the ubiquitination cascade generally requires the activity of an E3 ubiquitin ligase, which functions as the substrate recognition receptor of the system and is capable of interacting with both the E2 and the substrate. (Image obtained from http://en.wikipedia.org/wiki/Image:Ubiquitylation.png on 5/10/2007 with permission granted by Roger B. Dodd).

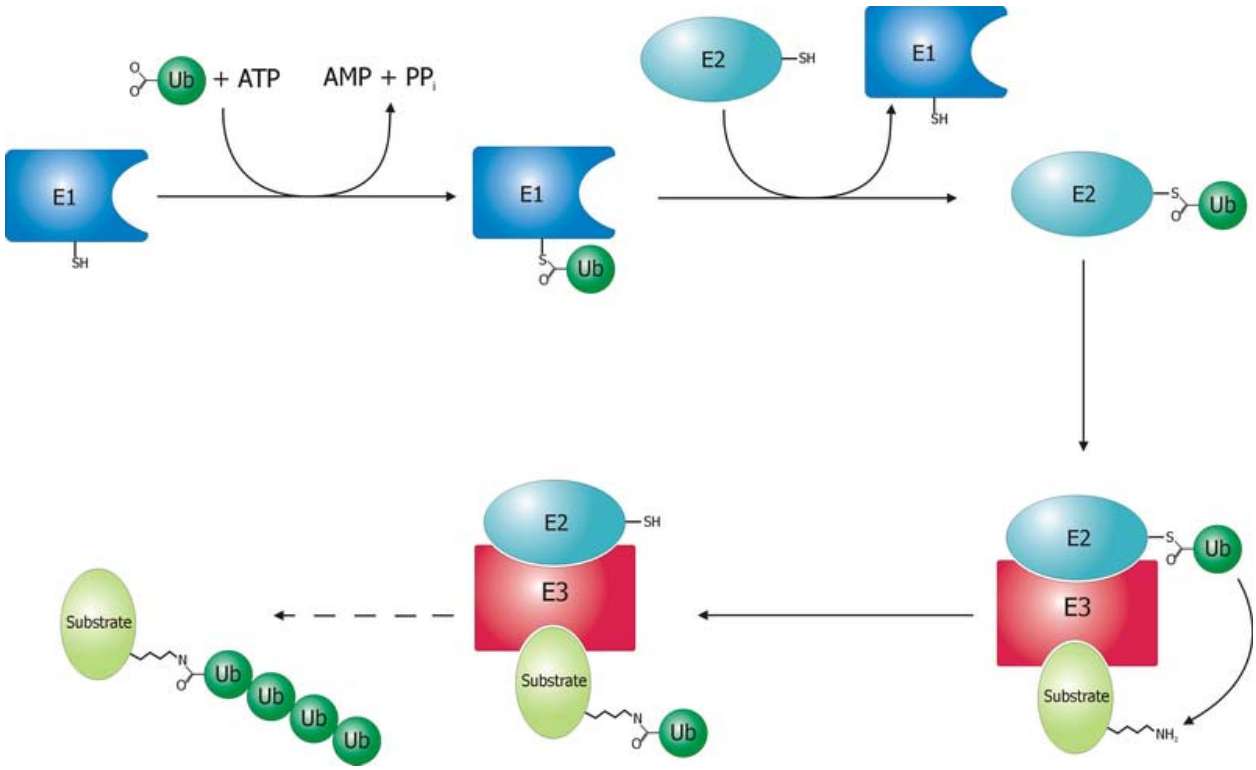

Figure 1. The ubiquitination pathway

cleaves a polypeptide at multiple sites until the final peptide sequences, ranging from 3 to 25 amino acid residues, are delivered from the particle, while a cytosolic protease may only cleave a substrate once or twice (Kisselev *et al.*, 1999).

The 26S proteasome is located in the cytoplasm, predominantly in a peri-nuclear sub-cellular localization, and accounts for approximately 1% of the total cell mass (Peters *et al.*, 1994; Enenkel *et al.*, 1998; Voges *et al.*, 1999). The 26S complex contains a central 20S proteolytic core particle (CP) and two 19S regulatory particles (Figure 2) (Voges *et al.*, 1999; Nandi *et al.*, 2006). The symmetrical, 20S barrel-shaped core particle of the proteasome is comprised of two half-proteasome complexes (15S) which result from two stacked hollow rings, per 15S complex, of seven subunits per ring. These half-proteasomes contain an outer ring of seven alpha subunits and an inner ring of seven beta subunits, in which three of the beta subunits are responsible for the CP's proteolytic activity (Orlowski and Wilk, 2000). The two outer alpha rings are identical to each other in composition and to the two inner beta rings also are identical in composition to each other. The 20S core harbors three distinct proteolytic activities; a chymotrypsin-like (CTL), a trypsin-like (TL), and a peptidylglutamyl-peptide hydrolyzing (PGPH) activity (Voges *et al.*, 1999; Heinemeyer *et al.*, 2004). The beta subunits that are responsible for the proteolytic activity of the CP, belong to a family of hydrolases, designated as *N*-terminal nucleophilic (Ntn) hydrolases, and can hydrolyze amine bonds as well as peptide bonds (Bochtler *et al.*, 1999). These conserved beta subunits orient the region responsible for proteolytic activity towards the inner lumen of the CP, allowing efficient proteolysis of substrates within the CP. Genes that encode Ntn hydrolases belong to a super-family of proteins and show great variability in protein structure as well proteolytic mechanisms. However, the subunits

Figure 2. The 26S proteasome.

Composite model of the three-dimensional structure of the 26S proteasome from *Drosophila* based on electron microscopy and using the crystal structure of the 20S proteasome from *Thermoplasma* (Walz *et al.*, 1998). The 19S cap (blue) attaches to one or both ends of the 20S core (yellow).

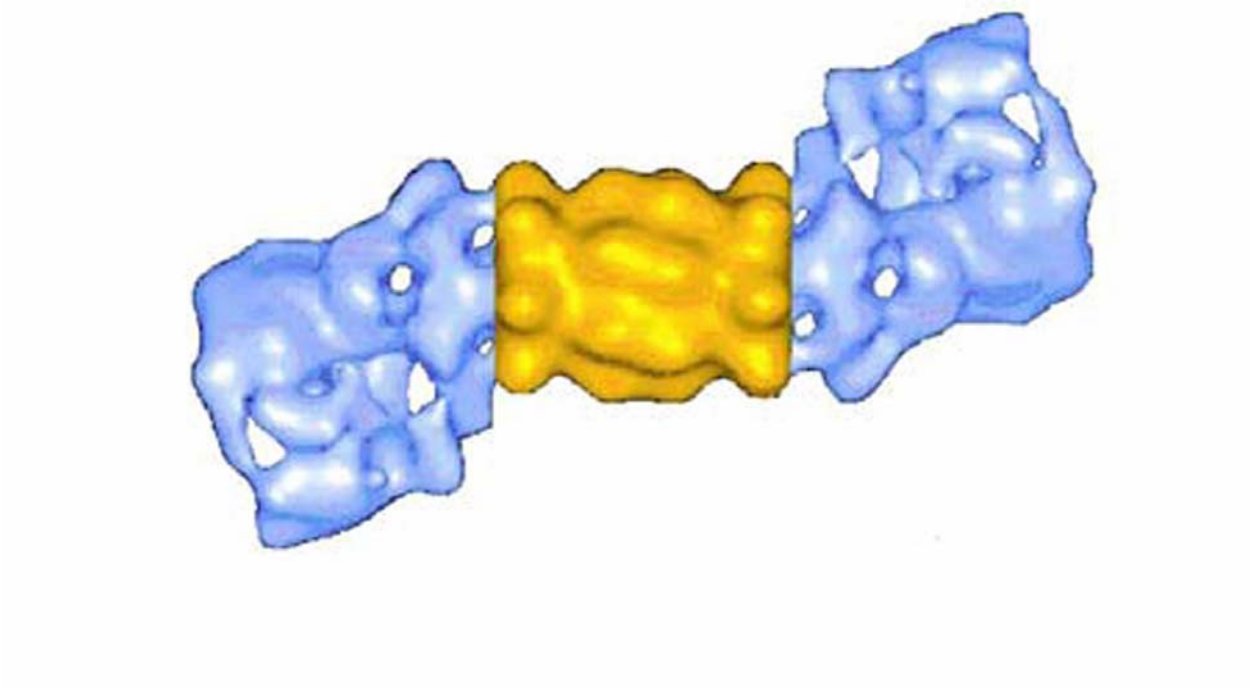

Figure 2. The 26S proteasome

responsible for proteolytic activity (Pre3p, Pre2p, and Pup1p) contain a conserved threonine (Thr1) and/or a conserved lysine (Lys33) residue that are required for proteolytic activity (Seemuller *et al.*, 1995).

Substrate entry into the 26S proteasome is gated by the 19S (also known as PA700) regulatory cap through a complex process. The outer alpha rings of the CP create a narrow pore through which substrates enter and degradation products exit with the assistance of the 19S complex (Groll *et al.*, 2000). The 19S cap confines proteolysis within the 20S core and prevents nonspecific proteolysis of proteins in the cytoplasm. The 19S particle contains polyubiquitin-binding subunits, enzymes required for polypeptide de-ubiquitination, and six AAA ATPases (Glickman *et al.*, 1998; Voges *et al.*, 1999; Leggett *et al.*, 2002; Verma *et al.*, 2002; Guterman and Glickman, 2004; Soboleva and Baker, 2004). These subunits are responsible for recognition, unfolding, de-ubiquitination, and translocation of the substrate into the lumen of the 20S core.

The 19S cap is made up of at least 19 different subunits and is conserved from yeast to mammals (Bochtler *et al.*, 1999; Voges *et al.*, 1999; Sharon *et al.*, 2006). This complex can be further divided into two sub-complexes, the base that binds directly to the 20S CP and the peripheral lid. The base contains the AAA ATPases (Rpt1-Rpt6), as well as four non-ATPase subunits (Rpn1, Rpn2, Rpn10, Rpn13). The ATPases are responsible for protein unfolding as well as CP channel opening (Glickman *et al.*, 1998). The lid is comprised of nine different non-ATPase subunits (Rpn3, Rpn5-9, Rpn11, Rpn12, and Sem1). The major activity of the lid is proposed to be de-ubiquitination (Yao and Cohen, 2002; Guterman and Glickman, 2004; Soboleva and Baker, 2004). De-ubiquitinating enzymes (DUBs, Rpn11p is one example), which are thiol proteases, facilitate the recycling of Ub by cleaving ester, thiol ester, and amide bonds

which link Ub to amino acids (Yao and Cohen, 2002; Guterman and Glickman, 2004; Soboleva and Baker, 2004). Rpn10p and Rpt5p have been shown to reversibly bind to ubiquitinated proteins and subsequently deliver them to the CP for degradation in an ATP dependent manner (Deveraux *et al.*, 1994; Lam *et al.*, 2002). Thus, these various subunits, working in concert allow multi-ubiquitinated proteins to bind to the 19S cap, undergo de-ubiquitination, unfold, and be fed into the CP for proteolysis. This exquisitely selective process allows only certain polypeptides to be degraded within the 26S proteasome.

1.1.2 26S proteasome assembly and maturation

The eukaryotic 26S proteasome serves as a vital final step in regulated protein degradation. To ensure that this complex is present, a complex sequence of stages exists that allows the step-by-step assembly and maturation of a proteolytic complex. There are two distinct steps required for proteasome assembly: 20S core assembly and 19S assembly.

While there have been significant strides to elucidate the mechanism for 20S core assembly over the last decade, the early steps in this process are still not clear. At this time, a generalized theory of core assembly has been proposed, and is outlined in Figure 3 (Ramos *et al.*, 1998; Griffin *et al.*, 2000; Witt *et al.*, 2000; Tone and Toh, 2002; Heinemeyer *et al.*, 2004; Hirano *et al.*, 2006; Li *et al.*, 2007). In brief, alpha subunits assemble a ring structure which acts as a scaffold, and allows the beta subunits to combine and create a second stacked ring. Thus, alpha ring formation provides the foundation for beta subunit ordering and orientation. By expressing these subunits in bacteria, several groups have been able to recapitulate stages of alpha ring assembly *in vitro* from eukaryotic cells (Gerards *et al.*, 1997; Gerards *et al.*, 1998; Huang *et al.*, 1999; Yao *et al.*, 1999). However, observations from these studies demonstrate

Figure 3. 20S Proteasome assembly and maturation

A model outlining the steps involved in proteasome assembly. Seven free alpha subunits (yellow circles) form a ring structure and then associate with free beta subunits (red and green circles). Subpopulations of beta subunits are proteolyticly inactive due to the retention of a pro-peptide sequence. The association of beta subunits with the alpha ring results in the formation of the half-proteasome. The two half proteasomes dimerize and allow the pro-peptides to be cleaved, thus activating the 20S CP. The approximate molecular mass of each intermediate is given.

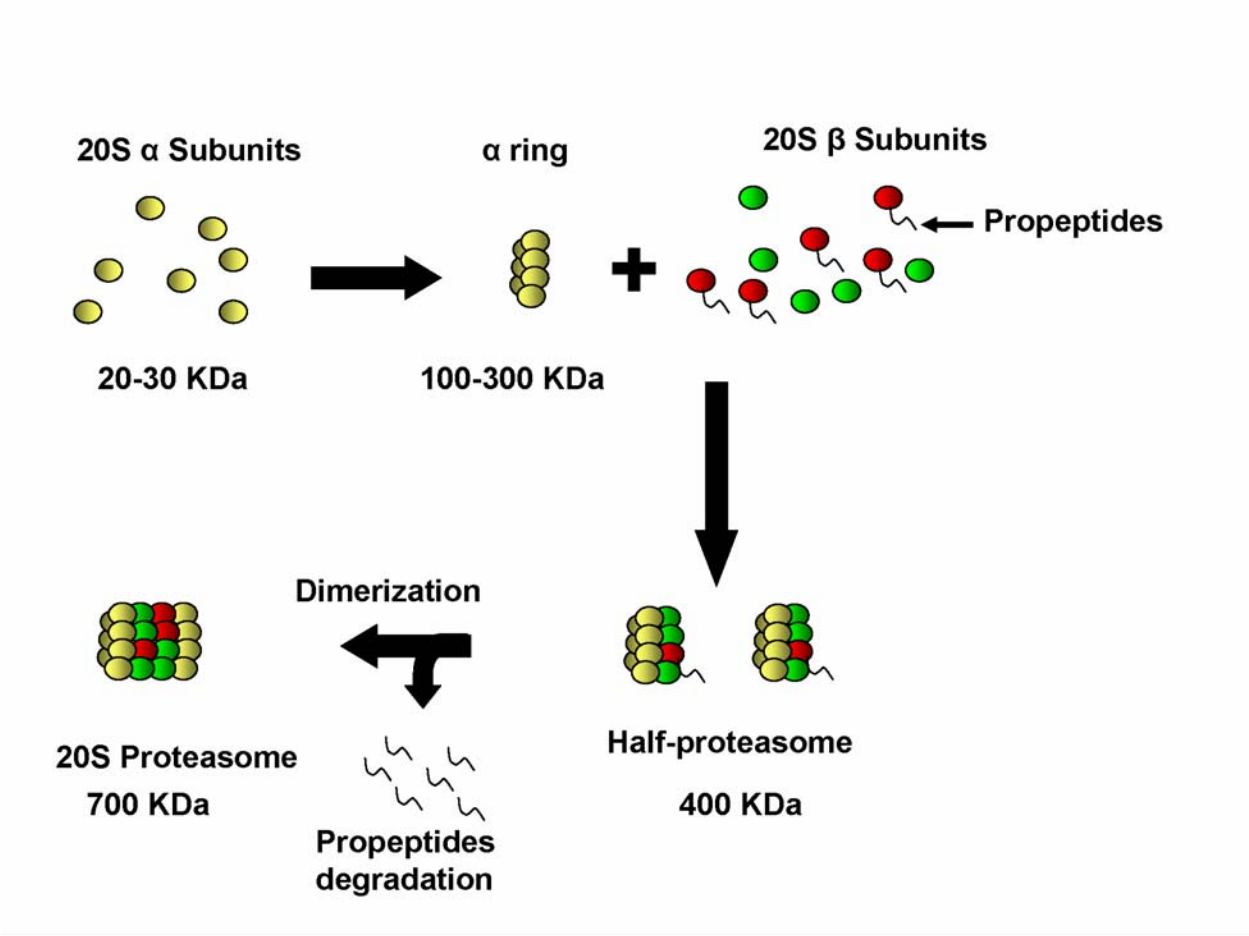

Figure 3. 20S Proteasome assembly and maturation

that the alpha subunits do not contain all the information necessary for their correct positioning within the ring structure *in vitro*. This suggests that alpha subunits either require other factors to properly assemble in the correct orientation or that the subsequent addition of beta subunits promotes reordering or replacement of alpha subunits to yield the final and complete ring structure. Putative early structures in the proteasome assembly pathway, such as dimers or ring structures containing predominantly alpha subunits, appear to be short lived as they have yet to be completely identified and characterized.

Once alpha ring formation has occurred, beta subunits associate with this structure to provide various intermediate complexes of different molecular masses and sizes (Frentzel *et al.*, 1994; Yang *et al.*, 1995; Chen and Hochstrasser, 1996; Nandi *et al.*, 1997; Ramos *et al.*, 1998). One structure of note is the half proteasome of approximately 400 kDa in size that sediments at 15S (Schmidtke *et al.*, 1997). The half proteasome consists of one ring of alpha and one ring of beta subunits. Many of the beta subunits are considered unprocessed when they are components of the half proteasome, as a pro-peptide sequence in the *N*-terminal region is still present. The pro-peptide sequence prevents proteolytic activity by masking the catalytic Thr1 in the Ntn hydrolases. However, some non-catalytic beta subunits also retain a pro-peptide sequence (Heinemeyer *et al.*, 1997). In the absence of pro-peptide cleavage, indiscriminate proteolysis in the cell by the various beta subunits is prevented. Upon the dimerization of the two assembled half-proteasomes, proteolytic beta subunits undergo autocatalytic processing, resulting in the cleavage and subsequent removal of the pro-peptide sequence associated with the Ntn hydrolases. Several beta subunits (Pre2p, Pre3p, Pre4p, and Pup1p) have been shown to be involved in subunit precursor processing and activating the 20S core complex (Heinemeyer *et al.*, 1997).

In general, less is known about the assembly and maturation of the 19S regulatory particle. The regulatory particles are believed to assemble as two distinct subcomponents, the ATPase-containing base and the ubiquitin-recognizing lid (Deveraux *et al.*, 1994). The six ATPases in the base may assemble in a pair-wise manner mediated by coiled-coil interactions (Gorbea *et al.*, 1999). The order in which the nineteen subunits of the regulatory particle bind to each other may also prevent non-specific proteins becoming exposed to the 20S core active site before assembly is complete (Sharon *et al.*, 2006).

While the exact nature of proteasome assembly is not completely understood, it has become very evident in recent years that a class of proteins has emerged that facilitate the proper assembly and maturation of the 20S CP. These proteins are termed proteasome assembly chaperones and are described in detail in the next section.

1.1.3 Proteasome assembly chaperones (PACs)

Work in the yeast *Saccharomyces cerevisiae* as well as in human cells over the past few years has established a series of dedicated proteasome assembly chaperones (PACs), which are proteins that facilitate and regulate proteasome assembly and maturation (Hirano *et al.*, 2005). The first member of this class of proteins was identified in yeast and was termed "Underpins the Maturation of the Proteasome" or Ump1p (Ramos *et al.*, 1998). This protein was isolated in a screen that identified mutants involved in ubiquitin/proteasome degradation. From this study, it was observed that yeast harboring the *ump1* deletion mutation are viable but are sensitive to cellular stresses that lead to an accumulation of proteins destined for degradation (Ramos *et al.*, 1998). Furthermore, deletion of *UMP1* results in a reduction of all three proteolytic activities of the 26S proteasome. Examination of beta subunits in the deletion strain revealed the retention of

the pro-peptide sequence and subsequently showed a drastic impairment of the proteolytic activity associated with the three beta subunits (Pre2p, Pre3p, and Pup1p). Furthermore, Ump1p associates with the half proteasome, but not with the fully assembled CP or the 26S proteasome. Ump1p is also extremely short lived and is degraded upon proteasome maturation (Ramos *et al.*, 1998). In fact, analysis of a defective CP strain, obtained by a point mutation in *PRE1* which compromises the CP CTL activity, demonstrated stability of Ump1p as well as an association with the CP previously not seen. This latter observation indicates that upon CP activation, Ump1p is degraded due to its association within the lumen of the CP (Ramos *et al.*, 1998). More recent work showed that Ump1p acts as a quality control checkpoint for half-proteasome dimerization (Li *et al.*, 2007). It is proposed that β7, believed to be the last subunit to associate with the partially assembled half-proteasome, associates with Ump1p, which was previously preventing pre-mature half proteasome dimerization. Upon β7 and Ump1p association, the half proteasome undergos dimerization (Li *et al.*, 2007). Taken together, these studies indicate that Ump1p associates with CP subunits and early CP intermediates in order to facilitate the assembly and maturation of the proteasome. Since the identification of Ump1p, other eukaryotic homologs, as well as a human homolog (Pomp1), have been isolated, and these homologs possess many of the same characteristics as Ump1p (Griffin *et al.*, 2000; Witt *et al.*, 2000).

Subsequent to the discovery of Ump1p, a second protein was identified that facilitates the proper assembly of the 20S CP (Tone *et al.*, 2000; Tone and Toh, 2002). This second proteasome assembly chaperone, Nob1p, exhibited many of the same features as Ump1p. Based on work performed by the Toh-e lab in Japan, Nob1p was hypothesized to play four major roles in proteasome function (Tone *et al.*, 2000; Tone and Toh, 2002). First, Nob1p associates with 20S and 19S complexes the in nucleus. This was demonstrated by Nob1p's association with

Pno1p, an uncharacterized nuclear protein. If either Nob1p or Pno1p was mutated, this led to an accumulation of proteasomes in the cytoplasm. Second, Nob1p facilitates the maturation of the 20S proteasome and degradation of Ump1p. A genetic interaction between Nob1p and Ump1p was established. Specifically, the over-expression of Nob1p complemented proteasome assembly defects observed in the *ump1Δ* mutant strains. Also, the *nob1-4* mutant strain exhibited defects in the processing of beta subunits and accumulated CP intermediates, similar to those observed in the *UMP1* deletion strain. Third, disruptions in *NOB1* also resulted in a significant reduction in the chymotrypsin-like proteolytic activity of the 26S proteasome. Fourth, Nob1p resides within the lumen of the CP and is subsequently degraded by the 26S proteasome upon its activation. Finally, it should be noted that no Nob1p orthologs have been identified in other eukaryotes.

Studies conducted in mammalian cells have also isolated a few proteins that seem to be involved in proteasome assembly and maturation (Hirano *et al.*, 2005; Hirano *et al.*, 2006). Three particular proteins, PAC1, PAC2, and PAC3 have been shown to be required for the efficient assembly of mammalian 20S CP. Unlike Ump1p or Nob1p, these proteins must dimerize to be active: PAC 1 and PAC2 form a heterodimer while PAC3 forms a homodimer. The Murata lab demonstrated that over-expression of both PAC1 and PAC2 proteins accelerates proteasome assembly, while the induction of RNAi against either PAC1 or PAC2 resulted in an accumulation of immature 20S proteasomes (Hirano *et al.*, 2005). Furthermore, disruption of either PAC1 or PAC2 resulted in a reduction of the CTL activity of the 26S proteasome. It was also established that PAC1 and PAC2 facilitate efficient alpha ring formation, which allows the rings to remain competent for half-proteasome formation. Early studies in proteasome assembly demonstrated that expression of alpha subunits *in vitro* resulted in ring structures with incorrect

alpha subunit positions (Gerards *et al.*, 1997; Gerards *et al.*, 1998; Huang *et al.*, 1999; Yao *et al.*, 1999). The Murata lab's observations provide valuable insight into early CP assembly by suggesting these proteasome assembly chaperones regulate competent alpha ring formation. Finally, the PAC1 and PAC2 heterodimer disassociates from the 20S CP and subsequently is degraded by the proteasome (Hirano *et al.*, 2006). This observation differs from the Ump1p and Nob1p degradation pathways, as they are internalized during half proteasome dimerization and then degraded (Ramos *et al.*, 1998; Tone and Toh, 2002).

Until very recently, all previous work regarding PACs elucidated proteins that associate with early CP intermediates and which facilitate the assembly of and are finally degraded by the activated CP. Recently published work shows the mammalian PAC3 homodimer also associating with early 20S intermediates, but then disassociates prior to half proteasome assembly (Hirano *et al.*, 2006). PAC3 seems to associate with both alpha and beta subunits and is required for alpha ring formation, but upon coupling with Pomp1, PAC3 disassociates from the complex. This PAC3 disassociation occurs prior to half proteasome formation and prevents PAC3 degradation upon 20S CP activation. This suggests that PAC3 may be recycled for future proteasome assembly processes. All these observations together suggest that not all proteasome assembly chaperones behave in the same manner or at the same step in the proteasome assembly pathway. Yet, interactions and cooperation between the various PACs seem to be required for proper assembly, since a triple PAC1/PAC2/PAC3 knockdown by RNAi resulted in an accumulation of incompetent half proteasome that were unable to properly dimerize (Hirano *et al.*, 2006).

1.2 SECRETORY PATHWAY

The proteasome functions as the final destination of a significant number of proteins, some of which have traveled through the secretory pathway. The secretory pathway is a series of compartments a cell uses to move proteins out of the cell or deposit them in the ER, Golgi network, or vacuole/lysome (Figure 4). The pathway is under high demand as approximately 20% of all proteins reside in or traverse the secretory pathway, as determined by analysis of various eukaryotic genomes (Lander *et al.*, 2001).

The path of a protein destined for secretion begins in the rough endoplasmic reticulum (ER), a membrane bound compartment located within the cell that is continuous with the nuclear membrane (Johnson and van Waes, 1999). Newly synthesized polypeptides are translocated into the ER. Proteins can be imported into the ER either co-translationally or post-translationally. Co-translationally translocated proteins that enter into the ER contain a signal peptide that is recognized by the signal recognition particle (SRP) as the signal sequence emerges from the ribosome (Keenan *et al.*, 2001). The SRP, while associated with the ribosome and the newly synthesized polypeptide, binds to the SRP receptor located on the ER membrane. At this point, the polypeptide is threaded into the Sec61 translocation channel which facilitates polypeptide entry into the ER. Post-translationally translocated polypeptides disassociate completely from the ribosome and do not bind the SRP (Rapoport *et al.*, 1999). Regardless of the mode of import, entry into the ER is immediately followed by cleavage of the signal sequence (Jackson and Blobel, 1977).

A major role of the ER is to post-translationally modify and package proteins destined for secretion or deposited along the secretory pathway (Gorlach *et al.*, 2006). Various alterations in the ER include glycosylation, disulfide bond formation, folding, and multi-protein complex

Figure 4. Secretory pathway

Co-translational translocation is depicted by ribosomes (grey circles) associated with mRNA (green line) which are then attached to the rough ER. Newly synthesized polypeptides (red lines) are hereby referred to as the substrate. As translation is started, the substrate is inserted into the lumen of the ER or into the membrane (not shown). Molecular chaperones (blue lines), begin assisting the substrate in its folding through association or modifications of the substrate. Grey lines illustrate the various resident proteins found in all compartments of the pathway. The substrate is then translocated into the *Cis-Medial-Trans* Golgi network where further folding, modifications, and associations occur. Finally, the substrate in its final conformation is transported to the plasma membrane and can be secreted. The substrate may also be targeted to the vacuole or lysosome as its final destination or for degradation if a non-native state is adopted and not reversed.

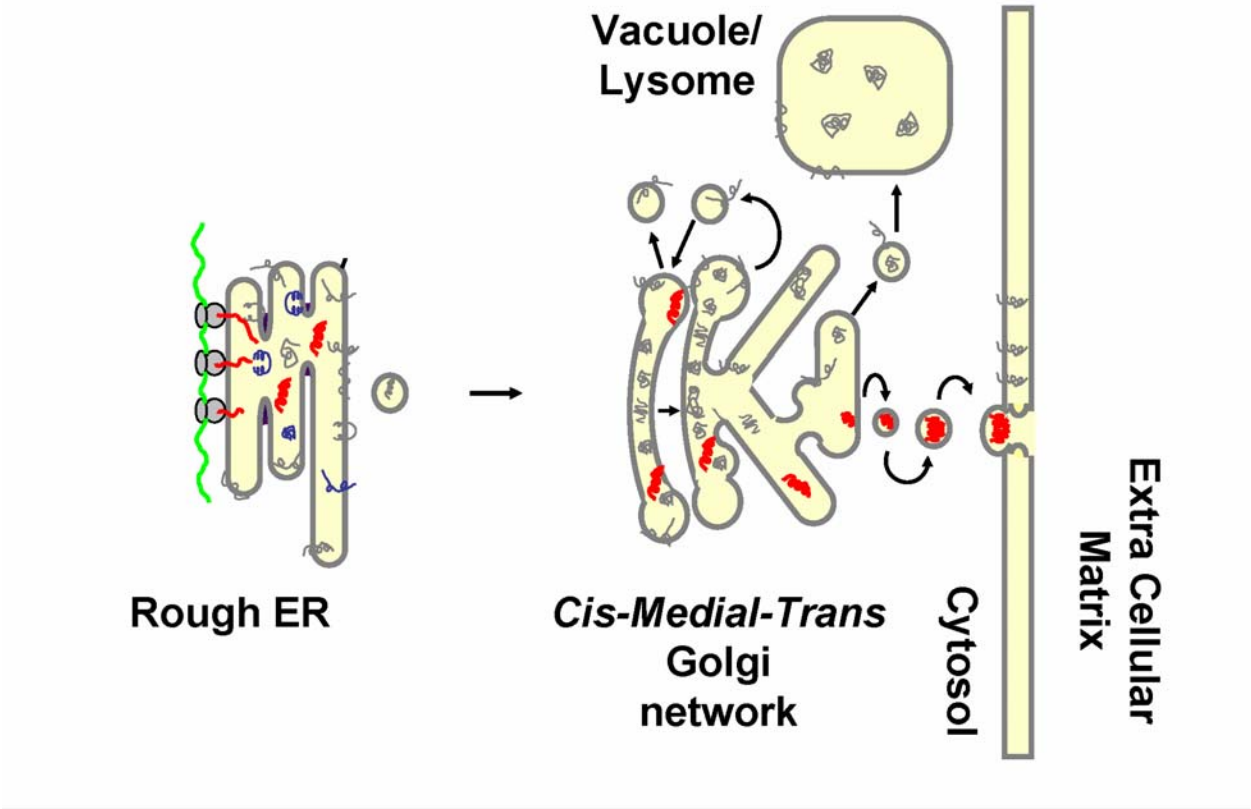

Figure 4. Secretory pathway

assembly. Therefore, the lumen of the ER is a highly specialized compartment containing high levels of Ca^{2+} and ATP, as well as a high oxidation potential (Clairmont *et al.*, 1992; Hwang *et al.*, 1992; Michalak *et al.*, 2002). Furthermore, there is a high concentration of molecular chaperones (see below) that reside within the ER lumen and whose function is tailored to prevent improper folded states of nascent polypeptides.

Molecular chaperones are a large and diverse group of proteins that associate with substrates non-covalently and facilitate the folding and unfolding of proteins as well as the assembly or disassembly of larger protein complexes (Brodsky *et al.*, 1999; Fewell *et al.*, 2001; Nishikawa *et al.*, 2005). Since molecular chaperones assist other proteins, they are not permanent components of their substrates. Molecular chaperones were first characterized during nucleosome assembly in amphibians (Laskey *et al.*, 1978), but have grown to include a diverse population of different proteins of various sizes. These proteins are required in all cells to prevent and/or reverse improper conformations or associations of the chaperones' substrates; which include proteins or RNAs (Cristofari and Darlix, 2002). Chaperones may be classified into two categories, constitutively expressed (Hsc) or heat shock proteins (Hsp). Constitutively expressed chaperones are considered house-keeping proteins that maintain the balance of protein synthesis during non-stressful conditions. On the other hand, heat shock proteins are induced during cellular stress since the requirement for chaperones increases, and these conditions cause proteins to misassemble or misfold at an increased rate.

After folding in the ER and passing ER quality control (see below), secreted proteins are selectively incorporated into budding vesicles to be transported into the ER-Golgi intermediate compartment or the Golgi complex (Bonifacino and Glick, 2004). These vesicles, which are coated with the COPII protein complex, collect the selected cargo from the ER and migrate to

the Golgi complex (Barlowe *et al.*, 1994). Proteins that are retained in the ER require retrograde transport back to the ER from the Golgi, which occurs via COPI coated vesicles and through the recognition of an ER retention signal (Letourneur *et al.*, 1994). Protein substrates will then traffic along the *Cis-Medial-Trans* Golgi Network and can be transported to the plasma membrane, lysosome (or the vacuole in Fungi or plants). Proteins can also be recycled within several compartments via components associated with the endocytic pathway (Clague, 1998).

Regardless of their final destination, the cell employs a series of quality control check-points at various stages along the secretory pathway. These check-points help regulate protein traffic by ensuring that only properly maintained proteins or protein complexes may pass further along the pathway. One of the earliest check-points in the secretory pathway is ER protein quality control, which is discussed next.

1.3 ENDOPLASMIC RETICULM PROTEIN QUALITY CONTROL

There are quality control systems required at every step during DNA replication and RNA and protein synthesis, which prevents the accumulation of misfolded proteins within the cell. In eukaryotic cells, it is estimated that approximately 25% of all newly synthesized secretory proteins misfold and are subsequently degraded (Schubert *et al.*, 2000). This accounts for only normal housekeeping quality control, and thus an increase in the production of mutant proteins greatly increases the rate of protein turnover immediately after biosynthesis (Lomas and Parfrey, 2004). As stated earlier, proteins that traverse the secretory pathway are translocated into the ER during or immediately after translation. Upon entry to the ER, nascent proteins must fold and assemble into a mature state prior to being transported further along the pathway. A mechanism

known as ER quality control (ERQC) monitors protein folding and assembly and prevents the transport of immature molecules (Ahner and Brodsky, 2004; Nishikawa *et al.*, 2005; Sayeed and Ng, 2005). Failure to achieve a competent state might subject the protein to degradation by the 26S proteasome after removing the aberrant protein from the ER. This process has been dubbed ER associated degradation, or ERAD. ERAD eliminates the formation of possibly toxic or aggregation-prone substrates within the crowded ER.

1.3.1 ER- associated degradation (ERAD)

Soluble proteins that fail to pass quality control within the ER will be targeted for degradation by the 26S proteasome in a multi-step process referred to as ERAD (Cabral *et al.*, 2002; McCracken and Brodsky, 2003; Ahner and Brodsky, 2004; Meusser *et al.*, 2005; Nishikawa *et al.*, 2005; Romisch, 2005; Sayeed and Ng, 2005). Since all proteins entering the secretory pathway have the potential to become misfolded, ERAD must be able to identify a range of substrates from large and complex proteins such as the cystic fibrosis transmembrane regulator (CFTR) to relatively small soluble proteins like antitrypsin (A1Pi) (Coughlan and Brodsky, 2003, 2005). ERAD may be generalized into a five step process: selection of substrate, retrotranslocation, polyubiquitination of the substrate and transport to the proteasome, de-ubiquitination, and degradation by the proteasome (Figure 5).

Recent evidence has suggested that while the proteasome is the final destination for all ERAD substrates, the requirements for the earlier steps differ for different substrates, particularly if the substrate is an ER lumenal protein or a transmembrane protein (Brodsky and McCracken, 1999; Vashist *et al.*, 2001; Vashist and Ng, 2004; Nishikawa *et al.*, 2005). Proteins with misfolded lumenal domains are monitored by ERAD- lumenal (ERAD-L) pathway components.

Figure 5. ERAD pathway

A model of the steps during the ERAD of a polypeptide (string of red circles). First, the polypeptide is identified as a misfolded substrate by molecular chaperones (purple circle) (step 1) and retrotranslocated from the ER into the cytoplasm through a putative pore in the ER membrane (step 2). The misfolded substrate is then polyubiquitinated via the ubiquitin conjugating pathway (step 3) and transported to the 26S proteasome (blue/yellow macromolecule). Substrate binding to the 19S regulatory cap (blue segment of 26S proteasome) results in substrate unfolding and de-ubiquitination (step 4). Finally the substrate is degraded into small peptides by the 20S CP (yellow segment of the 26S proteasome) (step 5).

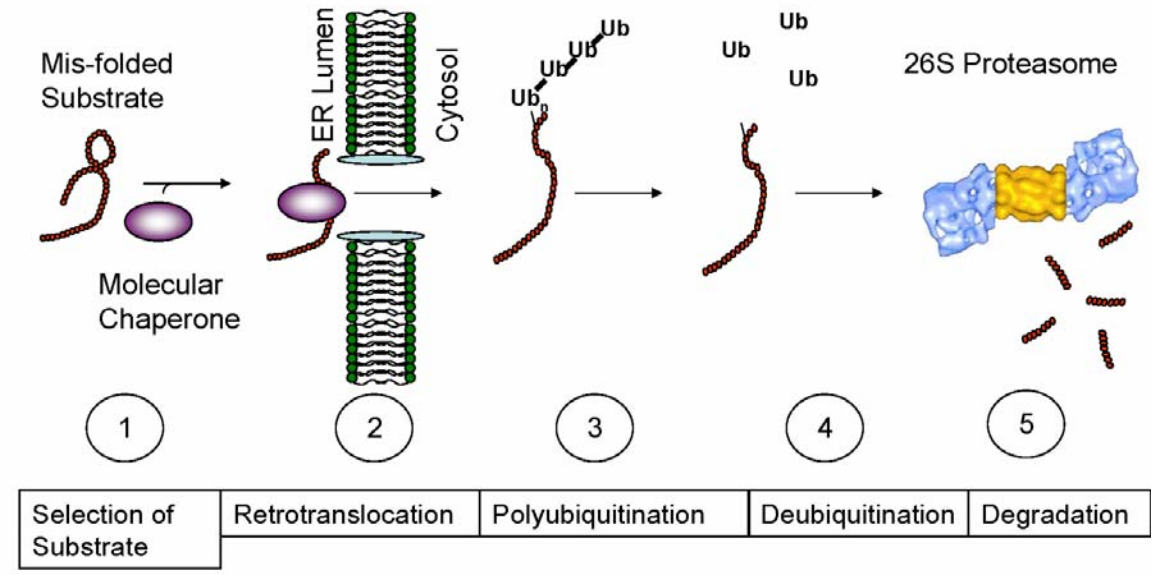

Figure 5. ERAD pathway

ERAD-L substrates seem to require ER to Golgi transport, the molecular chaperone BiP (see below), the transmembrane protein Der1p (see below), and Hrd1p, an E3 ubiquitin ligase. The requirement for ER-to-Golgi transport suggests that ERAD-L substrates are sequestered to an exit site located within the ER prior to degradation (Nishikawa *et al.*, 1994). In contrast, substrates with aberrant cytosolic domains fall under the ERAD-cytosolic (ERAD-C) pathway. ERAD-C substrates are not transported from the ER to the Golgi and do not utilize Hrd1p. Instead, Doa10p, another E3 ubiquitin ligase, is required. ERAD-C substrates also seem to be sequestered within a specialized sub-compartment of the ER prior to their degradation (Huyer *et al.*, 2004). It should be noted that both ERAD-L and ERAD-C substrate compartmentalization has only been examined for a limited number of substrates; thus these phenomena might not hold true for all ERAD substrates.

Potential substrates for ERAD are recognized as being misfolded by molecular chaperones within the lumen of the ER (ERAD-L) or in the cytoplasm (ERAD-C). The actual mechanism in which chaperones target a protein for entry into ERAD is not completely understood at this time, but this may be the result of a global defect in the structure of the protein instead of a particular altered residue. In some instances prolonged association of some chaperones with an unfolded protein might select the substrate protein. While at other times, different molecular chaperones that do not assist in proper folding and protein assembly might help target a substrate for ERAD (Zhang *et al.*, 2001; Youker *et al.*, 2004). One protein that is required for post-translational and co-translational entry into the ER, protein folding, and the ERAD of many lumenal proteins, is the lumenal Hsp70, BiP (Kabani *et al.*, 2003; Vashist and Ng, 2004). The analysis of various BiP mutants has demonstrated discrete roles of this molecular chaperone during protein folding, sensing ER stress, and targeting proteins for

degradation (Mori *et al.*, 1992; Brodsky *et al.*, 1999; Zhang *et al.*, 2001; Cabral *et al.*, 2002; Kabani *et al.*, 2003).

Prior to retrotranslocation from the ER, a protein needs to be disassociated from any associated macromolecular complexes, such as those complexes with molecular chaperones, in order to remain in a soluble state (Nishikawa *et al.*, 2001). In recent years, the search for the putative pore complex responsible for retrotranslocation has led to the characterization of two different multi-transmembrane protein complexes that form pores (in the case of one complex) within the ER membrane that seem to be required for retrotranslocation (Romisch, 2005). The heterotrimeric Sec61 complex in mammals was first identified as associated with ERAD substrates prior to their degradation by the 26S proteasome (Wiertz *et al.*, 1996). In yeast, mutant *sec61* alleles display reduced ERAD efficiency for various substrates as demonstrated by pulse chase analysis (Plemper *et al.*, 1997). But, these observations are difficult to intepet conclusively due to the pleiotropic effects of the mutant allele. The second putative pore complex was identified in 2004, by the Ploegh and Rapoport labs, who concluded that Derlin-1 associates with ERAD substrates during their extraction from the mammalian ER (Lilley and Ploegh, 2004; Ye *et al.*, 2004). Mutations in the yeast homolog of Derlin-1, Der1p, result in ERAD substrate stabilization (Knop *et al.*, 1996). Recently, Derlin-1, and not Sec61p, was shown to be required for the retrotranslocation of a derivative of the yeast mating pheromone pro-alpha-factor (Wahlman *et al.*, 2007). Due to the observation that Der1p is involved with the export of select ERAD substrates, while having little or no effect on other ERAD substrates, it is unlikely that there is only one major export pore within the ER.

As discussed above, the ubiquitination of ERAD substrates is facilitated by the ER resident E3 ligases, Hrd1p and Doa10p (Hampton *et al.*, 1996; Bays *et al.*, 2001; Swanson *et al.*,

2001). Hrd1p as well as Doa10p both work in conjunction with the ubiquitin conjugating enzymes, Ubc6p and Ubc7p (Bays *et al.*, 2001; Swanson *et al.*, 2001). It should be noted that the 26S proteasome-mediated clipping of the transmembrane protein Ole1p is independent of both Hrd1p and Doa10p but relies on Ubc6p and Ubc7p (Braun *et al.*, 2002). These observations suggest that other E3 ligases may be involved with ubiquitination of ERAD substrates.

After polyubiquitination, the substrate binds to the surface of the 19S cap of the 26S proteasome. Rpn10p and Rpt5p, subunits of the 19S regulatory cap of the proteasome, recognize the proteolytic degradation signal, polyubiquitin, in an ATP dependent manner (Deveraux *et al.*, 1994; Lam *et al.*, 2002). Upon substrate association with the 19S cap, the protein unfolds and is de-ubiquitinated and finally translocated into the lumen of the 20S CP for degradation. A subunit (Rpn11p) of the 19S regulatory cap of the 26S proteasome was identified as a metalloprotease responsible for the de-ubiquitinating enzymatic (DUB) activity prior to substrate degradation (Verma *et al.*, 2002). These observations for Rpt5p, Rpn10p and Rpn11p have provided evidence for the necessity of the 19S regulatory cap by coupling its roles in substrate recognition and de-ubiquitination prior to protein degradation.

During the degradation of some substrates, it has been shown that de-ubiquitination is a rate-limiting process during proteasomal degradation (Yao and Cohen, 2002; Guterman and Glickman, 2004; Hanna *et al.*, 2006). However, some ERAD substrates, such as the mutant form of antitrypsin, can be degraded in both a ubiquitin-dependent and -independent manner (Teckman *et al.*, 2000).

Overall, it appears that each ERAD substrate requires different factors to promote the efficient degradation of the misfolded substrate (Fewell *et al.*, 2001). Although many of these factors are unknown, further examination of different ERAD substrates will provide further

insight into essential, redundant, and/or unique factors required for ERAD.

1.3.2 Unfolded protein response (UPR)

As stated earlier, approximately 25% of all secretory proteins that are newly synthesized may misfold and be subsequently degraded (Schubert *et al.*, 2000). This percentage represents only the basal levels of protein turnover and does not account for environmental or genetic stresses that might enhance protein miss-assembly and turnover within the cell. While ERAD performs normal housekeeping degradation, the system can get overwhelmed in the presence of many misfolded proteins. Thus, a second quality control mechanism is induced within the cell, known as the Unfolded Protein Response or UPR (Patil and Walter, 2001; Schroder and Kaufman, 2005). The UPR is an intracellular signaling pathway that transcriptionally up-regulates a specific population of genes whose role is to alleviate or eliminate the accumulation of unfolded proteins within the ER.

The UPR signaling pathway responds to a variety of different stimuli. For example, the UPR is induced by viral infection (Dimcheff *et al.*, 2003). Furthermore, the UPR is induced by nutrient or carbohydrate reduction and/or starvation (Schroder *et al.*, 2000; Kuhn *et al.*, 2001). Finally, the accumulation of various misfolded proteins within the ER induce the UPR (Mori *et al.*, 1992; Shamu and Walter, 1996; Casagrande *et al.*, 2000; Travers *et al.*, 2000).

No matter what conditions induce the UPR signaling pathway, it begins within the ER membrane, through the three domain transmembrane serine kinase, Ire1p (Figure 6) (Cox *et al.*, 1993; Shamu and Walter, 1996). Association of two or more Ire1p molecules with an unfolded protein allows Ire1p dimerization and subsequent phosphorylation of the cytosolic kinase domain (Shamu and Walter, 1996; Welihinda and Kaufman, 1996). This activates the cytosolic

Figure 6. UPR Pathway

BiP, a molecular chaperone, is associated with Ire1p, a transmembrane protein kinase. It is unclear if this is a direct or indirect interaction (see text for details). During non-stressful conditions, this BiP/Ire1p complex is maintained, which prevents the translation of *HAC1* mRNA, which encodes for a transcription factor. During ER stress, BiP disassociates from Ire1p. This allows Ire1p homodimerization and removal of the *HAC1* mRNA intron which allows complete translation of the mRNA. Hac1p then translocates into the nucleus and up-regulates approximately 380 genes in yeast that help compensate for ER stress.

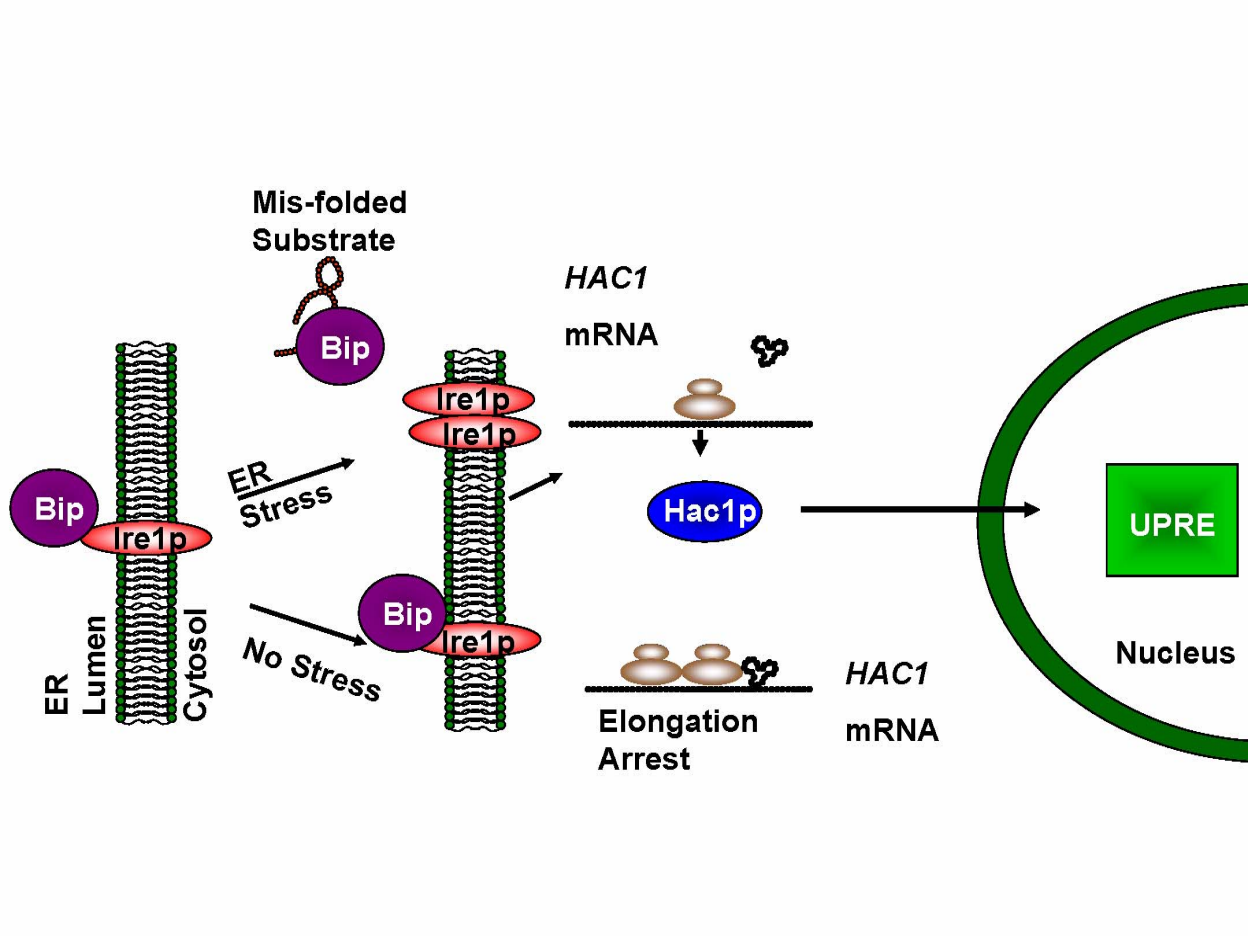

Figure 6. UPR pathway

endoribonuclease activity of Ire1p which cleaves an intron from a basic lucine zipper transcription factor Hac1p (Cox and Walter, 1996). The removal of this classical intron allows *HAC1* mRNA to be efficiently translated (Sidrauski and Walter, 1997). Notably, removal of the *HAC1* intron is not dependent on the spliceosome but only on Ire1p and is similar to tRNA splicing rather than mRNA splicing since a tRNA ligase is needed to repair the cleavage (Sidrauski *et al.*, 1996). Upon translation of Hac1p, the transcription factor is translocated into the nucleus and activates target gene transcription by binding a UPR specific upstream activating sequence, the unfolded protein response element (UPRE, see below) (Cox and Walter, 1996; Mori *et al.*, 1996; Kawahara *et al.*, 1997).

The amino terminal domain of Ire1p resides in the ER lumen and recent structural examinations of this lumenal domain have created contradictory models for the mechanism of sensing unfolded proteins (Credle *et al.*, 2005; Zhou *et al.*, 2006). Seminal work from the Kohno lab showed that BiP, a molecular chaperone, is tethered to Ire1p and upon accumulation of unfolded proteins within the ER, BiP dissociates from Ire1p to help fold substrates (Okamura *et al.*, 2000). This then lowers the level of the BiP-Ire1p complex, allowing Ire1p to homodimerize (Okamura *et al.*, 2000; Zhou *et al.*, 2006). The Walters group disagrees with this model and suggests that Ire1p contains a groove in its lumenal domain which associates with unfolded proteins directly. Ire1p dimerization is due to close association of Ire1p to a neighboring Ire1p along with a possible internal rearrangement of both Ire1ps when bound to an unfolded protein (Credle *et al.*, 2005).

The UPRE was originally defined as a 22-bp sequence that is involved in the up-regulation of *KAR2*, the gene that encodes yeast BiP (Mori *et al.*, 1992). The 22-bp sequence has subsequently been reduced to an essential seven nucleotide E-box-like palindrome (CAGNGTG)

(Mori *et al.*, 1998). Furthermore, the UPRE has been identified in the promoter sequence for a variety of different UPR targets (Mori *et al.*, 1998). Mutations of the conserved sequence or the deletion of the central nucleotide result in reduced induction of UPR targets during times of ER stress (Mori *et al.*, 1998). Taken together, the specific sequence of the UPRE explains why only a discrete set of proteins are induced by the UPR to cope with ER stress.

The target genes of the UPR encode factors that are involved in many different processes, such as phospholipid biosynthesis, protein maturation in the ER and secretory pathway function (Travers *et al.*, 2000). Yeast genomic microarray data indicate intimate interactions between ERAD and the UPR (Ng *et al.*, 2000; Travers *et al.*, 2000): [1] Strains lacking nonessential genes required for ERAD lead to an induction of the UPR. [2] Strains lacking ERAD required genes as well as *IRE1* are inviable during heat stress. [3] ERAD is less efficient in strains lacking Ire1p. [4] Induction of the UPR increases the efficiency of ERAD. Taken together, these observations indicate that cell viability is dependent on both ERAD and the UPR pathways and disruption of both will force cells to succumb to aberrant protein accumulation.

Approximately 380 genes are induced during times of ER stress, and are thus putative targets of Hac1p (Travers *et al.*, 2000). However, initial examination of the promoter sequences in most of these genes failed to uncover a recognizable UPRE. However, computational analysis of upstream activating sequences (UAS) 5' of UPR targets identified a second conserved sequence that is recognized by the Gcn4p transcription factor (Patil *et al.*, 2004). Gcn4p is up-regulated during times of cellular stress by its activator Gcn2p. Basal levels of Gcn4p are not sufficient to bind UPR targets, though its up-regulation during ER stress induces the UPR. Furthermore, dimerization with Hac1p facilitates the induction of many UPR targets. These observations suggest that Gcn4p is a second UPRE-binding transcription factor that works in

parallel and/or downstream of Hac1p (Patil *et al.*, 2004).

1.4 AUTOPHAGY

Eukaryotic cells have two complementary and conserved mechanisms to degrade proteins, the proteasome and the vacuole/lysosome. The proteasome selectively degrades proteins that are misfolded, under metabolic regulation, a part of the major histocompatibility complex, or degraded for cell cycle progression (see above). While the proteasome efficiently degrades soluble proteins, it may be limited in its ability to degrade aggregated proteins, membrane proteins, protein complexes, and even whole organelles. To this end, the vacuole in yeast and plants or the lysosome in mammalian cells is designed to degrade larger and more complex substrates (Abeliovich and Klionsky, 2001; Huang and Klionsky, 2002; Noda *et al.*, 2002). Autophagy is a membrane trafficking process that translocates bulk cytosoplasm and even entire organelles into the vacuole/lysosome during times of nutrient starvation or other physiological conditions (Clark, 1957; Ashford and Porter, 1962; Deter *et al.*, 1967; Deter and De Duve, 1967). The vacuole/lysosome is a double membrane organelle that contains a plethora of hydrolases in a segregated compartment that forgoes the need for substrate selection upon entry into the organelle. Entry into the vacuole/lysosome occurs through one of four different autophagic pathways: macroautophagy, the CVT pathway, microautophagy, and pexophagy (Figure 7). For simplicity, the vacuole/lysosome will here by be referred to as the vacuole.

Macroautophagy is often referred to as autophagy, and involves the *de novo* formation of a vesicle in the cytosol that sequesters cytoplasm and/or organelles which are then delivered to the vacuole (Noda *et al.*, 2002). One pre-vacuolar structure has been identified, the

Figure 7. Autophagy

Macroautophagy and CVT vesicle formation begin with the preautophagosomal structure, PAS (green circle), which then engulfs cargo and transports it to the vacuole. CVT pathway operates during vegetative conditions whereas macroautophagy is induced during nutrient starvation. Pexophagy (micro and macro) regulates the number of peroxisomes within the cell. Macroautophagy, macropexophagy, and the CVT pathways all begin with vesicle formation independent of the vacuole, whereas microautophagy and micropexophagy occur directly at the vacuole or lysosome membrane. Figure obtained from (Huang and Klionsky, 2002).

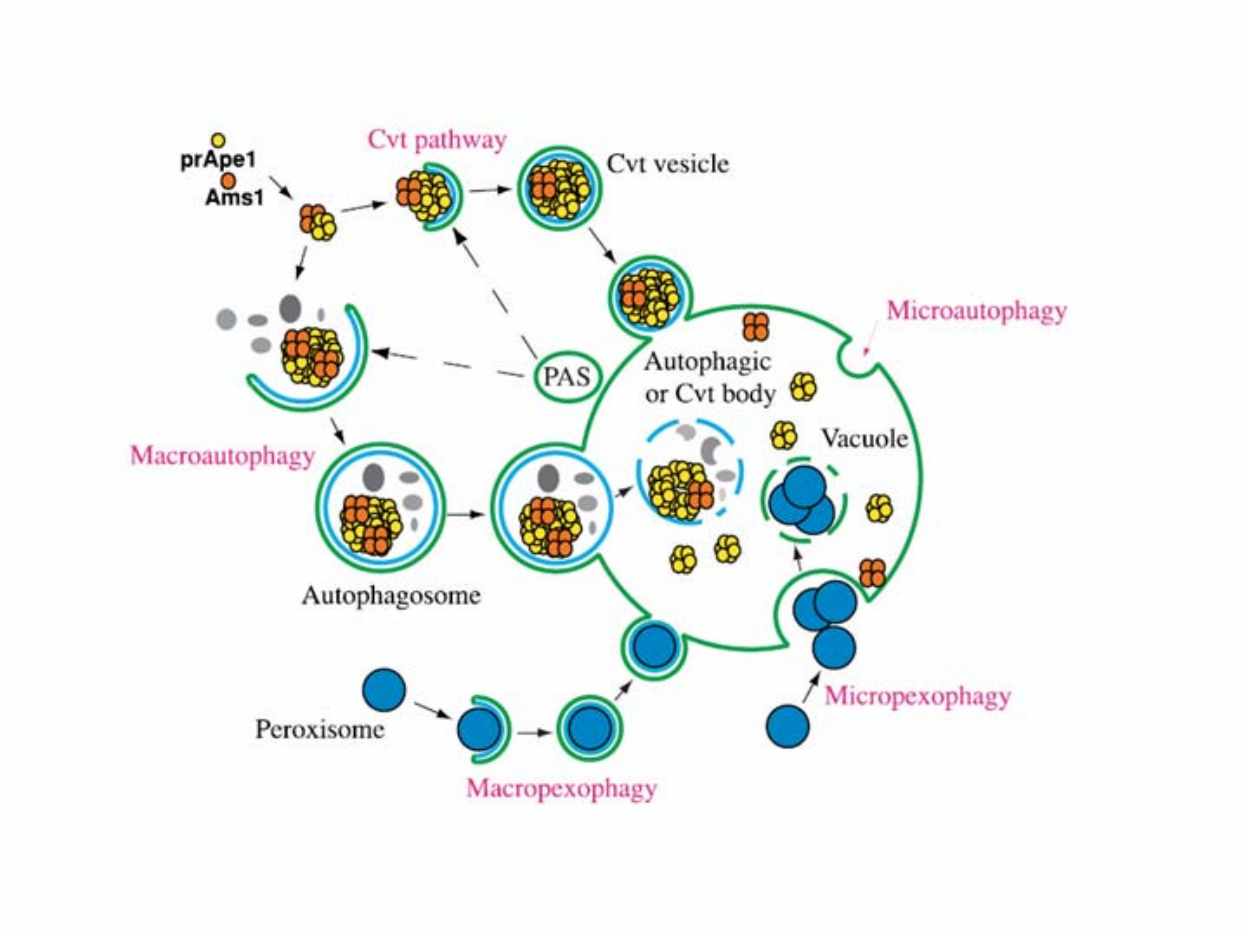

Figure 7. Autophagy

preautophagosomal structure (PAS), which contains various gene products that localize together transiently and catalyze vesicle formation (Suzuki *et al.*, 2001). However, it is unclear how the PAS forms at this time. The transport vesicle, or autophagosome, is a double membrane vesicle that is targeted to the vacuole by an unknown mechanism, and allows fusion of the outer membrane of the vesicle with the vacuole. The interior membrane vesicle, or autophagic body, is then released into the lumen of the vacuole and its contents are degraded. Autophagy requires a panoply of different proteins for vesicle formation, transport to the vacuole, and fusion of autophagosomes to the vacuole (partial list of autophagy factors located in Table 1 of Abeliovich and Klionsky, 2001).

Macroautophagy is an inducible pathway that is up-regulated during times of nutrient stress or cell arrest. The receptor that senses stress has been identified as the TOR (Target Of Rapamycin) receptor (Rohde *et al.*, 2001). TOR is a serine/theronine protein kinase that coordinates multiple cell responses due to nutrient conditions (Raught *et al.*, 2001). Through a signaling pathway involving a series of protein complexes, phosphorylation, and dephosphorylation, the result is the association of Atg13p and Atg1p, proteins required for macroautophagy initiation. This association activates the Atg1p kinase function which is thought to in turn activate vesicle formation (Kamada *et al.*, 2000). Though, recent studies suggest that Atg1p may simply be required for macroautophagy (Abeliovich *et al.*, 2003).

While macroautophagy is an inducible catabolic pathway, a second conserved and constitutive pathway has been identified which operates similar to macroautophagy and is termed the cytoplasm-to-vacuole-targeting (CVT) pathway. The majority of vacuolar hydrolases are transported to the vacuole via the secretory pathway due to the presence of specific vacuolar targeting sequences (Bryant and Stevens, 1998). However, two vacuole hydrolases, Ams1p and

Ape1p, have been shown to be delivered to the vacuole independently of the secretory pathway (Yoshihisa and Anraku, 1990; Klionsky *et al.*, 1992). Ams1p and immature Ape1p (prApe1p) are encased in a densely compacted double membrane vesicle, called the CVT vesicle. The overall process of Ams1p and prApe1p delivery to the vacuole is very similar to macroautophagy, but the process is not regulated by nutrient starvation. It is interesting to note that CVT vesicles have been isolated inside autophagosomes in starved yeast (Baba *et al.*, 1997). This suggests that the CVT pathway is co-opted by macroautophagy during times of ER stress and CVT vesicles are engulfed by autophagosomes.

A third type of autophagy, which is not well defined, is microautophagy. Microautophagy is a process of invaginating a portion of the vacuole membrane to engulf neighboring cytoplasm and/or organelles (Yuan *et al.*, 1997). The fourth method of autophagy involves the degradation of peroxisomes, either by micro- or macropexophagy (Tuttle and Dunn, 1995; Kim and Klionsky, 2000).

1.5 PROTEIN CONFORMATIONAL DISEASES

Over the past two decades a variety of human disorders have been identified and characterized due to our better understanding of how mutations affect synthesis, maturation, and regulation of specific proteins. Human disorders are classified into various groups; inflammatory, degenerative, infectious, neoplastic, or conformational. Conformational disorders are the result of abnormal folding and subsequent aggregation of a particular protein (Carrell and Lomas, 1997). This is different than other genetic disorders, which result from a failure of protein production. Proteins in this group are extremely diverse and are associated with a variety of

disorders: prion disorders such as encephalopathies, to neurodegenerative disorders like Huntington's and Alzheimer's disease, and the misfolded members of the serpin family protease inhibitors. The focus of this section is on one disorder, Antitrypsin Deficiency, which arises from a misfolded serpin.

1.5.1 Antitrypsin Deficiency

Alpha-1 Antitrypsin Deficiency (ATD) is a genetic disorder characterized by production of abnormal antitrypsin proteins (Carrell and Lomas, 1997, 2002; Parfrey *et al.*, 2003; Lomas and Parfrey, 2004; Richmond and Zellner, 2005; Rudnick and Perlmutter, 2005). Antitrypsin (AT) is a 53 kDa neutrophil inhibitor of pulmonary elastase that is induced during times of lung infection or due to lung irritation or injury (Myerowitz *et al.*, 1972; Perlmutter, 2002). Therefore, AT protects the tissue matrix of the pulmonary system from being damaged by proteolytic enzymes. AT is a serpin (short for serine protease inhibitor), which are a group of structurally related protein, that inhibit proteases (Law *et al.*, 2006). Most serpins, like antitrypsin, target trypsin-like serine proteases, such as trypsin, which are characterized as having a serine residue in their catalytic site. The structure of AT as well as over 80 other serpin family members have been solved and reveal the archetypical serpin fold (Figure 8). All serpins typically have three beta sheets and eight or nine alpha helices. Serpins also possess an exposed variable region termed the reactive central loop (RCL) that includes the specificity determining region and forms the initial interaction with the target protease. The AT RCL loop contains key methionines and serines that act as bait for elastase and are essential for its inhibition (Carrell and Lomas, 2002). Inhibition is initiated when the RCL region is cleaved by the protease. Elastase, which is then tethered to the RCL fragment, is flung to the other side of AT, which subsequently distorts the

Figure 8. 2.0A structure of alpha-1 antitrypsin

The X-ray crystal structure of native human antitrypsin is shown (protein database code 1QLP). The RCL variable loop has been annotated. The image was obtained and modified from http://www.rcsb.org/pdb/explore.do?structureId=1QLP on May 16, 2007).

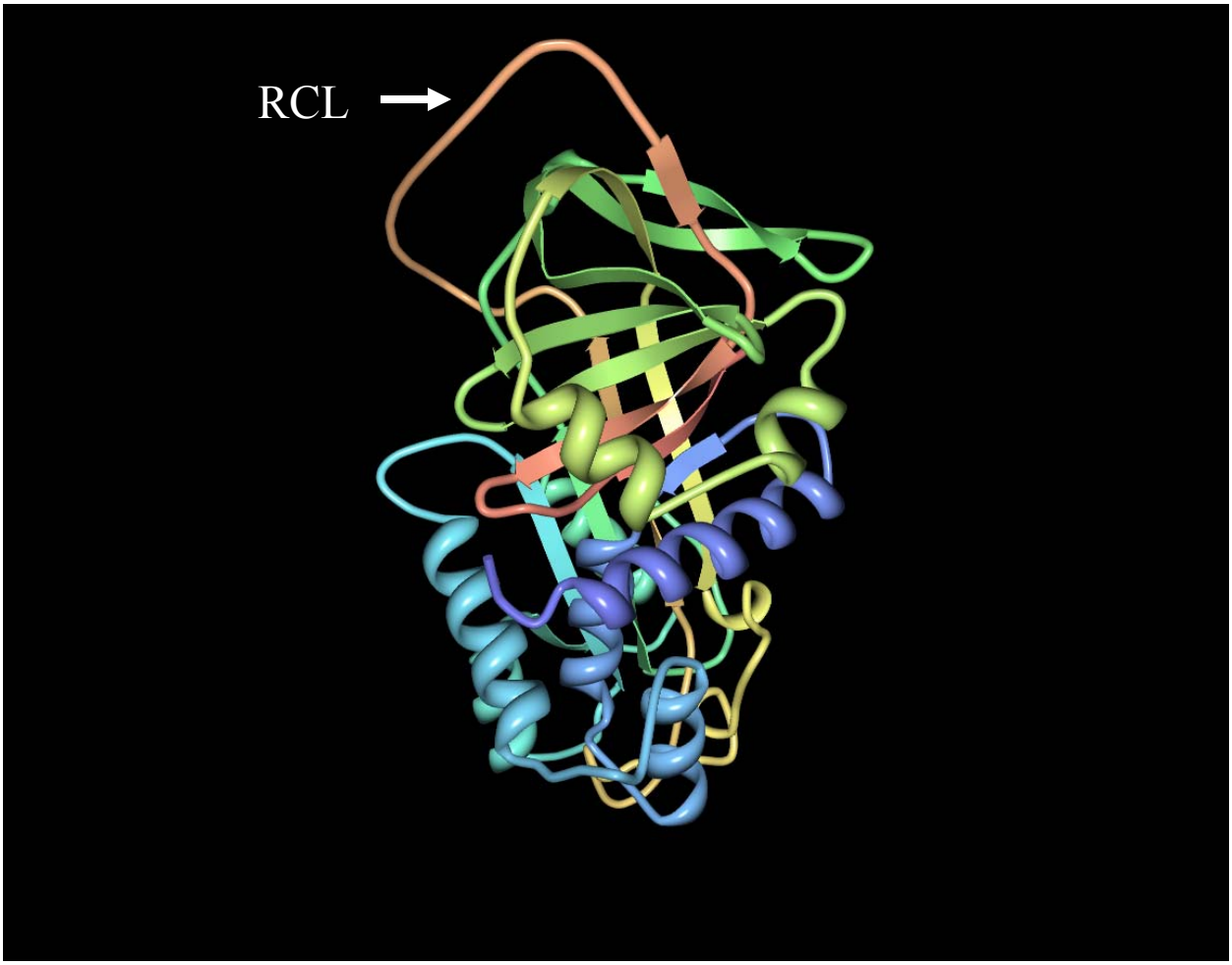

Figure 8. Antitrypsin structure

elastase structure and presents the protease for removal from tissue in a manner that is not fully understood (Janoff, 1985).

AT is secreted predominantly by hepatocytes, and significant reduction of secreted AT results in ATD (Carrell and Lomas, 2002; Perlmutter, 2002; Parfrey *et al.*, 2003; Lomas and Parfrey, 2004; Richmond and Zellner, 2005; Rudnick and Perlmutter, 2005). The rate of incident of the disorder is rather high in the Caucasian population in the United States with an estimate of 1/3000 individuals affected. In comparison, the genetic disorder cystic fibrosis has an occurrence of 1/2500 in the Caucasian population.

Individuals afflicted with ATD present with low levels of secretion of an abnormal AT protein, which results in pulmonary tissue damage. Chronic lung diseases, such as emphysema, asthma, and bronchitis, are the most common symptoms of ATD in adults and present as early as the second decade of life in humans (Colp *et al.*, 1993; King *et al.*, 1996; Eden *et al.*, 1997; Rudnick and Perlmutter, 2005). Those individuals that smoke present the disease at a much earlier age with an increased severity of symptoms (Larsson, 1978). Specifically, when comparing normal individuals and ATD individuals, including if they smoked or did not smoke, there is a significant decrease in the level of forced expiratory volume per second for the ATD individuals, which is compounded if the same person smoked (Piitulainen and Eriksson, 1999).

The accumulation of abnormal protein bodies within hepatocytes results in various forms of liver disease. Liver diseases, such as cirrhosis of the liver, can result from ATD at any age and is the second most common reason for liver transplants in the United States. The major risk factor for liver cirrhosis is an increased level of aberrant AT polymers, which normally occur in patients that maintain two copies of a genetically unstable allele of AT (Campra *et al.*, 1973; Cruz *et al.*, 1976; Mahadeva *et al.*, 1999). Abnormal AT retained in the liver dilates the ER and

large globules of aggregated AT are evident (Figure 9, see below). This retention of abnormal AT results in widespread necrosis of hepatocytes and thus is known as a global liver disease.

Although the exact mechanism is unknown, some ATD individuals (approximately 10%) present with various forms of hepatocellular carcinoma (Sveger, 1988). Recent work from the Perlmutter lab suggests that AT globule-devoid cells are "sick but not dead" compared to hepatocytes that contain large globules of aggregated AT undergoing necrosis (Rudnick and Perlmutter, 2005). This hypothesis has three implications: [1] these cells have activated a variety of stress response pathways, such as autophagy; [2] the cells are deficient in proliferation as well as growth; and [3] the globule containing cells are somehow inducing regenerative signals. The reason that only some hepatocytes contain globules may be age, as younger liver cells may have insufficient time to accumulate abnormal AT to sufficient levels. Also, the third implication suggests that the neighboring globule devoid cells would have a proliferation advantage compared to those globule containing cells. This increased rate of proliferation could subsequently lead to an increase rate of liver carcinomas.

There are currently four major treatment plans for those individuals with confirmed diagnosis of ATD (refer to http://www.alphaone.org/ for more information); behavioral and lifestyle modification, drug therapy for lung problems, specialized therapy for ATD, and surgical options. [1] Behavioral and lifestyle modifications involve the cessation of smoking, avoidance of environmental pollutants, and implementation of an exercise program. The ultimate goal of this treatment plan is to strengthen the lung capacity of an ATD patient. [2] Drug therapy for lung problems includes vaccinations against influenza as well as medications for lung infections, thereby preventing further lung damage. [3] ATD patients may undergo specialized therapy for ATD by receiving intravenous infusions of alpha-1 antitrypsin derived from donated human

Figure 9. The accumulation of an aberrant form of antitrypsin in hepatocytes.

A liver section from an ATD individual. AT stains dark purple with an immunoperoxidase stain. Nuclei were stained blue with haematoxylin, and eosin stained the cytoplasm a light blue or lavender. Image obtained from http://www.meddean.luc.edu/Lumen/MedEd/orfpath/cellch2.htm on May 16, 2007).

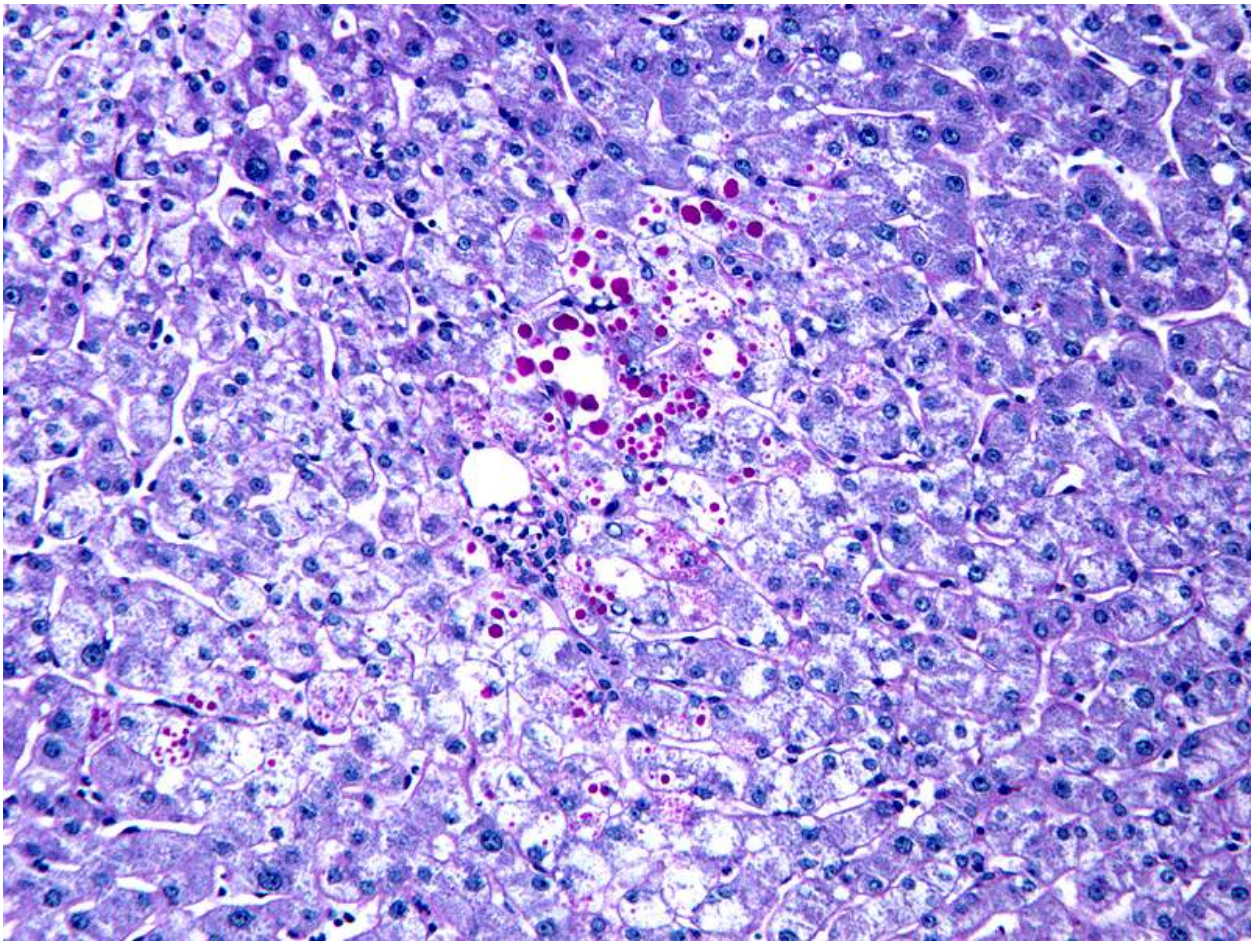

Figure 9. The accumulation of an aberrant form of antitrypsin in hepatocytes

plasma. This augmentation therapy is thought to arrest the course of the disease and halt any further damage to the lungs. [4] ATD patients may undergo liver or lung transplants in cases of extreme damage to either organ.

1.5.1.1 A1PiZ

AT isolates were first defined by electrofocusing (isoelectric focusing) analysis, in which the protein underwent electrophoresis through a pH gradient (Myerowitz *et al.*, 1972). Normal wild type AT is termed "M", as it is neutral and does not migrate very far. Other variants, which are less active, are termed A-L and N-Z, dependent on whether they run more proximal or more distal to the M band. The presence of deviant bands by electrofocusing can signify the presence of ATD. One allele of AT has been extensively studied and is linked to the most severe presentations of ATD; A1PiZ (or alpha-1 protease inhibitor, Z) (Lomas *et al.*, 1992; Yu *et al.*, 1995). Although secreted A1PiZ does retain partial activity, individuals expressing this protein have significantly lower circulating levels of the protein because the E342K mutation compromises its folding in the ER, rendering it a substrate for ERAD (Werner *et al.*, 1996). However, when the A1PiZ variant accumulates, it can form loop-sheet polymers or aggregates that may trigger cirrhosis (Figure 9) (Foreman *et al.*, 1984; Perlmutter *et al.*, 1985; Mornex *et al.*, 1986; Verbanac and Heath, 1986; Brantly *et al.*, 1988; McCracken *et al.*, 1989; Lomas *et al.*, 1992; Mast *et al.*, 1992; Kim *et al.*, 1995; Sidhar *et al.*, 1995; Carrell and Lomas, 2002; Parfrey *et al.*, 2003) and hepatocellular carcinoma (Carlson *et al.*, 1989; Rudnick and Perlmutter, 2005). Thus, A1PiZ is also a gain-of-function allele of ATD. The loop sheet polymer formation of A1PiZ is due to aberrant alignment of the RCL due to steric interference of E342K, which results in a cleft at the top of the protein. Thus, the RCL from one A1PiZ protein will then bind in the groove of a second A1PiZ protein, who's RCL will then bind to a third A1PiZ protein, and so on,

until a loop-sheet polymer of A1PiZ aggregates are formed within hepatocytes.

Extensive studies of AT have been conducted over the years resulting in the elucidation of some of the processes by which both A1PiM as well as A1PiZ are secreted. Unfortunately, the exact nature of how AT is expressed, processed, degraded, and secreted is unknown. Also, due to the difficulty of manipulating and examining cultures from patients afflicted with ATD, the Brodsky and McCracken laboratories developed a yeast expression system to begin to address these questions (see below). The results from the A1PiZ yeast expression system were valid for two reasons (McCracken and Kruse, 1993): [1] Components of the protein quality control machinery are highly conserved, and [2] yeast expression systems for several human disease-causing proteins have led to a better understanding of the pathological consequences of aberrant protein production (Coughlan and Brodsky, 2003).

Notably, the A1PiZ yeast expression system helped establish this protein as a *bona fide* ERAD substrate (Werner *et al.*, 1996). Specifically, strains defective for the CTL activity of the proteasome degraded A1PiZ 3-times slower than wild type yeast strains (Figure 10). Furthermore, expression of wild type Pre1p and Pre2p in a *pre-1-1 pre2-2* (proteasome mutant strain) strain complemented the A1PiZ degradation defect. Later work identified BiP as an important player in A1PiZ turnover (Brodsky *et al.*, 1999). This result was subsequently confirmed in mammalian cells (Cabral *et al.*, 2002; Schmidt and Perlmutter, 2005).

The seminal work described above and more recent studies indicate that there are many possible fates for A1PiZ within the cell (Figure 11). First, the AT gene product from cells containing the Z allele fails to properly mature and is not secreted from hepatocytes. Therefore, the retained protein polymerizes to create large globules of aggregated protein that ultimately cause the cell to undergo apoptosis due to mitochondrial injury.

Figure 10. The proteasome is required for the ERAD of A1PiZ.

Pulse chase analysis of A1PiZ in the following yeast strains; *pre1-1 pre2-2, pre1-1 pre2-2* expressing Pre1p or Pre2p (*pre1-1 pre2-2* + *PRE1* or *pre1-1 pre2-2* + *PRE2*), or an isogenic wild type. (a) Mutations in the proteasome lead to an increase accumulation of A1PiZ in yeast. A representative phosphorimage of radiolabeled A1PiZ. Immunoprecipitation products from samples taken at discrete time points (0, 60, 90, 120 mins) were treated (+) or not (-) with endoglycosidase H (EndoH) to remove carbohydrate chains that are added to A1PiZ within the ER. (b) Quantification of the degradation rates of A1PiZ in the above strains from three independent experiments. Figure obtained from Werner *et al*. 1996.

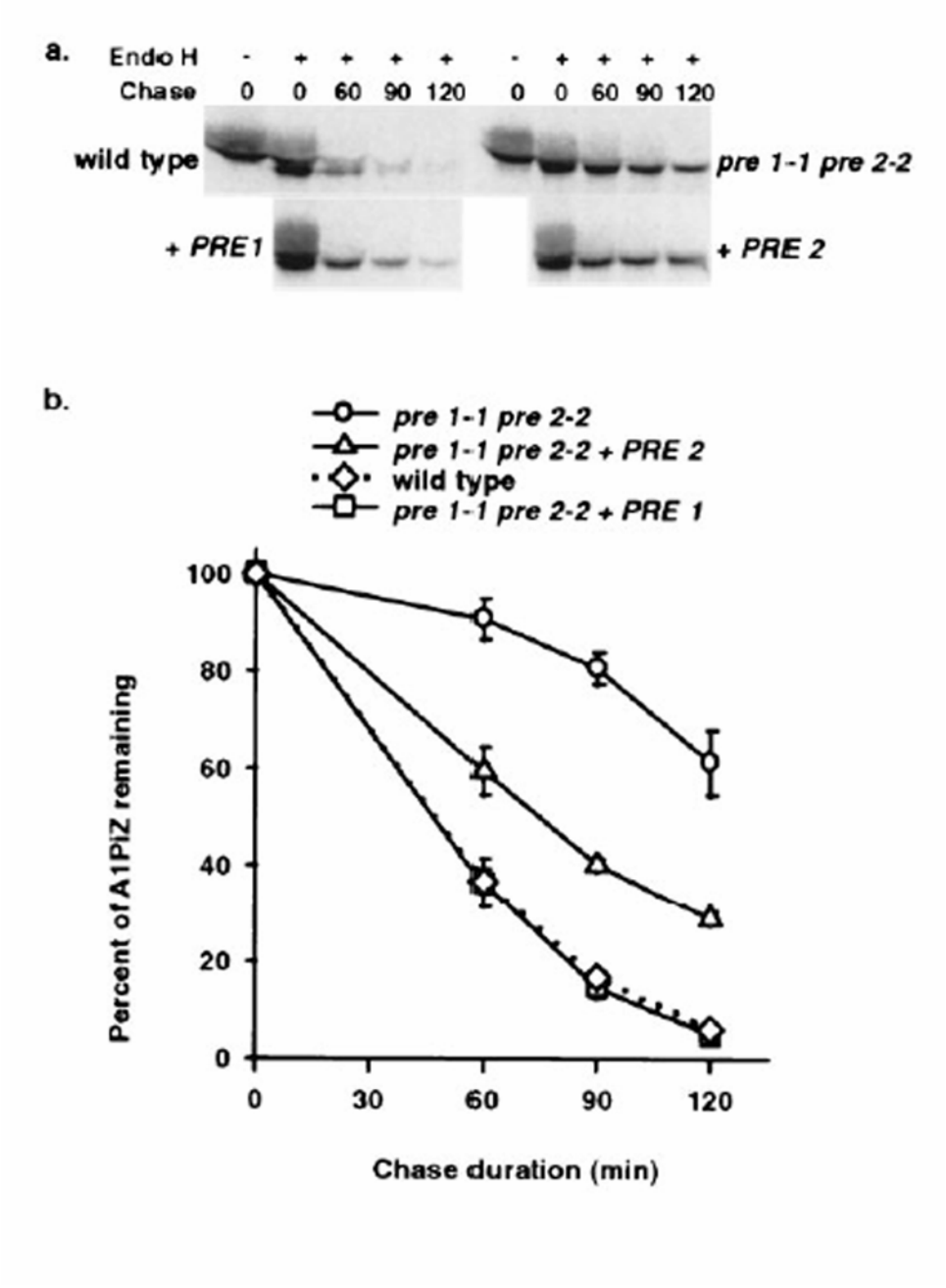

Figure 10. The proteasome is required for the ERAD of A1PiZ

Figure 11. The fate of A1PiZ.

Generalized model showing the possible fates of A1PiZ (red circles). The aberrant protein is not secreted by the cell, and the retained A1PiZ can form loop-sheet polymer aggregates, or if soluble, can be degraded via ERAD. However, the retained mutant protein will not induce the UPR. The aggregated protein can also be degraded by the lysosome via the autophagic pathway.

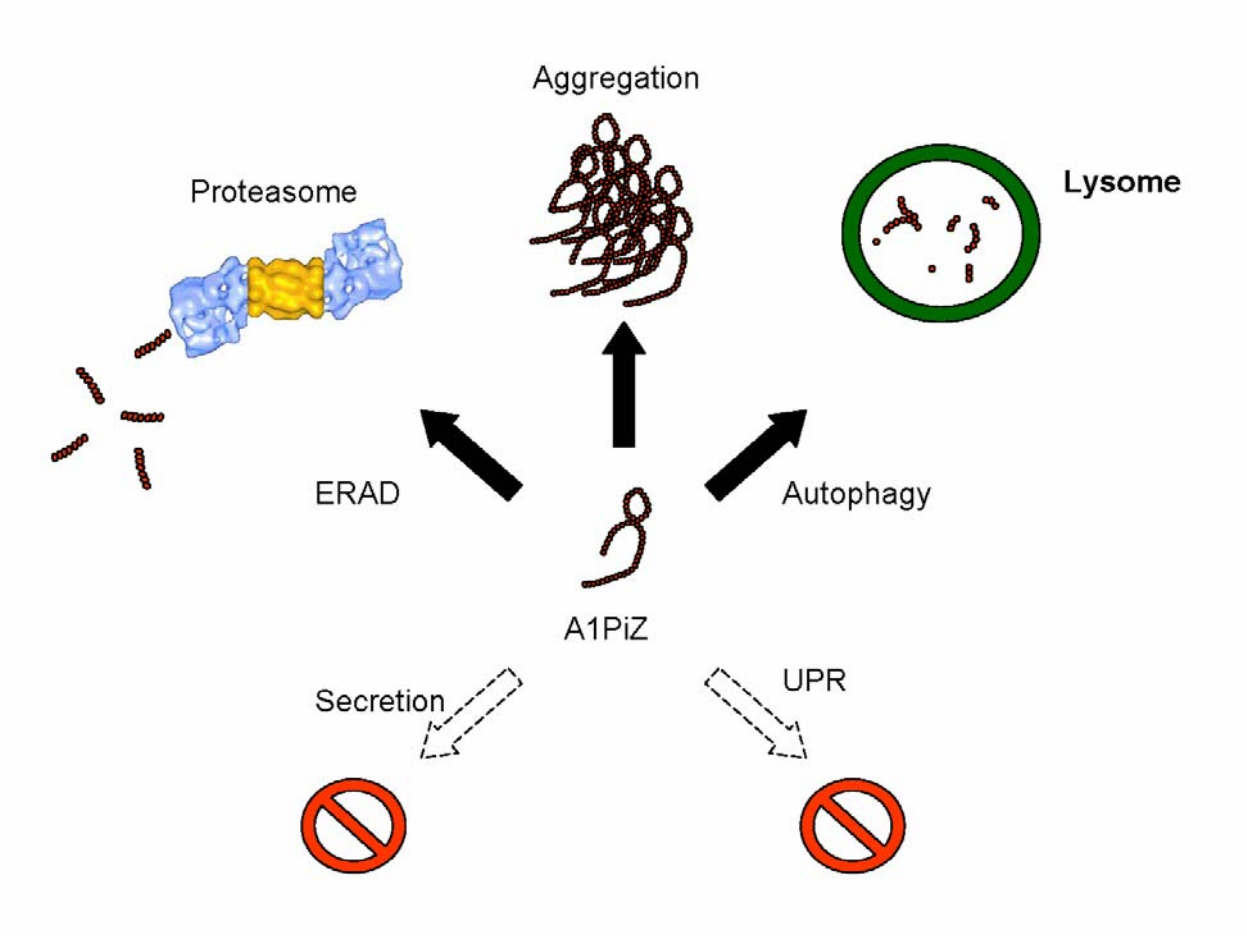

Figure 11. The fate of A1PiZ

(Van Molle *et al.*, 1997; Teckman and Perlmutter, 2000; Perlmutter, 2002). In addition, a portion of the aggregated protein is degraded by the lysosome via the autophagic pathway in mammals and in the vacuole of yeast (Teckman and Perlmutter, 2000; Kruse *et al.*, 2006). However, it is not completely clear whether mitochondrial dysfunction is the result of the autophagic response to ER retention of A1PiZ or arises from the UPR, which is known to induce apoptosis when chronically stimulated (Wang and Ron, 1996; Nakagawa *et al.*, 2000; Yoneda *et al.*, 2001). One can imagine that mitochondria are damaged nonspecifically by the autophagic response, which is activated to remove and subsequently degrade the aggregated mutant protein. But, the retention of this aberrant protein does not induce the UPR, even though A1PiZ is an ERAD substrate and soluble A1PiZ is degraded by the 26S proteasome in yeast and mammals (Qu *et al.*, 1996; Werner *et al.*, 1996). Therefore, A1PiZ ERAD or autophagy may lead to apoptosis. Overall, because of its unique attributes, it is likely that many proteins play a role in the removal of this mutant protein from the secretory pathway.

1.5.2 Antitrypsin degradation deficient (*ADD*) Genes

The Brodsky and McCracken laboratories wished to identify genes that affect the degradation of A1PiZ. This was accomplished utilizing both a classical genetic approach (McCracken *et al.*, 1996) as well as a targeted approach (Palmer *et al.*, 2003), and a class of genes termed antitrypsin degradation deficient (*ADD*) genes were identified. While many of these *ADD* genes have not been characterized for their roles in A1PiZ degradation, some have allowed valuable insights into the complex nature of quality control within the secretory pathway.

One of the genes isolated was *ATG6/VPS30/ADD3*, which is required for autophagy (Kametaka *et al.*, 1998). This gene was originally identified because of a slower degradation rate

of A1PiZ compared to wild type yeast strains (McCracken *et al.*, 1996; Palmer *et al.*, 2003). Mutations in this gene lead to compromised targeting of proteins to the vacuole via the autophagic pathway (Kruse *et al.*, 2006). Consistent with these data, yeast cells over-expressing A1PiZ, deliver the aggregated protein to the autophagic pathway (Kruse *et al.*, 2006), and autophagic vesicles are abundant in liver biopsies from individuals with late-stage ATD (Teckman and Perlmutter, 2000). In addition, A1PiZ-expressing autophagy-deficient cell lines degrade A1PiZ less efficiently than wild type cells (Kamimoto *et al.*, 2006). Taken together, this work demonstrates that A1PiZ degradation is linked to autophagy when expression levels are increased or the aberrant protein escapes ERAD.

Given that a subset of the genes that are the ultimate targets of the unfolded protein response are also required for ERAD (Ng *et al.*, 2000; Travers *et al.*, 2000), the Brodsky and McCracken lab examined yeast strains deleted for the targets of the UPR to determine if these genes had an effect on the degradation of A1PiZ (Palmer *et al.*, 2003). This targeted approached examined approximately 70 non-essential and uncharacterized yeast genes which had robust induction via the UPR (Casagrande *et al.*, 2000; Travers *et al.*, 2000). Utilizing a novel colony blot immunoassay screen, yeast strains lacking the gene of interest and expressing A1PiZ were examined and the level of A1PiZ accumulation was measured compared to wild type yeast strains (Palmer *et al.*, 2003 and Section 2.2.5 for details). A total of 6 *add* mutants were identified (Figure 12). *ADD66* was one of these six identified genes and its characterization is the focus of this dissertation.

1.5.3 Antitrypsin degradation deficient 66 (*ADD66*)

ADD66 (YKL206c) is predicted to encode a protein with a molecular mass of 30kDa. The initial

Figure 12. Identification of *ADD66*

A representative image of the colony blot immunoassay used to identify the *ADD* genes. In brief, yeast strains (1-73), deleted for the non-essential candidate genes and expressing A1PiZ were grown and spotted in duplicate on nitrocellulose paper and lysed *in situ*. The filters were then probed for antitrypsin using a colorimetric detection assay to identify yeast genes that had elevated levels of A1PiZ. The levels of A1PiZ accumulated in WT yeast strains expressing A1PiM (M), A1PiZ (Z), or containing an empty vector (O) were compared to the mutant yeast strains. The *add66Δ* samples have been highlighted by a red oval. Image obtained from Palmer *et al.*, 2003.

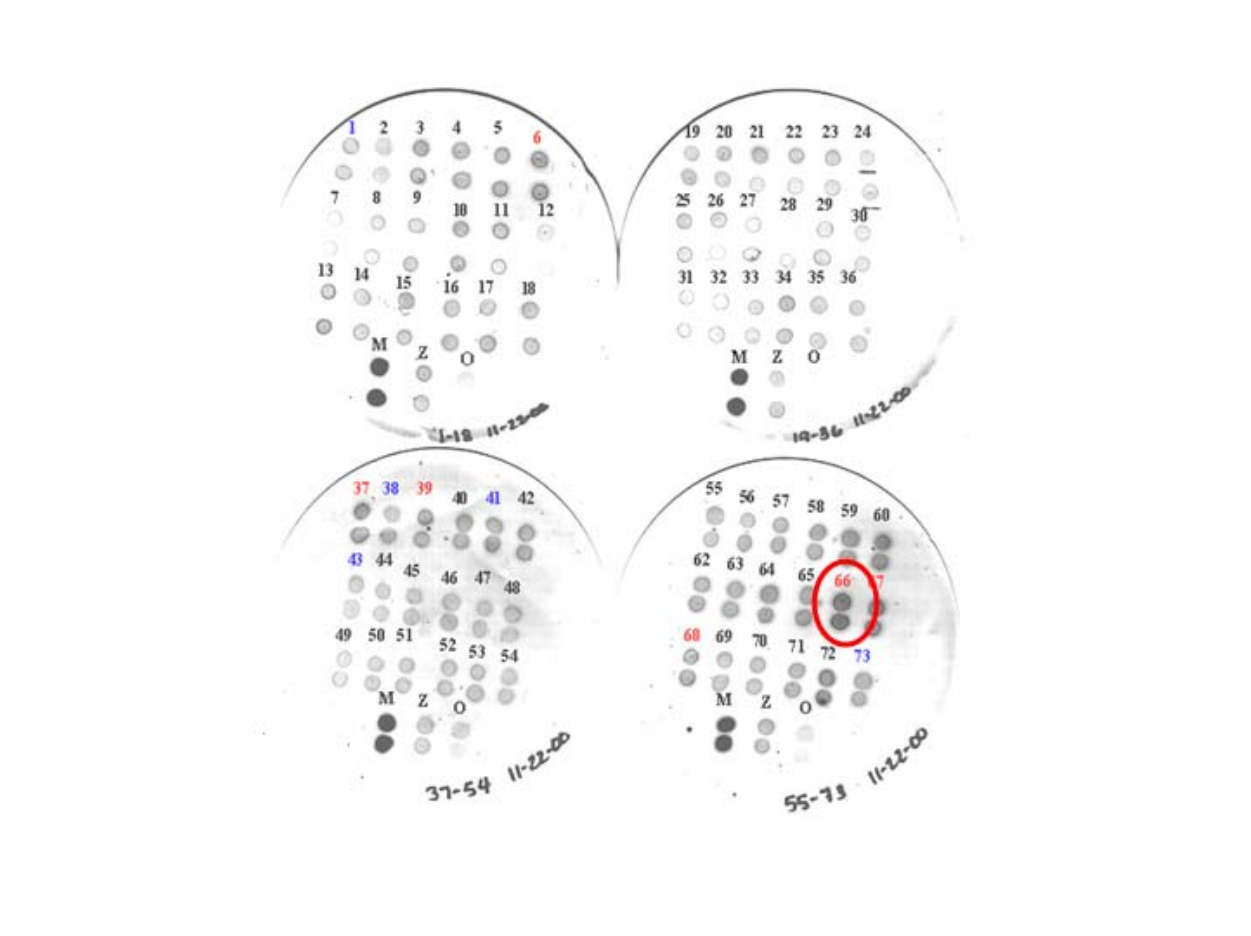

Figure 12. Identification of *ADD66*

analysis of *ADD66* demonstrated that the deletion of the gene caused an accumulation of A1PiZ and slowed the rate of degradation of A1PiZ (Figure 12 and Figure 13A), but the ERAD of other substrates such as the mutated form of carboxypeptidase (CPY*) was not affected (Figure 13B) (Palmer *et al.*, 2003). CPY* is a soluble ERAD substrate which requires BiP for its efficient degradation (Plemper *et al.*, 1997; Zhang *et al.*, 2001). The deletion of *ADD66* modestly slowed the degradation of CFTR, but had no effect on the degradation of pro-alpha factor, a yeast pheromone and another ERAD substrate (Palmer *et al.*, 2003). This supports the view that each ERAD substrate requires a unique set of factors for their degradation (Fewell *et al.*, 2001).

As detailed above, *ADD66* was a candidate for the colony blot assay because it is up-regulated by the UPR (Casagrande *et al.*, 2000; Travers *et al.*, 2000). Specifically, *ADD66* mRNA expression is increased 9.8 fold when cells were treated by tunicamycin, which inhibits *N*-linked glycosolation (Travers *et al.*, 2000). Furthermore, expression of mouse major histocompatability complex class I heavy chain (H-2K^b), a substrate for ERAD, led to a 2.5 fold increase of *ADD66* mRNA in yeast (Casagrande *et al.*, 2000). These data indicate that *ADD66* is a *bona fide* target of the UPR.

Global ERAD defects can lead to UPR induction due to the wide-spread accumulation of aberrant proteins within the ER (Fewell *et al.*, 2001). On the other hand, subtle or specific substrate ERAD defects might not be sufficient to induce a noticeable UPR. Interestingly, deletion of *ADD66* itself disrupted ER homeostasis in yeast significantly enough to cause a 3-fold increase in the UPR when compared to the isogenic wild type strain (Palmer *et al.*, 2003). Therefore, not only is *ADD66* a target of the UPR, but Add66p plays a significant role in minimizing ER stress.

Figure 13. Deletion of *ADD66* exhibits differential effect on the degradation of two ERAD substrates.

Pulse chase radiolabeling experiments were performed in the various *add* mutant strains characterized in Palmer, *et al.* 2003, and the results were compared to the isogenic wild type yeast strain. For simplicity, *ADD66* (blue) and *add66Δ* (red) are highlighted. (A) A1PiZ was immunoprecipitated from cell extracts at 0, 20, 40, 60 minutes and resolved by SDS PAGE. The relative amounts of A1PiZ were quantified and the amount of A1PiZ at 0 min was set to 100%. (B) CPY* was immunoprecipitated from cell extracts at 0, 20, 40, 60 minutes and resolved by SDS PAGE. The relative amounts of CPY* were quantified and the amount of CPY* at 0 min set to 100%. Results shown are the average of five independent experiments, +/- SD.

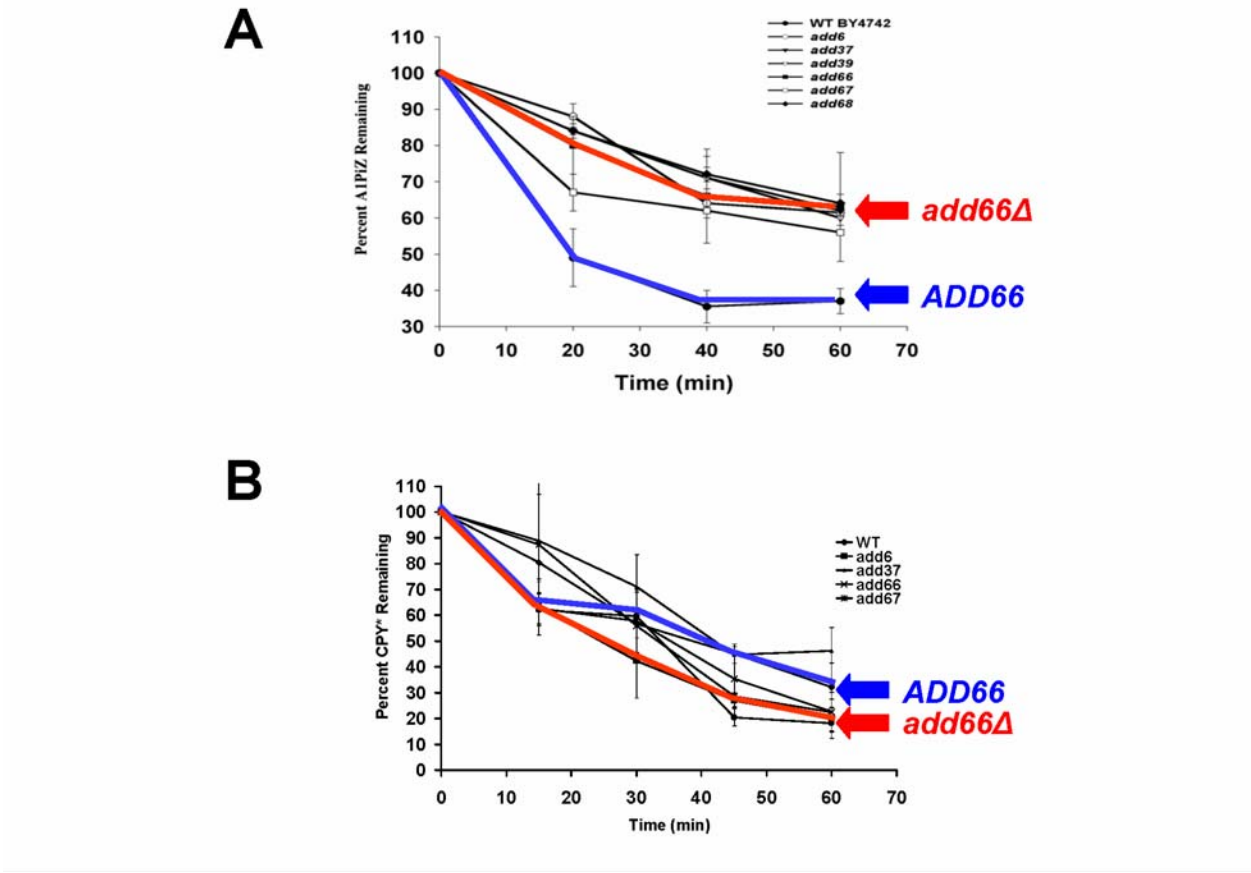

Figure 13. Deletion of *ADD66* exhibits differential effect on the degradation of two ERAD substrates

Overall, the initial studies of the putative functions of Add66p suggest that: [1] Add66p is required for the degradation of only a subset of ERAD substrates examined (Palmer *et al.*, 2003). [2] *ADD66* mRNA is induced by the UPR (Travers *et al.*, 2000). [3] Yeast cells deleted for *ADD66* induce the UPR (Palmer *et al.*, 2003). Because of these observations, I suggested that Add66p might play a more general role in ER protein quality control.

1.6 YEAST AS A MODEL ORGANISM

The yeast species *Saccharomyces cerevisiae,* also known as baker's or brewer's yeast*,* has been used in baking bread and fermenting alcoholic beverages for millennia. In the last century, it has become extremely important as a model organism in modern cell biology research, and is one of the most thoroughly researched eukaryotic microorganisms to date. Researchers utilize yeast as a model organism to gather information on the biology of the eukaryotic cell and ultimately human biology (Ostergaard *et al.*, 2000). For the purpose of this dissertation, the use of the yeast system is possible since many aspects of protein synthesis, trafficking, and degradation are conserved between yeast and mammals. Furthermore, *S. cerevisiae* was the first eukaryote to have its genome, consisting of 12 million base pairs and approximately 6,000 open reading frames sequenced (Williams, 1996). In addition, yeast can perform homologous recombination, allowing researchers to isolate, delete, or manipulate individual genes. Also, the budding yeast *Saccharomyces cerevisiae* offers a variety of genetic and biochemical tools enabling me to investigate the impact of protein regulation and degradation.

1.7 DISSERTATION OVERVIEW

Proteasome assembly and maturation is complicated and requires a panoply of different proteins to form one of the largest multi-subunit complexes within the eukaryotic cell (Voges *et al.*, 1999). This choreographed assembly would not be possible without the assistance of a class of proteins recently termed proteasome assembly factors (Heinemeyer *et al.*, 1997; Ramos *et al.*, 1998; Tone and Toh, 2002; Hirano *et al.*, 2005; Hirano *et al.*, 2006; Li *et al.*, 2007). Only a few proteins have been identified as PACS in yeast and mammals (Yeast: Ump1p and Nob1p; Mammals: Pomp1, PAC1, PAC2, and PAC3). While the recent identification of these PACs has provided some insights into the order of assembly and regulation of maturation, it is difficult to believe that these few PACs represent the complete list of proteasome assembly chaperones.

In this work, I discuss the further characterization of the Add66p protein and determine its cellular function. Specifically, I show that Add66p is a *bona fide* PAC and is required for maximal proteasome activity. This work complements earlier studies on Add66p and explains why the deletion of *ADD66* affects the clearance of some but not all ERAD substrates. Finally, my examination of Add66p is strengthened by recently published work from the Hochstrasser lab that suggests that Add66p (named Pba2p by that group) is involved in early CP assembly (Li *et al.*, 2007).

2.0 CHARACTERIZATION OF *ADD66* AND ITS ROLE IN PROTEASOME ASSEMBLY AND MATURATION

2.1 INTRODUCTION

Newly synthesized secreted proteins must pass a stringent quality control check-point in the endoplasmic reticulum (ER), which ensures that only properly folded, assembled, and processed proteins transit the secretory pathway (Ellgaard and Helenius, 2003). Polypeptides that fail to pass this check-point may be targeted for ER associated degradation (ERAD), a process in which aberrant proteins are selected and then delivered—or retro-translocated—to the cytoplasm and degraded by the 26S proteasome (Fewell *et al.*, 2001; Tsai *et al.*, 2002; Kostova and Wolf, 2003; Meusser *et al.*, 2005; Romisch, 2005; Sayeed and Ng, 2005; Nandi *et al.*, 2006). The 26S proteasome is an ~2.5 MDa multi-subunit complex that contains a central 20S proteolytic core particle and two 19S regulatory particles (Voges *et al.*, 1999; Nandi *et al.*, 2006). The 20S core harbors three distinct proteolytic activities—a chymotrypsin-like (CTL), a trypsin-like (TL), and a peptidylglutamyl-peptide hydrolyzing (PGPH) activity—whereas the 19S "cap" (also known as PA700) functions as a gate-keeper at the entrance of the core particle. In addition, the 19S particle contains polyubiquitin-binding subunits, enzymes required for polypeptide de-ubiquitination, and 6 AAA ATPases that are thought to unfold and feed polypeptides into the

core (Glickman *et al.*, 1998; Voges *et al.*, 1999; Leggett *et al.*, 2002; Verma *et al.*, 2002; Guterman and Glickman, 2004; Soboleva and Baker, 2004).

Some ERAD substrates in humans are mutated versions of wild type proteins. Not surprisingly, the absence of these functional proteins may lead to the onset of specific diseases (Aridor and Hannan, 2000, 2002; Coughlan and Brodsky, 2003). One substrate in which the connection between ERAD and loss-of-function disease is quite clear is the Z-variant of alpha-1-antitrypsin, also known as A1PiZ (or alpha-1 protease inhibitor, Z). Wild type A1Pi, originally termed the "M" variant or A1PiM (Myerowitz *et al.*, 1972), is an ~53 kDa serine protease inhibitor that is primarily synthesized in and secreted by hepatocytes (Perlmutter, 2002). Serum A1Pi inhibits neutrophil proteases, which are released during inflammatory responses and can mediate proteolysis of the pulmonary connective tissue matrix (Richmond and Zellner, 2005; Rudnick and Perlmutter, 2005). Although secreted A1PiZ retains partial activity, individuals expressing this protein have lower circulating levels of the protein because the E342K mutation compromises its folding in the ER. The subsquent decrease in plasma levels of the protease inhibitor lead to antitrypsin deficiency (ATD), which is exemplified by uninhibited neutrophil elastase activity and destruction of the pulmonary extracellular matrix. However, when the A1PiZ variant accumulates, it can form loop-sheet polymers or aggregates that may trigger cirrhosis (Foreman *et al.*, 1984; Perlmutter *et al.*, 1985; Mornex *et al.*, 1986; Verbanac and Heath, 1986; Brantly *et al.*, 1988; McCracken *et al.*, 1989; Lomas *et al.*, 1992; Mast *et al.*, 1992; Kim *et al.*, 1995; Sidhar *et al.*, 1995; Carrell and Lomas, 2002; Parfrey *et al.*, 2003) and hepatocellular carcinoma (Carlson *et al.*, 1989; Rudnick and Perlmutter, 2005). Thus, ATD is also a gain-of-function disease.

Interestingly, only ~10% of *A1PiZ*-homozygotes develop liver disease (Sveger, 1988).

Although the reason for this remains a mystery, this phenomenon may arise because a subset of individuals is unable to efficiently clear this aggregation-prone molecule from the ER. Indeed, A1PiZ-expressing fibroblasts from individuals with liver disease degrade the substrate less efficiently than A1PiZ-expressing fibroblasts from healthy homozygotes (Wu *et al.*, 1994). Therefore, factors that alter the efficiency of A1PiZ ERAD may represent genetic modifiers of ATD.

To identify putative ATD modifiers, the Brodsky and McCracken labs developed an A1PiZ yeast expression system (McCracken and Kruse, 1993) because: [1] Components of the protein quality control machinery are highly conserved, and [2] yeast expression systems for several human disease-causing proteins have led to a better understanding of the pathological consequences of aberrant protein production (Coughlan and Brodsky, 2003). Notably, the A1PiZ yeast expression system helped establish this protein as a *bona fide* ERAD substrate (Werner *et al.*, 1996) and identified an Hsp70 molecular chaperone in the lumen of the ER, known as BiP, as an important player in A1PiZ clearance (Brodsky *et al.*, 1999). This result was subsequently confirmed in mammalian cells (Cabral *et al.*, 2002; Schmidt and Perlmutter, 2005). The Brodsky and McCracken labs also identified antitrypsin degradation deficient (*ADD*) mutants using both a classical genetic (McCracken *et al.*, 1996) and a targeted approach (Palmer *et al.*, 2003). One of the genes isolated was *ATG6/VPS30*, which is required for autophagy (Kametaka *et al.*, 1998), and yeast over-expressing A1PiZ deliver the aggregated protein to the autophagic pathway (Kruse *et al.*, 2006). Similarly, autophagic vesicles are abundant in liver biopsies from individuals with late-stage ATD (Teckman and Perlmutter, 2000) and A1PiZ-expressing autophagy-deficient cell lines degrade A1PiZ less efficiently than wild type cells (Kamimoto *et al.*, 2006).

Another yeast gene that was isolated is *ADD66* (YKL206c). Even though Add66p is required for the degradation of only a subset of ERAD substrates examined (Palmer *et al.*, 2003), the *ADD66* transcript is induced by the Unfold Protein Response (UPR) (Travers *et al.*, 2000), which serves as an indicator of ER stress; moreover, the UPR and ERAD provide complementary mechanisms to lessen the effects of aberrant protein accumulation in the ER (Fewell *et al.*, 2001; Patil and Walter, 2001; Schroder and Kaufman, 2005). Because of these observations, and because cells deleted for *ADD66* also induce the UPR (Palmer *et al.*, 2003), I examined the hypothesis that Add66p might play a more general role in ER protein quality control.

Here, I report that Add66p facilitates the maturation of the 20S proteasome particle, is vital for maximal proteasome activity, and like some other proteasome chaperones (Ramos *et al.*, 1998; Tone and Toh, 2002; Hirano *et al.*, 2005) is a substrate for proteasome-mediated degradation. Based on these results and on the sequence similarity between *ADD66* and the mammalian proteasome assembly chaperone-2 (PAC2) (Hirano *et al.*, 2005; Hirano *et al.*, 2006), I propose that the *S. cerevisiae* Add66p and PAC2 share similar functions. Together, these results provide the first direct link between PAC activity and ERAD.

2.2 MATERIALS AND METHODS

2.2.1 Strains and growth conditions

The *E. coli* strain used in this study was DH5α (*endA1 hsdR17 supE44 thi-1 recA1 gyrA relA1* Δ [*lacZYA-argF*] *U169 deoR* [Φ80 *dlac* Δ *lacZ M15*]). Bacteria were grown in Luria-Bertani (LB) medium supplemented with ampicillin (50 μg/ml) for plasmid selection. An *add66Δ* disruption cassette was obtained by amplifying pRS400 (Brachmann *et al.*, 1998) with the following oligonucleotides: 5' ACT TCA GGA AAG AAT AGC ACA AAA CCC AAA GGA ACA TAC GCT GTG CGG TAT TTC ACA CCG 3' and 5' ATA TAT GCA CTT GTA TAG AAA ACA GAT ATA CTT CTC GGT TAG ATT GTA CTG AGA GTG CAC. *ADD66* mutants were obtained as previously described (Brachmann *et al.*, 1998). A *pdr5Δ* haploid strain was isolated by sporulation and dissection of the yeast *pdr5Δ* homozygous diploid (Invitrogen). All other yeast strains used in this study are detailed in Table 2 located in Appendix A and were grown on yeast extract-peptone (YP)-dextrose (YPD) medium or on synthetic complete (SC) medium lacking the indicated nutrient but supplemented with a carbohydrate source to a final concentration of 2% with or without the addition of the various indicated chemicals (Table 1). Yeast were grown at the indicated temperatures and all genetic and molecular manipulations followed standard published protocols (Adams *et al.*, 1997).

2.2.2 Detection of polyubiquitinated proteins in yeast

Yeast were transformed with a plasmid engineered for the expression of a ubiquitin-*myc* fusion protein under the transcriptional control of a copper inducible promoter ((Ecker *et al.*, 1987); sub-cloned and provided by A. Caplan, Mount Sinai School of Medicine), and transformants were isolated on selective medium (SC-*HIS*) containing glucose. A culture containing 20 ODs (optical density measured at 600 nm) of cells was grown to mid-log phase (~1.0 OD per ml) at 30°C before $CuSO_4$ was added at a final concentration of 100 μM and the cells were incubated for 1 h. The yeast were harvested and re-suspended in 100 μl of sample buffer (1.0% beta-mercaptoethanol, 1% SDS, 5% glycerol, 0.05 mg/ml bromophenol blue, 65 mM Tris, pH 6.8), 0.2 g of glass beads were added, and lystates were prepared by vigorous agitation on a Vortex mixer ten times for 1 min with a 1 min incubation in an ice bath between each treatment. The total protein in a 5 μl aliquot of each sample was resolved by SDS-PAGE and transferred onto nitrocellulose blots. The nitrocellulose was incubated for 30 min, while sandwiched in Whatman filter paper, in boiling double-distilled de-ionized water. Ubiquitin and Sec61p, a component of the translocon that served as a loading control, were identified by western blotting using anti-*myc* (kindly provided by G. Apodaca and O. Weisz, University of Pittsburgh School of Medicine) and anti-Sec61p (Stirling *et al.*, 1992). Western blots were developed using Enhanced Chemiluminescence (Pierce) according to the manufacturer's instructions. Images were obtained on a Kodak 440CF Image Station and the results were quantified using Kodak 1D (version 3.6) imaging software.

2.2.3 Expression of wild type and the Z variant of alpha-1-antitrypsin, PAC2, and

epitope-tagged Add66p

Yeast were transformed with plasmids containing the genes encoding A1PiM or A1PiZ under the transcriptional control of a galactose inducible promoter (McCracken *et al.*, 1996) and transformants were isolated on selective medium (SC-*URA*) containing glucose. As a control, the indicated strains were also transformed with the pYES2 vector (Invitrogen) lacking an insert.

To create an epitope-tagged version of Add66p, a single *myc* epitope was appended onto the *C*-terminus of Add66p by PCR amplification of genomic yeast DNA with the following oligonucleotides: 5' CGC GGA TCC ATG AGC TGC CTG GTG TTG 3' (to construct the pGPD vectors, see below) or 5' CGC GGA TCC TCC TCG ATT TGA CTG GAA AC 3' (to construct the pRS vector) and 5' CCC AAG CTT TCA CAG GTC CTC CTC TGA GAT CAG CTT CTG CTC CTC ATT GTA TAA ATC TAC AAA TTT ATC TCT TGC 3' (the underlined portion encodes the 11 amino acid *myc* epitope (Evan *et al.*, 1985)). The PCR fragment was inserted into the *Bam*H1 and *Cla*I sites in the pPRS315, pGPD425, and pGPD426 vectors (Sikorski and Hieter, 1989; Mumberg *et al.*, 1995) and the in-frame insertion and integrity of *ADD66* were confirmed by DNA sequence analysis. The corresponding vectors or the vectors lacking an insert were introduced into the indicated strains and transformants were isolated on selective media. Next, yeast were grown to mid-log phase, 2.0 ODs of cells were harvested, and total cell extracts were prepared as previously published (Brodsky *et al.*, 1998). Add66p-*myc* expression was assessed after SDS-PAGE by western blotting, as described above, using anti-serum against *myc*.

To create a mammalian PAC2 expression vector, I obtained PAC2 cDNA maintained in a Bluescript expression vector (Stratagene) which was received from Dr. Jiyang O-Wang (Riken Yokohama Institute, Japan). The PAC2 cDNA is similar to the one reported previously, but with

a shortened 5' UTR (Bahar *et al.*, 2002). The PAC2 cDNA insert was excised from the Bluescript vector and inserted at the same sites into a pcDNA 3.0 (Invitrogen) vector at the *Xho1* and *EcoR1* restriction sites. The in-frame insertion and integrity of *ADD66* were confirmed by DNA sequence analysis.

2.2.4 A yeast colony blot assay for A1PiZ accumulation

A colony blot immunoassay was performed to assess A1PiZ levels in wild type and select mutant yeast as previously described (Palmer *et al.*, 2003). In brief, 3 µl (0.001 OD) of cells from a saturated culture were spotted onto nitrocellulose that had been overlaid onto selective medium containing 2% galactose to induce expression of A1PiZ. After a 36 h incubation at 35°C, the cells were lysed. A1Pi was detected by immunoblotting and the results were quantified using the Molecular Analyst program (Bio-Rad). The signals corresponded to cell and protein levels in the linear range of detection. Previous work established the validity of using the colony blotting protocol as a means to report on AiPiZ turn-over in wild type and the *add66Δ* mutant (Palmer *et al*., 2003).

2.2.5 Add66p localization

The residence of Add66p-*myc* was assessed by biochemical fractionation using a previously published method, with minor modifications (Kabani *et al.*, 2002). Specifically, detection of Add66p-*myc* by western blotting required 1000 ODs of mid-log phase yeast that contained the

pGPD425-Add66p-*myc* expression vector and that had been grown at 30°C.

To assess Add66p-*myc* localization by indirect immunofluorescence (IF) microscopy, a previously described protocol was used (Coughlan *et al.*, 2004) employing yeast containing either the Add66p-*myc* expression vector under the transcriptional control of a constitutive promoter (pGPD) or the vector lacking an insert (as a negative control). Images were captured on an Olympus BX60 microscope fitted with a Hamamatsu C4742-95 digital camera and were analyzed using QED Imaging software (Pittsburgh, PA).

2.2.6 Purification of yeast 26S proteasomes

FLAG-tagged 26S proteasomes were purified from RJD1144 as described (Verma *et al.*, 2000; Saeki *et al.*, 2005; Verma and Deshaies, 2005) with minor modifications. In brief, cells were grown to an OD of ~3, frozen in liquid nitrogen and ground in a Waring blender. The ground powder (~20 ml) was thawed with 9 ml of lysis buffer (50 mM Tris pH 7.5, 150 mM NaCl, 10% glycerol, 5 mM $MgCl_2$) plus 5 mM ATP, 2x ATP regenerating system (0.02 mg/ml creatine phophokinase, 20 mM creatine phosphate), 5 mM $MgCl_2$ and 1 mM DTT. After centrifugation at 15,000 rpm for 20 min at 4˚C in a Sorvall SS34 rotor, the supernatant (~13 ml) was supplemented with 5 mM ATP, 2x ATP regenerating system and 5 mM $MgCl_2$, and incubated with 300 µl of 50% (v/v) washed FLAG agarose beads (Sigma) at 4˚C for 1.5 h with rocking. The agarose beads were washed twice with 10 ml of lysis buffer plus 2 mM ATP and 1 mM DTT, once with 5 ml of lysis buffer plus 2 mM ATP, 1 mM DTT and 0.2% TritonX-100, once with 5 ml of lysis buffer plus 2 mM ATP and 1 mM DTT, once with 800 µl of lysis buffer plus 2 mM ATP and 1 mM DTT, and once with 1 ml of 26S elution buffer (25 mM Tris pH 7.5, 10 mM

$MgCl_2$, 150 mM NaCl, 15% glycerol) plus 2 mM ATP. The bound proteins were eluted with 400 µl of 26S elution buffer plus 2 mM ATP supplemented with 1/50 volume of 5 mg/ml 3xFLAG peptide (DYKDDDDK (Biotechnology Center, University of Pittsburgh)) by incubating for 3 h at 4˚C with rocking. The eluted proteasomes were enriched to ~0.9 mg/ml using a Centricon-30 micro-concentrator and stored at -80°C.

2.2.7 Proteasome activity assays and glycerol gradient analysis

Proteasome activity was assessed in clarified yeast cytosols that were obtained from 2 l of the indicated strains grown in selective medium to mid-log phase at 30 °C. The cell pellet was washed with water and re-suspended in 500 µl of Buffer 88 (20 mM HEPES pH 6.8, 150 mM KOAc, 5 mM MgOAc, 250 mM sorbitol), and the cell-slurry was frozen in liquid nitrogen. Frozen cells were lysed by grinding with a mortar-and-pestle in the presence of liquid nitrogen for 12 min and the cells were thawed in the presence of a minimal amount of Buffer 88 containing 1 mM DTT. Unbroken cells and debris were removed by centrifugation in a Sorvall SS34 rotor at 9,000x*g* for 10 min at 4 °C, and the supernatant was clarified by centrifugation at 300,000x*g* for 1 h at 4 °C. The clarified cytosol was then aliquoted and snap-frozen in liquid nitrogen and stored at -80 °C. Total protein was quantified using the Bio-Rad protein assay kit with bovine serum albumin (BSA) as a standard.

Proteasome activity was determined by modifying a previously described protocol (Glickman *et al.*, 1998). First, a total of 100 µg of clarified cytosol was diluted into 1.8 ml of Buffer A (50 mM Tris-HCl pH 7.4, 5 mM $MgCl_2$, 10% glycerol, 1 mM ATP, 1 mM DTT) and incubated on ice for 30 min in either the presence or absence of 100 µM MG-132 or leupeptin.

Next, a fluorescent substrate to detect each proteasome activity (CTL: Suc-LLVY-AMC [Sigma], TL: Cbz-AAR-AMC [Cal BioChem], PGPH: Cbz-LLE-AMC [Cal BioChem]) was added to a final concentration of 100 μM and the reactions were shifted to 30°C for the indicated time points and quenched by the addition of 1% SDS (final concentration). Where noted, a total of 0.5 μg of purified 26S proteasomes were utilized and treated identically. Fluorescence was determined on an Aminco-Bowman Series 2 Luminescence Spectrometer (excitation: 380 nm; emission: 436 nm). The CTL, TL, and PGPH activities were confirmed using the following inhibitors at a final concentration of 100 μM: MG-132 (for CTL and PGPH) and leupeptin (for TL) (Savory and Rivett, 1993; Gaczynska and Osmulski, 2005). The activity in each reaction and at each time point was obtained after the background fluorescence in the presence of each inhibitor was subtracted from the net fluorescence. When extracts were examined, the data were then normalized to the activities observed in lysates from the reaction containing 400 μg of cytosol (Figure 18) or 100 μg (Figure 19) of the respective isogenic wild type strains at reaction times of 10 min for the CTL activity, and at 60 min for the TL and PGPH activities. When highly enriched proteasomes were examined, the data were normalized to the activities observed in the absence of inhibitors at 180 min (Figure 19, third column), and when lysates were examined in this figure (Figure 19, first and second columns) the CTL, TL, and PGPH activities were normalized to the wild type activities observed at 180 min in the absence of inhibitors. Maximal, normalized activities are denoted as 100%.

To assess the integrity of the proteasome using glycerol gradient centrifugation, the indicated cells expressing Add66p-*myc* under its endogenous promoter (Figure 26), an over-expressing constitutive promoter (Figure 27), or an expression vector lacking an insert were grown in SC-*LEU* and 2% glucose at 30°C. A total of 100 ODs of mid-log phase cells were

harvested and washed once with water and resuspended in 2 ml of Buffer A lacking glycerol. (The *pdr5Δ* strain was incubated with 100 μg of MG132 for 1 h at 30°C prior to harvesting.) Cells were lysed as above and unbroken cells were removed by centrifugation in a Sorvall SS34 rotor at 9,000x*g* for 30 min at 4°C. Extracted proteins (5 mg total, as assessed using the Bio-Rad protein assay kit with BSA as the standard) were fractionated on a 30 ml 4-25% linear glycerol gradient in an SW28 rotor (Beckman) at 83,000x*g* for 24 h at 4 °C. Molecular mass markers (Sigma) were examined in parallel. One ml fractions were removed and the refractive index was examined to verify the establishment of a linear gradient. Fractionated proteins were precipitated with trichloroacetic acid (TCA: 25% final concentration) and were resolved by SDS-PAGE and analyzed as above by western blotting with anti-*myc*, anti-20S (BioMol), anti-HA (Roche Molecular Biochemicals), and anti-Cim5p (Ghislain *et al.*, 1993) anti-sera.

2.2.8 Non-denaturing PAGE proteasome activity assay

A non-denaturing PAGE proteasome activity assay was slightly modified from a previously described method (Glickman *et al.*, 1998). In brief, 100 μg of clarified cytosol or 1 μg of purified 26S and 20S proteasomes were resolved on a non-denaturing single layer gel (0.18 M Tris-borate (pH 8.3), 5 mg $MgCl_2$, 1mM ATP, 1mM DTT, and 4% acrylamide-bisacrrylamide (37:5:1 ratio)). The running buffer was the same as the gel buffer but lacked acrylamide. Xylene cyanol was added to the samples prior to loading onto the gels. The samples were resolved at 150mV at 4°C for approximately 2 h, allowing the xylene cyanol to run off. The gel was then incubated in 10 ml of 0.1 mM Suc-LLVY-AMC in buffer A (Section 2.2.7) for 10 min at 30°C. Bands corresponding to the cleaved fluorescent substrate were visualized via the Kodak 440CF Image Station when exposed to UV light (~360-380 nM wavelength).

2.2.9 Add66p-*myc* degradation assay

The *pdr5Δ* yeast strain expressing Add66p-*myc* was grown in SC-*LEU* to mid-log phase at 30°C and protein synthesis was arrested by the addition of cycloheximide to a final concentration of 100 µg/ml. Four ODs of cells were removed at the indicated time points. The cells were washed, and total protein was isolated by glass bead lysis as detailed above. Proteins were resolved on either 12.5% or 18% polyacrylamide gels under denaturing conditions, and analyzed and quantified as above by western blotting with anti-*myc* and anti-Sec61p anti-sera.

2.2.10 Induction of autophagy

The indicated strains were grown overnight in YPD and 2.5 ODs of cells were diluted into 10 ml of rich medium (YP with 2% galactose) or nitrogen-depleted media (SC lacking ammonium sulfate but supplemented with 2% galactose) to induce autophagy. After incubation for 5 h at 30°C, equal numbers of cells were harvested and lysates were prepared by glass bead lysis as described above. Equal amounts of protein (as assessed above) in each sample were resolved by SDS-PAGE and analyzed by western blotting using anti-Ape1p (Santa Cruz Biotechnology) and anti-Sec61p anti-sera.

2.2.11 A1PiZ degradation assay in a genetically engineered mammalian cell line

In collaboration with the Perlmutter laboratory, the HTO/Z cell line (HeLa cells with inducible expression of A1PiZ (Teckman *et al.*, 2001) was transiently transfected with constructs

engineered for the expression of PAC2 (pcDNA 3.0) or GFP (pCMV (Invitrogen)) using Superfect (Qiagen) and the manufacturer's recommendations. Twenty-four hours after transfection, the cells were harvested and homogenized by 12 passages through an 18 gauge needle in 10 mM Tris, pH 7.4, 1 mM EDTA, 150 mM NaCl, 0.5% NP40, 2 mM PMSF. The homogenate was centrifuged to remove the insoluble material. Total proteins in the soluble homogenate were then resolved by SDS-PAGE and subjected to western blot analysis by probing for A1PiZ (Diasorin), GFP (Abcam), or GADPH (US Biological).

2.2.12 Radiolabeling, immunoprecipitation and phosphorimaging

To assay A1PiZ expression, a previously published procedure was modified (Brodsky *et al.*, 1998). In brief, yeast strains were grown over night at 30°C on selective solid medium containing 2% glucose. A total of 20 OD_{600} cells were scraped from the plates using 4 ml of sterile water and switched to liquid selective medium lacking cysteine and methionine but containing 2% galactose to induce expression of A1PiZ. Cells were immediately pulsed with 200 μCi/ml of ^{35}S-Easy Tag (NEN) and grown for 2 h at 30°C with vigorous shaking. After this time, samples were harvested after the 2 h incubation. Cell lysis and immunoprecipitation were performed as described (Brodsky *et al.*, 1998) using antibodies against A1Pi (Rockland) and BiP and eluted off Protein A sepharose (GE Healthcare). Proteins were resolved by SDS-PAGE and visualized using a BAS-2500 (Fuji). Quantification was performed using ImageGuage version 3.45 (Fuji).

2.3 RESULTS

2.3.1 Pleiotropic phenotypes associated with *add66Δ*

Growth phenotypes associated with mutations are one of the most basic tools of genetic analysis since a particular phenotype or a set of phenotypes can suggest a function for the corresponding gene product. Therefore, a series of initial growth assays were performed comparing the wild type and mutant *ADD66* strains in the presence of various temperatures and chemicals. First, wild type cells and the *add66Δ* mutant strain were incubated on a variety of different growth media supplemented with various carbohydrate sources (Table 1). No detectable differences were observed. Second, exposure to media supplemented with different chemical compounds yielded no visible growth defects in the *add66Δ* strains relative to the wild type strain. Finally, the wild type and mutant *ADD66* strains grew identically when incubated at different temperatures (15, 26, 30, 35, and 37° C). Furthermore, additive or synergistic effects of media supplemented with different chemicals or carbohydrates, in addition to incubation at elevated temperatures, yielded no visible growth defects for the mutant strain. Many of these compounds have been linked to specific biochemical pathways; ideally, then any observed growth defects would indicate a relationship to a specific biochemical pathway (Hampsey, 1997).

Table 1. Growth Conditions and Associated Biochemical Pathways

Growth Condition	Associated Biochemical Pathway	Growth Condition	Associated Biochemical Pathway	Growth Condition	Associated Biochemical Pathway
YP Raf	Raffinose fermentation	YP Suc	sucrose fermentation	YP Gal	galactose fermentation
YP Gly	general respiration	8 mM DTT	ER protein folding	- Inositol	general transcription
15 nM Caffeine	MAP kinase pathway	Various Salt Conditions and Concentrations	osmotic sensitivity	Sorbitol	osmotic sensitivity
Hydroxyurea	nucleic acid metabolism	15 μM $CdCl_2$	general protein folding and/or proteasome		

2.3.2 Genetic interactions between *ADD66* and *IRE1*, a transducer of the Unfolded Protein Response (UPR)

The Brodsky and McCracken labs previously reported on the identification of UPR-target genes in yeast that, when deleted, result in A1PiZ stabilization (Palmer *et al.*, 2003). In turn, the deletion of one gene, *ADD66*, induced the UPR, suggesting that the corresponding protein might be involved in more general aspects of ER quality control. Therefore, I wished to examine the possible connection between Add66p and the UPR pathway. As a control, one strain lacked Ire1p, an ER-resident transmembrane protein that senses a rise in the concentration of misfolded ER lumenal proteins and initiates the transcription of genes whose products lessen ER stress (Cox *et al.*, 1993; Mori *et al.*, 1993; Shamu and Walter, 1996; Credle *et al.*, 2005; Zhou *et al.*, 2006). The *ire1Δ* strain was examined along with *add66Δ* yeast and an *ire1Δadd66Δ* strain. These cells, as well as an isogenic wild type strain (see Table 2 located in Appendix A) were transformed with either a control plasmid or with a plasmid that expresses a ubiquitin-*myc* fusion protein under the transcriptional control of a copper inducible promoter. As shown in Figure 14A (right half of figure), I first observed that strains lacking Add66p showed a modest increase in polyubiquitinated proteins compared to the *ADD66* strain (~2-fold in this experiment), and yeast deleted for *IRE1*—regardless of whether *ADD66* was present—accumulated somewhat greater amounts of polyubiquitinated protein. Though in another experiment, I found a more robust increase in polyubiquitinated proteins in the *add66* deletion strain when compared to the *ADD66* strain (~5-fold in this experiment (Figure 14B). Furthermore, I noted that yeast lacking both *ADD66* and *IRE1* exhibited a strong, synthetic growth defect when incubated on media

Figure 14. *ADD6* and *IRE1* synthetically interact.

ADD66, *add66Δ, ire1Δ* and *ire1Δ add66Δ* strains were transformed with a control plasmid or a plasmid expressing a ubiquitin-*myc* fusion protein under the transcriptional control of a copper inducible promoter ("pCu Ub*myc*"). (A) Representative western blots of extracts from cells containing a vector control or the ubiquitin expression vector are shown. Extracts were prepared after cells had been treated with 100 μM $CuSO_4$ for 1 h at 30°C. Blots were probed with anti-*myc* and anti-Sec61p (as a loading control). (B) A second representative western blot of extracts from cells containing a vector control or the ubiquitin expression vector is shown. Extracts were prepared after cells had been treated with 100 μM $CuSO_4$ for 1 h at 30°C. Blots were probed with anti-*myc* and anti-Sec61p (as a loading control). (C) Serial dilutions of the indicated strains (see Table 2 located in Appendix A) were grown on YPD in the presence or absence of 8 mM DTT, as indicated, for 48 h at 30°C. Of note, I chose to examine DTT-sensitivity on YPD media at pH 6.5 to reduce alternate stresses, although previously published work demonstrated a greater sensitivity to DTT in the *ire1Δ* strain when grown using other conditions (Frand and Kaiser, 1998; Pollard *et al.*, 1998).

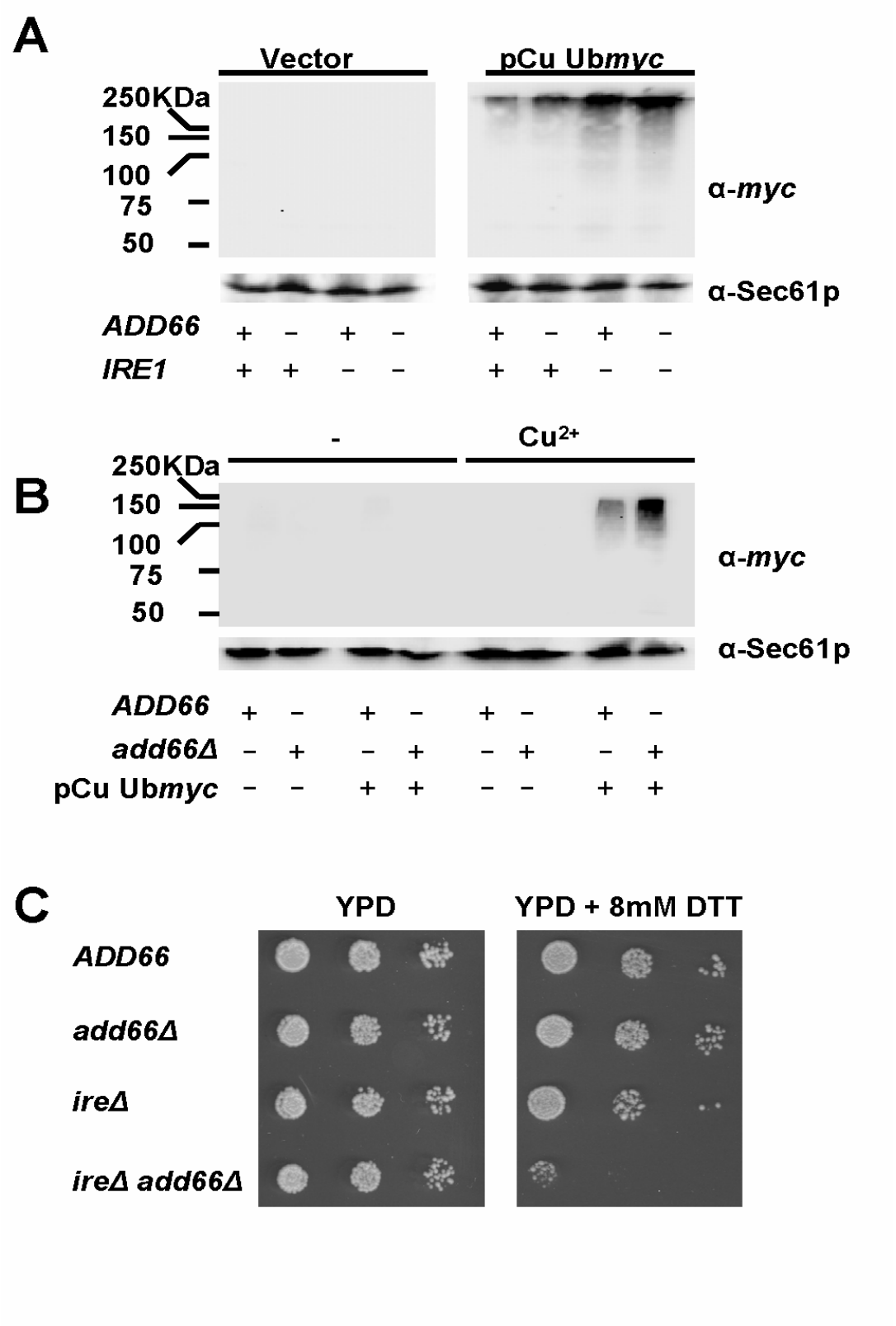

Figure 14. ***ADD6*** **and** ***IRE1*** **synthetically interact**

containing DTT, a reducing agent that induces the UPR (Figure 14C). These data support the hypothesis that Add66p plays a role in the turnover of polyubiquitinated proteins and ER quality control, and are consistent with reports indicating that mutations in genes required for both ERAD and the UPR exhibit synthetic phenotypes (Ng *et al.*, 2000; Travers *et al.*, 2000).

In recently published work, autophagy has been shown to play a significant role in mediating A1PiZ degradation in yeast, mammalian cell culture, and mouse models (Teckman and Perlmutter, 2000; Kamimoto *et al.*, 2006; Kruse *et al.*, 2006). Therefore, it was possible that deletion of *ADD66* leads to the accumulation of A1PiZ and exhibits synthetic interactions with *IRE1* because the autophagic pathway, which is induced by ER stress (Bernales *et al.*, 2006; He *et al.*, 2006; Ogata *et al.*, 2006), is compromised. To examine this hypothesis, the maturation of Ape1p, a protease that is targeted to the vacuole during autophagy, was assessed in both *ADD66* and *add66Δ* strains and in a well-characterized autophagy-deficient strain, *atg14Δ* (Kametaka *et al*., 1998). As Ape1p enters the vacuole it is proteolytically cleaved, and thus the conversion of immature-Ape1p ("pre-Ape1p") to mature Ape1p ("m-Ape1p") can be used to assess induction of autophagy (Suzuki *et al.*, 2002). As anticipated, I found that Ape1p failed to mature in the *atg14* mutant, regardless of whether autophagy was induced upon nutrient starvation. In contrast, greater amounts of mature Ape1p were evident in both the wild type and *add66Δ* strains upon starvation (Figure 15). These data indicate that autophagy is proficient in yeast lacking *ADD66*.

2.3.3 Add66p is a cytosolic, soluble protein

To determine why cells deleted for *ADD66* accumulate A1PiZ and polyubiquitinated proteins, I wished to characterize the gene product. To this end, a sequence encoding the *myc* epitope was

Figure 15. Autophagy is robust in the *add66Δ*strain.

ADD66, *add66Δ*, and *atg14Δ* strains were grown in rich media (YPD) or in synthetic complete medium lacking ammonium sulfate (starvation media, or "Strv"). Protein extracts were prepared from each strain, under each condition, and were resolved by SDS-PAGE and probed with an antiserum that recognizes the precursor (pre) and mature (m) forms of Ape1p. Anti-Sec61p antiserum was used as a loading control. It should be noted that this assay only measures macroautophagy induction.

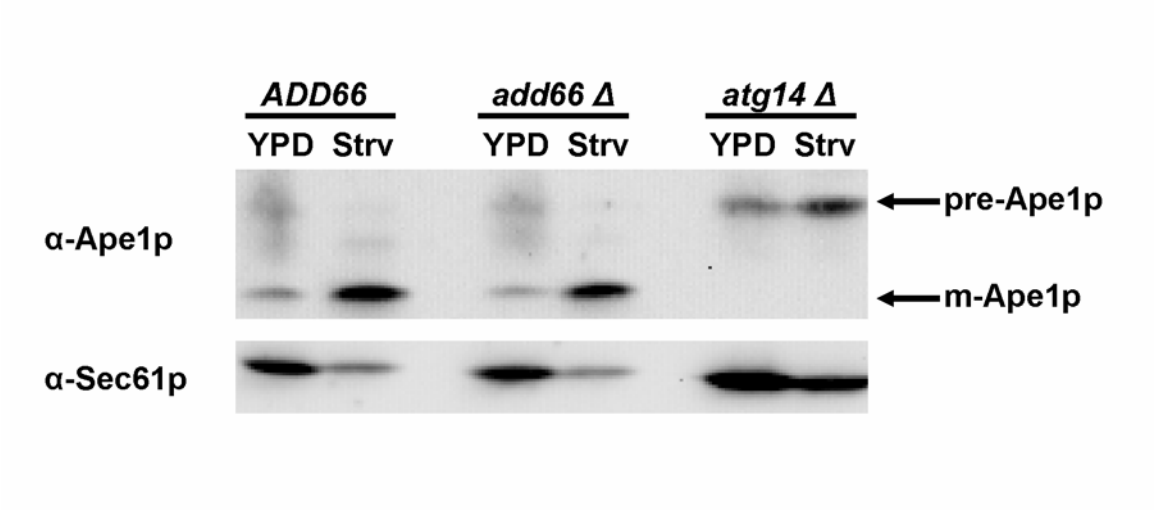

Figure 15. Autophagy is robust in the *add66Δ* strain

appended onto the *C*-terminus of Add66p and the construct was cloned into a vector designed for the strong, constitutive expression of the desired protein (pGPD425) (Mumberg *et al.*, 1995) or into a vector in which *ADD66* expression was driven by the endogenous promoter (pRS315; see Section 2.2.3). To determine if the tagged protein was active, I assessed whether A1PiZ degradation was restored to wild type levels in Add66p-*myc*-expressing *add66Δ* yeast. To this end, **Kristina** Kruse of the McCracken lab utilized my constructs and employed a quantitative colony blot assay that reports on A1PiZ expression levels and ERAD, and in fact was used to isolate the *ADD* mutants (McCracken *et al.*, 1996; Palmer *et al.*, 2003). As shown in Figure 16A-B, A1PiZ accumulated to wild type levels when *add66Δ* cells contained the Add66p-*myc* expression vector. I then examined the expression levels of A1PiZ in the various *ADD66* and *add66Δ* strains. As expected, Add66p-*myc* expression was observed only in *ADD66* and *add66Δ* strains that had been transformed with the expression vector (Figure 16C).

To determine Add66p's residence, lysates were prepared from cells constitutively expressing epitope-tagged Add66p or containing a vector control, and the lysates were analyzed by differential centrifugation. Add66p was found exclusively in a high-speed supernatant ("S2", Figure 17A), suggesting cytoplasmic residence. Similar results were observed in strains expressing Add66p-*myc* expressed under the endogenous promoter (data not shown). Cytoplasmic residence was further supported through the use of indirect immunofluorescence microscopy: The anti-*myc* fluorescent signal exhibited a diffuse, cytoplasmic staining, unlike a marker for the ER, BiP, which was evident in perinuclear and peripheral patterns (Figure 17B). These data are consistent with earlier studies that attempted to define the localization of the vast majority of *Saccharomyces cerevisiae* proteins through the use of engineered GFP insertions at

Figure 16. The A1PiZ degradation defect is rescued in *add66Δ* strains expressing Add66p-*myc*.

(A) A colony-blot immunoassay was performed with anti-antitrypsin antiserum on *add66Δ* strains expressing A1PiZ lacking a vector or were transformed with an empty vector (-) or with an *ADD66-myc* expression plasmid (+). (B) The results from three independent colony-blot immunoassays were quantified for wild type yeast (*ADD66*) and *add66Δ* yeast that lacked a vector or were transformed with the *ADD66-myc* expression vector (+) or a vector control (-). Data were quantified from signals detected in the linear range of the analysis. Data represent the means of three independent experiments, +/- SD: The p value for the data for the *ADD66* strain versus the *add66Δ* strain is <0.001. The p value for the data for the *ADD66* strain versus the *add66Δ* Add66p*myc* (+) strain is <0.0001. The p value for the data for the *ADD66* versus the *add66Δ* Add66pmyc (-) strain is <0.0005. (C) Protein extracts were prepared from *ADD66* and *add66Δ* yeast transformed with a vector control (-) or with the *ADD66myc* expression plasmid (+) and total proteins were resolved by SDS-PAGE. The blots were probed with anti-*myc* and anti-Sec61p anti-sera. Duplicate colonies were analyzed and are shown.

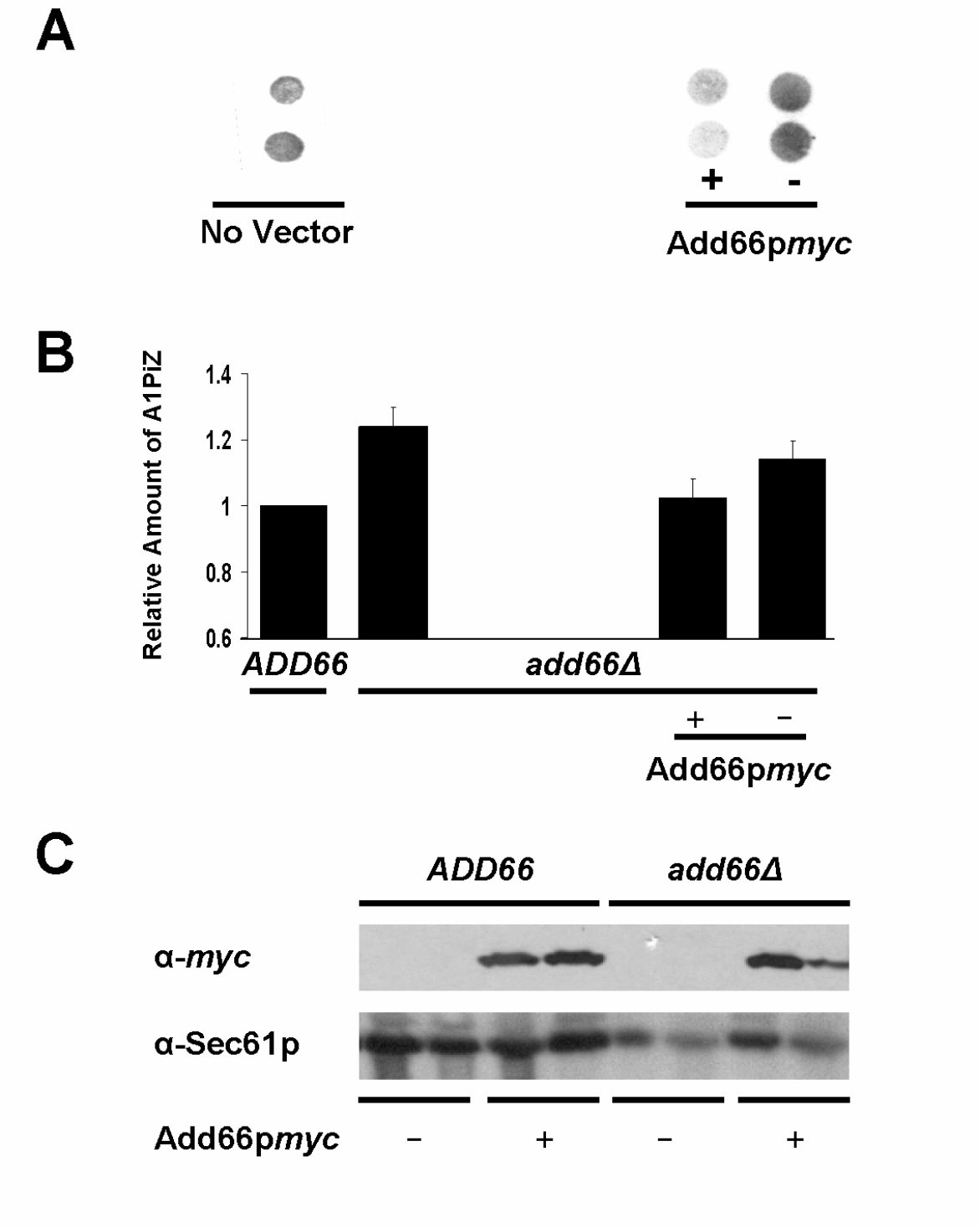

Figure 16. The A1PiZ degradation defect is rescued in *add66Δ* strains expressing Add66p-*myc*

Figure 17. Add66p is cytosolic.

(A) *add66Δ* cells were transformed with a control plasmid or with a 2μ plasmid engineered for the constitutive expression of Add66p-*myc*. Cell lysates (L) were subjected to 16,000*g* and 150,000*g* centrifugations. Total proteins in the pellets (P1 and P2) and supernatants (S1 and S2) were resolved by SDS-PAGE and analyzed by western blot analysis with anti-*myc*, anti-Sec61p (ER membrane protein), anti-Sse1p (a primarily cytosolic protein; (Goeckeler *et al.*, 2002)), and anti-Cim5p (a regulatory subunit of the 26S proteasome with cytosolic and ER membrane subcellular localizations) anti-sera. (B) Indirect immunofluorescence of *add66Δ* strains transformed with the plasmids described in part A were stained with DAPI (nuclear staining), and probed with anti-BiP (ER peri-nuclear and peripheral staining) and anti-*myc* anti-sera and signals were detected as described in Section 2.2.5.

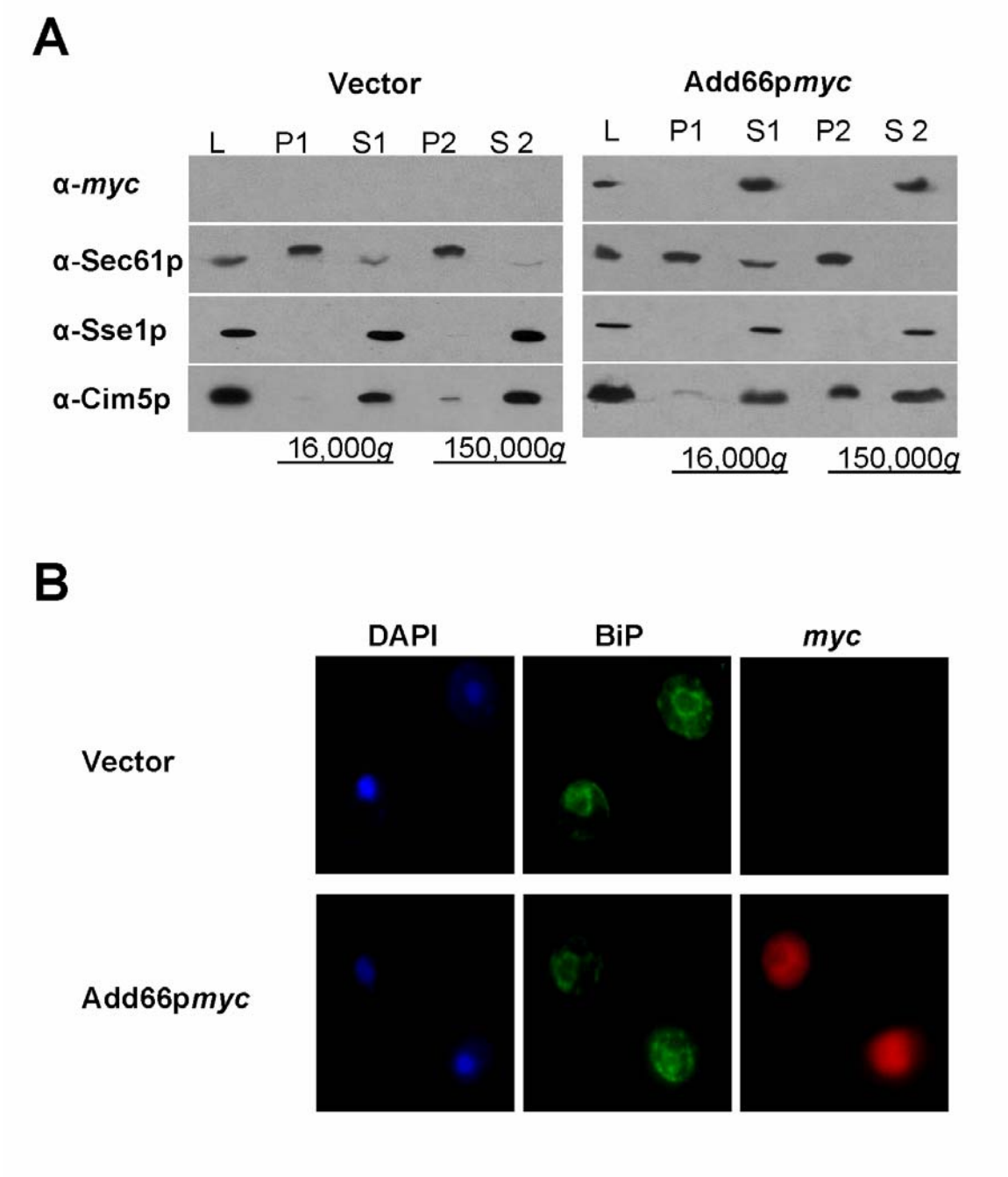

Figure 17. Add66p is cytosolic

their *C*-termini (http://yeastgfp.ucsf.edu/). Taken together, these data indicate that Add66p is a soluble cytosolic protein.

2.3.4 Add66p is required for maximal proteasome activity

A clue to Add66p's function was provided by a large-scale yeast proteomic analysis in which the gene product was found in a multi-protein complex that included Pre1p (Ho *et al.*, 2002). Pre1p is a subunit in the 20S proteasome core that is one of two subunits that facilitates CTL activity (Heinemeyer *et al.*, 1991; Hilt *et al.*, 1993). Add66p was also identified in a multi-protein complex with Pre5p (Krogan *et al.*, 2006), a non-proteolytic subunit of the 20S proteasome (Heinemeyer *et al.*, 1994), and with Ump1p, a protein required for the maturation of the proteasome core particle (Ramos *et al.*, 1998). These data suggested why *add66Δ* yeast accumulated polyubiquitinated proteins and why synthetic growth defects were observed when mutations in *ADD66* and *IRE1* were combined and ER stress was induced (Figure 14). Specifically, it suggests that Add66p is involved in proteasomal degradation and the removal of the protein results in the accumulation of misfolded protein substrates of the 26S proteasome. Therefore, I went on to examine the influence of Add66p on the proteolytic activity of the 26S proteasome.

The activity of purified proteasomes has been measured and quantified utilizing an established fluorescence assay (Glickman and Ciechanover, 2002 and Section 2.2.7). To facilitate the study of Add66p's role in proteasome function, I modified this protocol to examine clarified cytosol in which the activities of the proteasomes could be assessed. In each set of assays, the background (spontaneous) hydrolysis of the fluorogenic substrate was subtracted and

the resulting values for activity in the mutant lysates were normalized to the activity in the wild type lysates. Previous studies on proteasome activities worked with approximately 1μg of highly enriched 26S proteasome (Glickman *et al.*, 1998). Therfore, I examined 10-400 μg of clarified cytosol to determine if this was within the detectable and linear range of the CTL activity assay (Figure 18). From this titration of cytosol concentrations, 100 μg of clarified cytosol was determined to be in the approximate linear range and was consequently utilized for subsequent assays. The time dependence of the CTL, TL, and PGPH activity in each extract was also measured and compared to the activity in highly enriched 26S proteasomes (Figure 19). From these experiments, 10 minutes was determined to be in the linear range for examining the CTL activity in yeast cytosol, and one hour was in the linear range for the TL and PGPH activity assays.

To test directly whether the deletion of *ADD66* affected proteasome function, the three proteolytic activities of the proteasome were measured in clarified cytosolic extracts derived from *ADD66* and *add66Δ* strains using an established fluorescence assay (Glickman *et al.*, 1998). As shown in Figure 19 and Figure 20A, I observed that the proteasome's CTL activity—which constitutes most of the proteasome's activity—was markedly reduced in extracts from *add66Δ* yeast (BY4742). To ensure that this effect was not strain-specific, the *ADD66* gene was ablated in another strain background (W303) and a similar reduction in CTL activity was observed (Figure 20A, top panel, center). As a control for these assays, I noted that all three activities were compromised in extracts prepared from a *cim5-1* strain (Figure 20A, grey bars), which is known to exhibit delayed proteasome-dependent protein turnover, an elongated G2/M cell cycle transition, and growth arrest under various stress conditions (Ghislain *et al.*, 1993; Rubin *et al.*, 1998).

Figure 18. CTL activity detection of varying amounts of yeast cytosol.

The chymotrypsin-like (CTL) activity in extracts prepared from the *ADD66* strain was determined using a fluorogenic substrate, as described in section 2.2.7. The indicated concentration of cytosol for each reaction is labeled below each bar. Fluorescence was measured on a spectrofluorometer (emission at 380 nm and excitation at 436 nm) after 10 minutes. The relative activities were normalized to the fluorescent signals of 400 μg of yeast cytosol, which was set at 100%. Standard deviations were obtained from the results of three independent experiments. Data represent the means of three independent experiments, +/- SD.

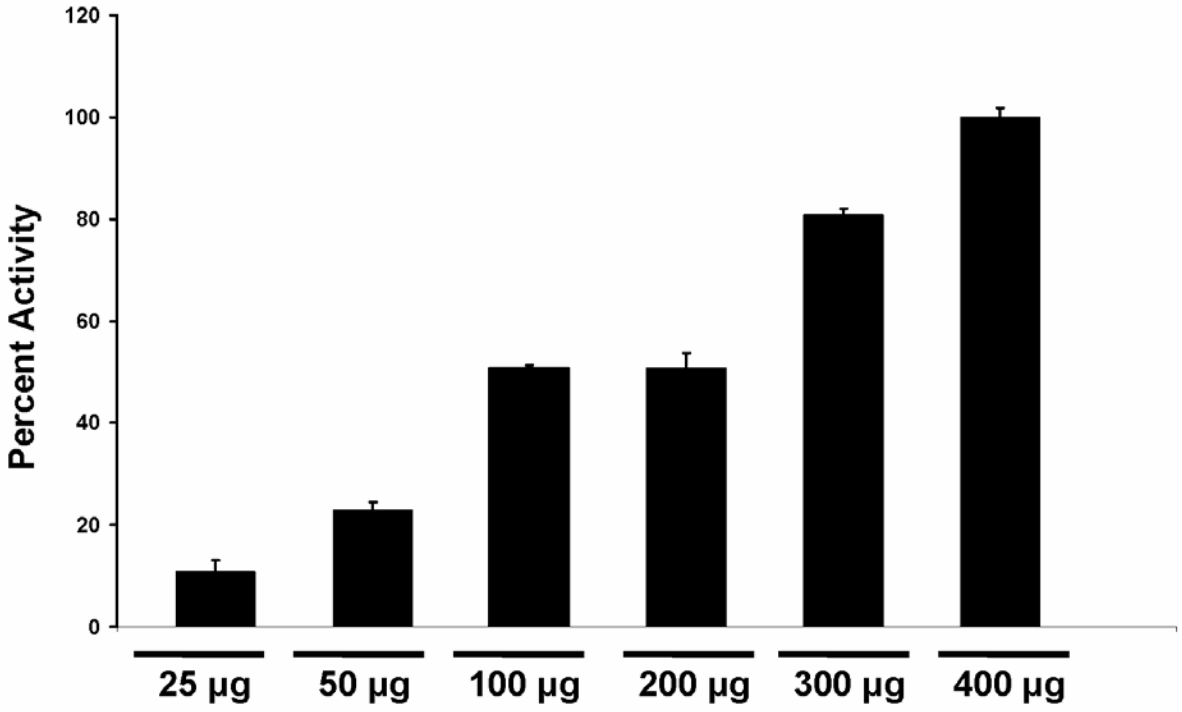

Figure 18. CTL activity detection of varying amounts of yeast cytosol

Figure 19. Expression of Add66p-*myc* from its endogenous promoter complements the chymotrypsin-like activity defect in *add66*Δ yeast.

The chymotrypsin-like (CTL), trypsin-like (TL) and peptidylglutamyl peptide hydrolyzing (PGPH) activities in extracts prepared from *ADD66* (blue square) or *add66Δ* (red triangle) strains containing either a vector control or an Add66p-*myc* expression vector, or purified 26S proteasome (circles, last column), were determined using a fluorogenic substrate, as described in Section 2.2.7. A total of 100 μg of cytosol and 0.5 μg of 26S proteasome was used in each reaction. Fluorescence was measured on a spectrofluorometer (emission at 380 nm and excitation at 436 nm) at the indicated time points treated with DMSO (closed symbols) or inhibitor (open symbols; CTL: MG132, TL: leupeptin, PGPH: MG-132). The relative activities were normalized to the fluorescent signals for wild-type levels (first two columns) or the DMSO-treated 26S proteasome (last column) at 180 min, which were set at 100%. Data represent the means of three independent experiments, +/- SD. The p value for the data for the CTL activity of the *ADD666* strain versus the *add66Δ* strain without MG132 is 0.0001. The p value for the data for the *ADD66* strain versus the *add66Δ* strain with or without Add66*myc* and lacking treatment of a proteasome inhibitor is 0.7 or greater. The p value for the data for the 26S proteasome in the presence versus the absence of inhibitor for the CTL, TL, and PGPH activities are less than or equal to 0.0001.

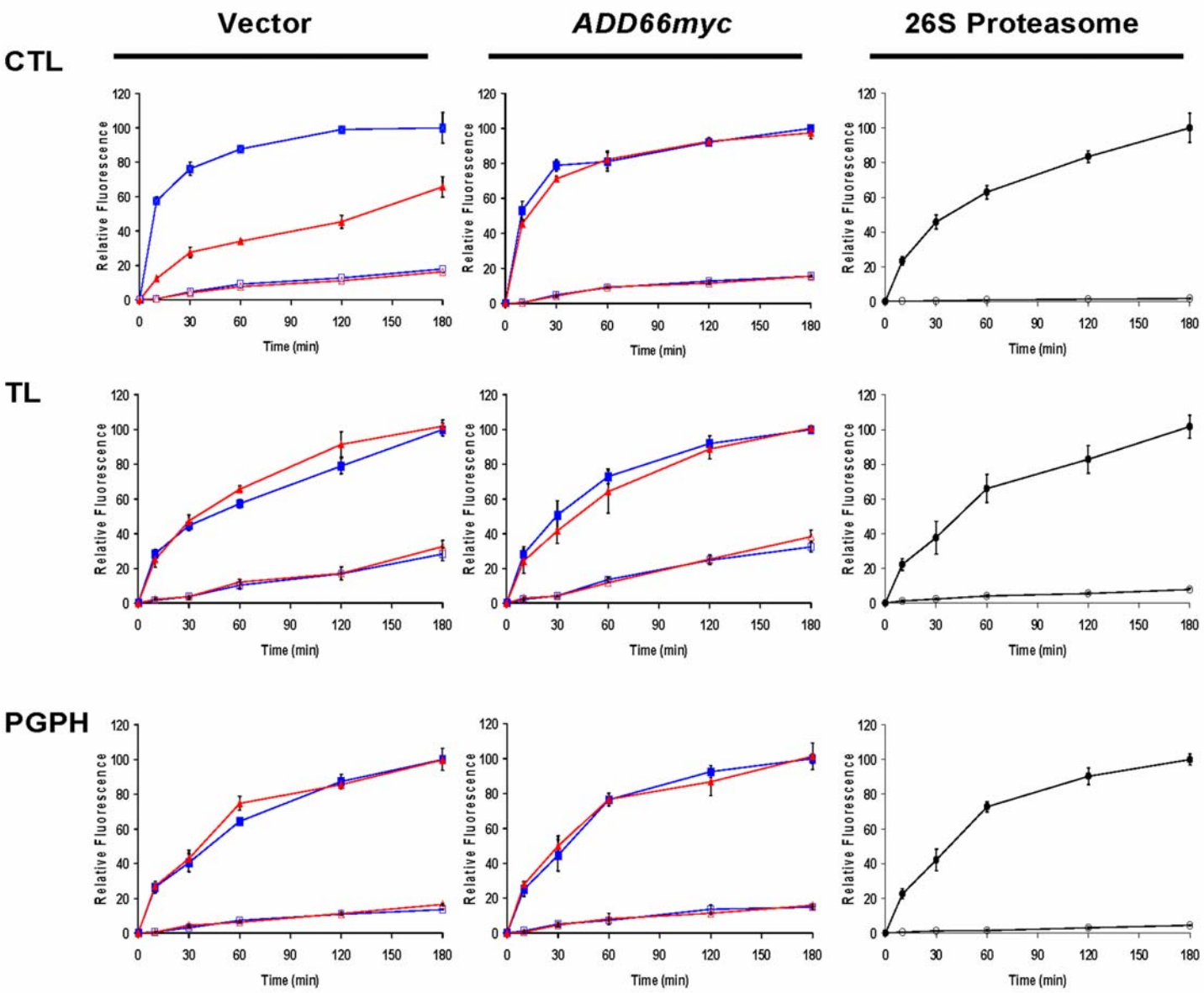

Figure 19. Expression of Add66p-*myc* from its endogenous promoter complements the chymotrypsin-like activity defect in *add66Δ* yeast

Figure 20. The chymotrypsin-like activity of the 26S proteasome is reduced in extracts prepared from the *add66Δ* strain.

The chymotrypsin-like (CTL), trypsin-like (TL) and peptidylglutamyl peptide hydrolyzing (PGPH) activities in clarified extracts from *ADD66* (black bar) or *add66Δ* (white bar) yeast in two different strain backgrounds (BY4742 and W303) were determined. Proteasome activities in extracts from *CIM5* and *cim5-1* (grey bar) strains were used as a positive control. The relative activity was determined by normalizing the fluorescent signals to the levels corresponding to the wild-type strains, as described in section 2.2.7. Data represent the means of three independent experiments, +/- SD. The p value for the data for the CTL activity of the *ADD666* strain versus the *add66Δ* (BY4742 or W303) strains is 0.0005 or less. The p value for the data for the *ADD66* strain versus *add66Δ* strains for the TL or PGPH activities is 0.1447 or greater. The p value for the data for the *CIM5* strain versus *cim5-1* strain for the CTL, TL, and PGPH activities are less than or equal to 0.001. (B) Constitutive expression of Add66p-*myc* restores the CTL activity in the *add66Δ* strain. Wild-type and *add66Δ* strains were transformed with an empty vector (-) or a vector engineered for the expression of Add66p-*myc* (+) and the CTL activity was analyzed as in part A. Data represent the means of three independent experiments, +/- SD of the means. The p value for the data for the CTL activity of the *ADD666* strain versus the *add66Δ* strain lacking the expression of Add66p-*myc* is 0.0023. The p value for the data for CTL activity from the *ADD66* strain versus the *ADD66* or the *add66Δ* strains expressing Add66p*myc* is 0.0875 or greater. (C) Cytosolic proteins from the strains in (B) were resolved by SDS-PAGE and probed for Add66p-*myc* and Sse1p expression by western blot analysis. Sse1p served as a loading control.

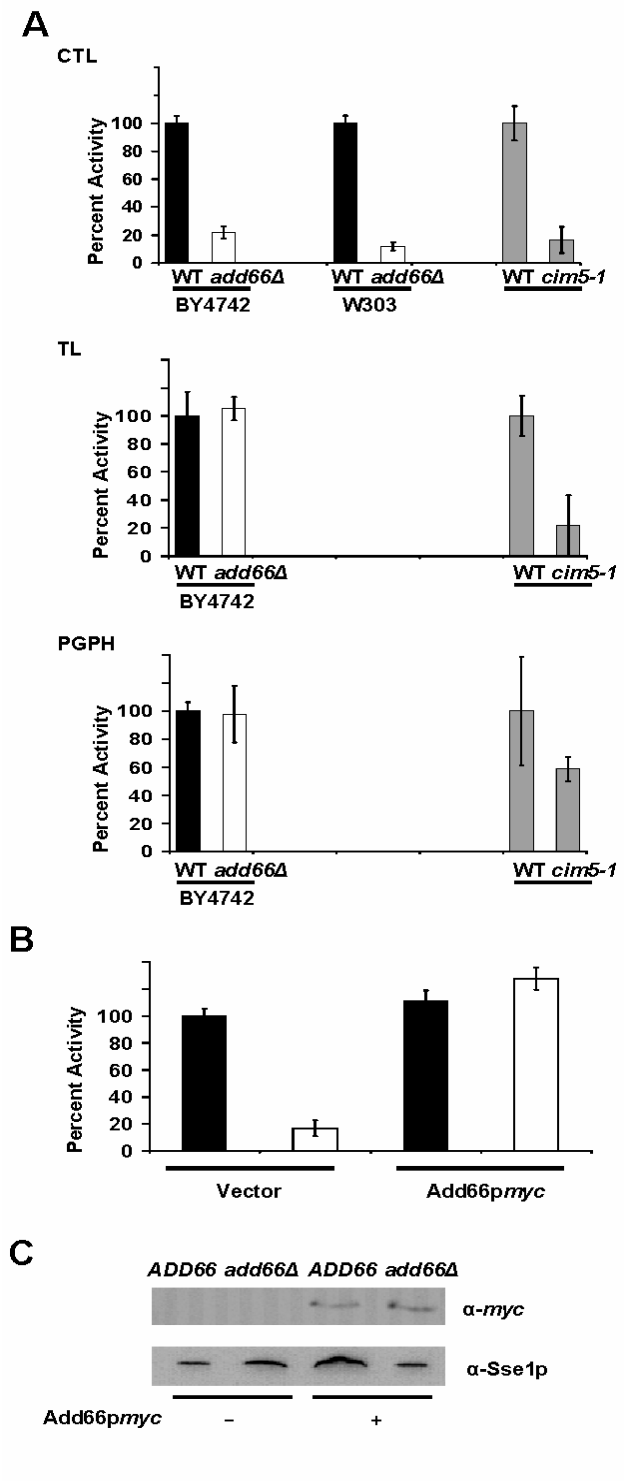

Figure 20. The chymotrypsin-like activity of the 26S proteasome is reduced in extracts prepared from the *add66Δ* complexes

I found that the constitutive, strong expression of Add66p-*myc* in the *add66Δ* strain complemented the CTL defect and restored activity to wild type levels (Figure 20B-C). However, it was unknown if over-expression of Add66p-*myc* would present some unforeseen secondary effect on proteasome activity. Therefore, Add66p-*myc* was also expressed in strains under the control of its endogenous promoter and lysates were prepared from *add66Δ* yeast containing a vector control and the expression vector. Here too I noted that the *add66Δ* CTL defect was complemented (Figure 19, "*ADD66myc*").

A complementary fluorescence assay was employed to confirm that the reduction in CTL activity observed in the *add66Δ* strain was due to a reduction of 26S proteasome activity (Glickman *et al.*, 1998). Equivalent amounts of *ADD66*, *add66Δ*, *CIM5* and *cim5-1* clarified cytosol, as well as purified 26S and 20S proteasomes, were resolved in a non-denaturing polyacrylamide gel and subsequently incubated with the fluorogenic substrate (Section 2.2.8). The gel was then subjected to UV light and the total signal of fluorescence was measured (Figure 21). Although this assay is not necessarily quantitative, I noted a general decrease in the CTL activity in the *add66Δ* mutant as well as in the *cim5-1* strain. It should be noted that there was no increase in 20S proteasomes in the *add66Δ* strain, while there was an increased level of CPs in the *cim5-1* strain when compared to their respective isogenic wild type strains.

The *add66Δ* mutant as well as five other *add* mutants were identified in the same screen (Palmer *et al.*, 2003). I therefore examined the proteolytic activities in four of the five other *add* mutants to determine if they had similar defects in proteasome activity (Figure 22). Although varying levels of proteolytic activities were observed, the *add66Δ* mutant consistently showed a reduction in the chymotrypsin-like activity. A possible explanation for this range of observed activities from each *add* mutant strain is that the strains were obtained from a commercial source

Figure 21. 26S proteasome activity is reduced in the *add66Δ* strain with no increase in the relative level of 20S particles.

One hundred μg of clarified cytosol from the *ADD66*, *add66Δ, CIM5 or cim5-1* or 1 μg of purified 26S or 20S proteasome were resolved on a non-denaturing PAGE gel. The gel was then incubated 0.1 mM Suc-LLVY-AMC and proteasome bands were visualized via a Kodak 440CF Image Station upon exposure to UV light (~360-380 nM). (A) Quantification of the relative proteasome activity by measuring the combined levels of 26S and 20S activities of the above yeast strains. The combined relative proteasome activity was determined by normalizing the fluorescent signals to the levels corresponding to the wild-type strains. Wild type strains were normalized to 100% activity. The bars show a range of activities from two independent experiments. (B) A representative blot of proteasome activity of all the above samples. The relative sizes of 26S and 20S proteasomes are depicted to the left of the gel. The faster migrating intermediate band in the 26S lane is possibly the result from one of the 19S regulatory caps disassociating from the 26S proteasome complex.

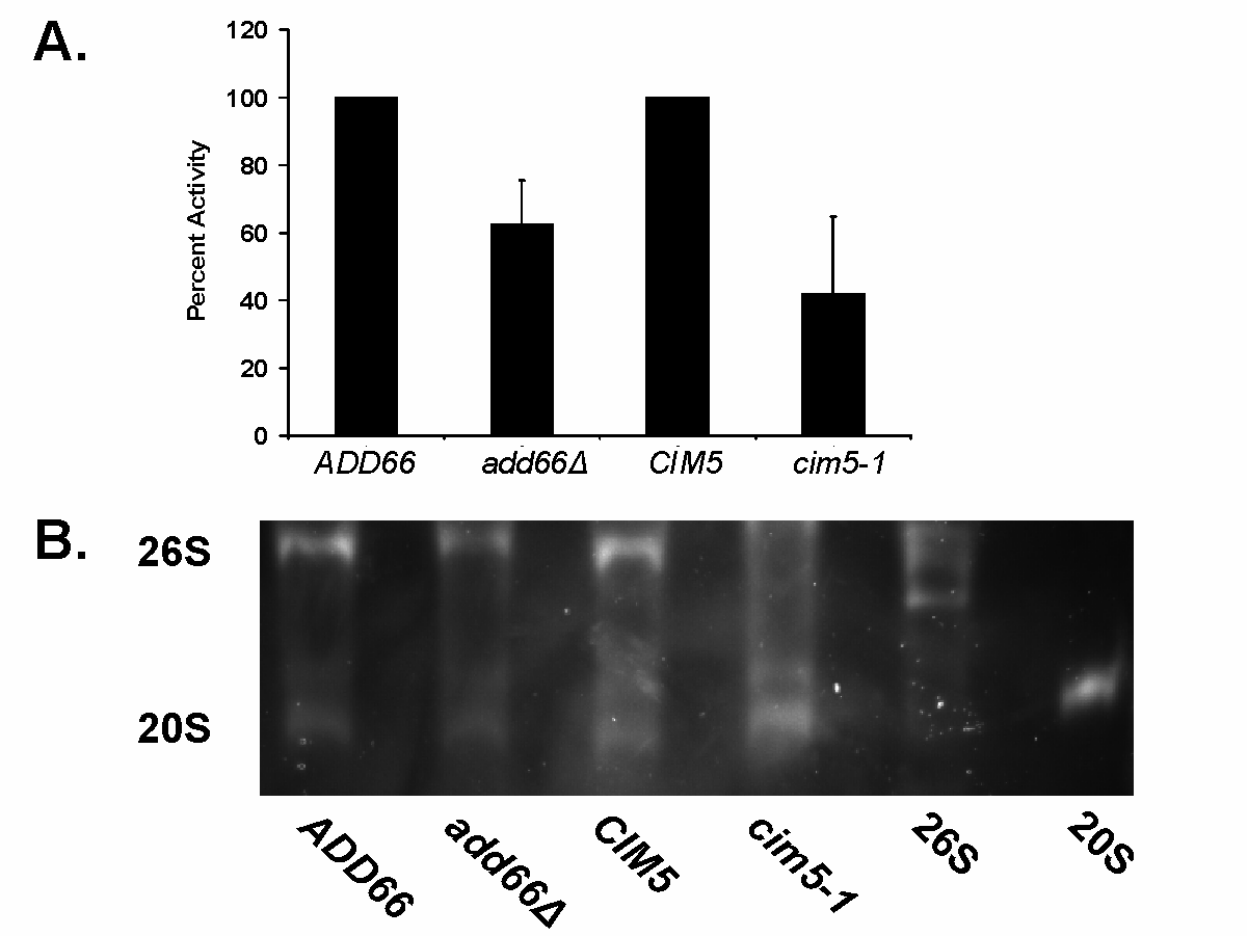

Figure 21. 26S proteasome activity is reduced in the *add66Δ* strain with no increase in the relative level of 20S particles

Figure 22. The proteolytic activities of the 26S proteasome extracts prepared from various *add* strains.

Extracts prepared from *ADD*, *add6Δ*, *add37Δ*, *add66Δ*, *add67Δ*, and *add68Δ* strains (Palmer *et al.*, 2003) were examined for the chymotrypsin-like (CTL), trypsin-like (TL), and peptidylglutamyl peptide hydrolyzing (PGPH) activities. 100 μg of clarified cytosol was used for each reaction. Fluorescence was measured on a spectrofluorometer (emission at 380 nm and excitation at 436 nm). The relative activities were determined by normalizing the fluorescent signals to those observed in extracts prepared from the *ADD* (wild-type) yeast, which was set at 100%. Standard deviations were determined from the means of four independent experiments with a p values comparing the data from the wild type strain to the isogenic mutant strain (CTL, PGPH, and TL respectively): *add6Δ* (0.001, <0.0001, and 0.0011), *add37Δ* (0.015, 0.004, and 0.0516), *add66Δ* (<0.0001, 0.0008, and < 0.0001), *add67Δ* (0.035, < 0.0001, and 0.0235), and *add68Δ* (0.001, 0.001, and 0.006).

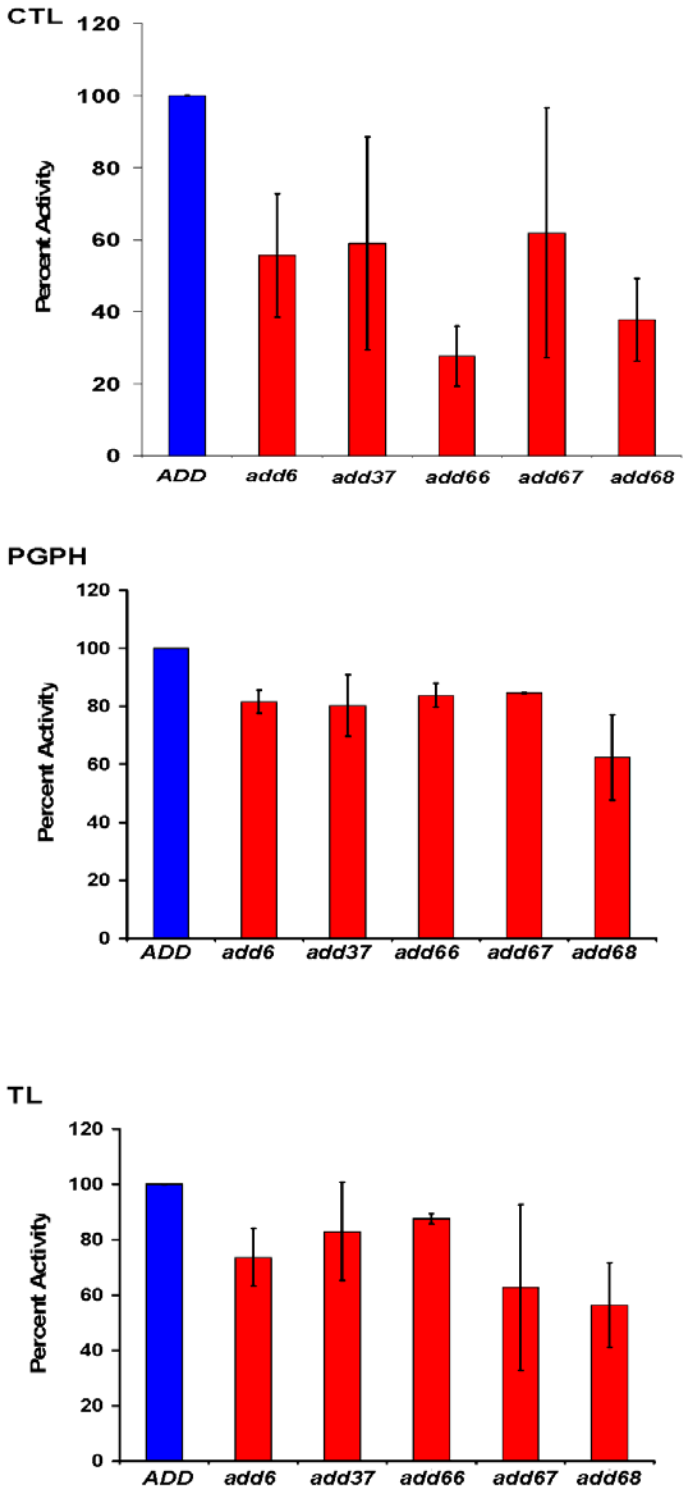

Figure 22. The proteolytic activities of the 26S proteasome extracts prepared from various *add* strains

(BY4742, Research Genetics). Strains in this commercial collection have been noted to have additional mutations and thus may not be homogeneous. In the future, it would be worthwhile to reconstruct these mutations in another strain background and reassess the CTL acitivty.

Combined with the fact that Add66p-*myc* rescues the A1PiZ degradation defect in *add66Δ* yeast (Figure 16), all these data indicate that Add66p is required for maximal CTL activity and strongly suggest that the A1PiZ degradation defect in *add66Δ* yeast arises from reduced proteasome activity.

2.3.5 The levels of 26S proteasome subunits are unaltered in the *add66Δ* strain

The simplest explanation for the reduced CTL activity in extracts derived from *add66Δ* yeast is that the number of proteasomes is decreased in this strain. As demonstrated earlier (Figure 21), there appeared to be no significant accumulation of 20S complexes in the *add66Δ* strain. However, the reduced CTL activity observed in the *ADD66* mutant strain could be the result of a decrease in the individual amount of subunits in the 26S complexes. To address this possibility, quantitative immunoblotting was employed to measure the levels of six 20S subunits, using a non-specific polyclonal antiserum, and one 19S subunit (Cim5p) in the *add66Δ* and wild type strains (Figure 23). However, no significant difference in the relative levels of these subunits was detected.

2.3.6 The relative affinities of the subunits that mediate the CTL activity for specific inhibitors are not altered in extracts prepared from *add66Δ* yeast

Pre1p is one of the two essential 20S subunits required for the CTL activity of the proteasome

Figure 23. The levels of 26S proteasome subunits are unaltered in the *add66Δ* strain.

(A) Proteins in clarified cytosol from *ADD66* (black bar) and *add66Δ* (white bar) yeast were resolved by SDS-PAGE and western blot analyses were performed to detect the levels of 20S subunits, a component of the 19S particle (Cim5p), Sse1p, and Hsp82p. Relative protein levels were determined by quantifying the intensities of the various proteins, and then normalizing these values to the levels measured in the isogenic wild type strain. Data represents the means of eight independent experiments, +/- SD, with a p value comparing the data for the *ADD66* strain to the *add66Δ* strain of 0.36559 or greater for each protein. (B) A representative western blot used to amass the data in part A.

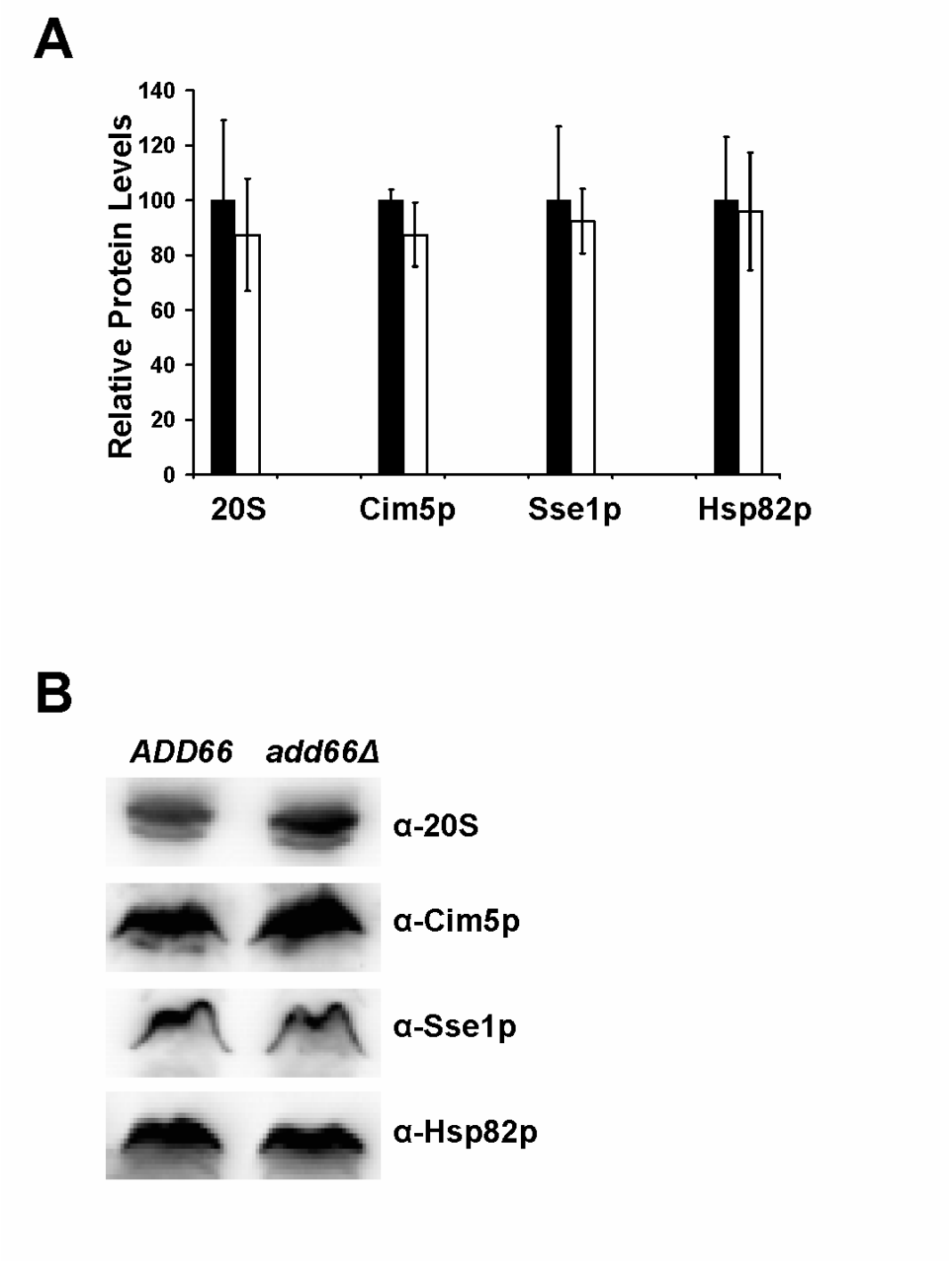

Figure 23. The levels of 26S proteasome subunits are unaltered in the *add66Δ* strain

(Heinemeyer *et al.*, 1991; Hilt *et al.*, 1993). Because reduced CTL activity was observed in extracts from *ADD66*-deleted cells (Figure 19, 20A, 21, and 22), it was possible that the absence of the corresponding protein might grossly alter the conformation of Pre1p's substrate binding site. To test this hypothesis, the CTL activity was assayed in extracts from wild type and *add66Δ* strains in the presence of increasing concentrations of MG-132 and epoximycin. MG-132 and epoxomicin specifically block the CTL activities in nearly irreversible non-covalent and covalent manners, respectively (Gaczynska and Osmulski, 2005). As shown in Figure 24, there was no difference in the apparent K_Is for these inhibitors (~5 x 10^{-7} M) when titrated into cytosols prepared from wild type or *add66Δ* yeast. This result suggests that the conformation of the Pre1p substrate-binding site was not radically altered.

2.3.7 20S precursors accumulate in yeast deleted for *ADD66*

The 26S proteasome is comprised of at least 31 different subunits that combine in a spatially and temporally defined manner via various intermediate complexes (Ramos *et al.*, 1998; Voges *et al.*, 1999; Tone *et al.*, 2000; Hirano *et al.*, 2005). Although little is known about the exact mechanism by which the proteins in the cap and the 7 distinct alpha and 7 beta subunits in the core assemble (See Section 1.1.1 for further details), two proteins were previously identified that are required for the proper maturation of the core particle in yeast: Nob1p and Ump1p (Ramos *et al.*, 1998; Tone *et al.*, 2000). Mutations in *NOB1* exhibit defects in the processing of 20S beta subunits, which are the central, proteolytic subunits, and in the assembly of the 20S and 26S particles (Tone and Toh, 2002). In addition, as described above, Ump1p co-precipitates with Add66p in a multi-protein complex (Krogan *et al.*, 2006) and mutations in *UMP1* affect the function of all three proteolytic activities due to defects in beta subunit maturation

Figure 24. The relative affinities of the subunits that mediate the CTL activity for specific inhibitors are not altered in extracts prepared from *add66Δ* yeast.

The CTL activities in extracts prepared from *ADD66* (open circles) and *add66Δ* (closed circles) strains were determined (as described in Section 2.2.7) at the indicated concentration of (A) epoxomicin and (B) MG-132. The relative activity was determined by normalizing the fluorescent signals to wild-type levels in reactions lacking inhibitor. The structures of the inhibitors are shown, and the data represents the means of four independent experiments, +/- SD.

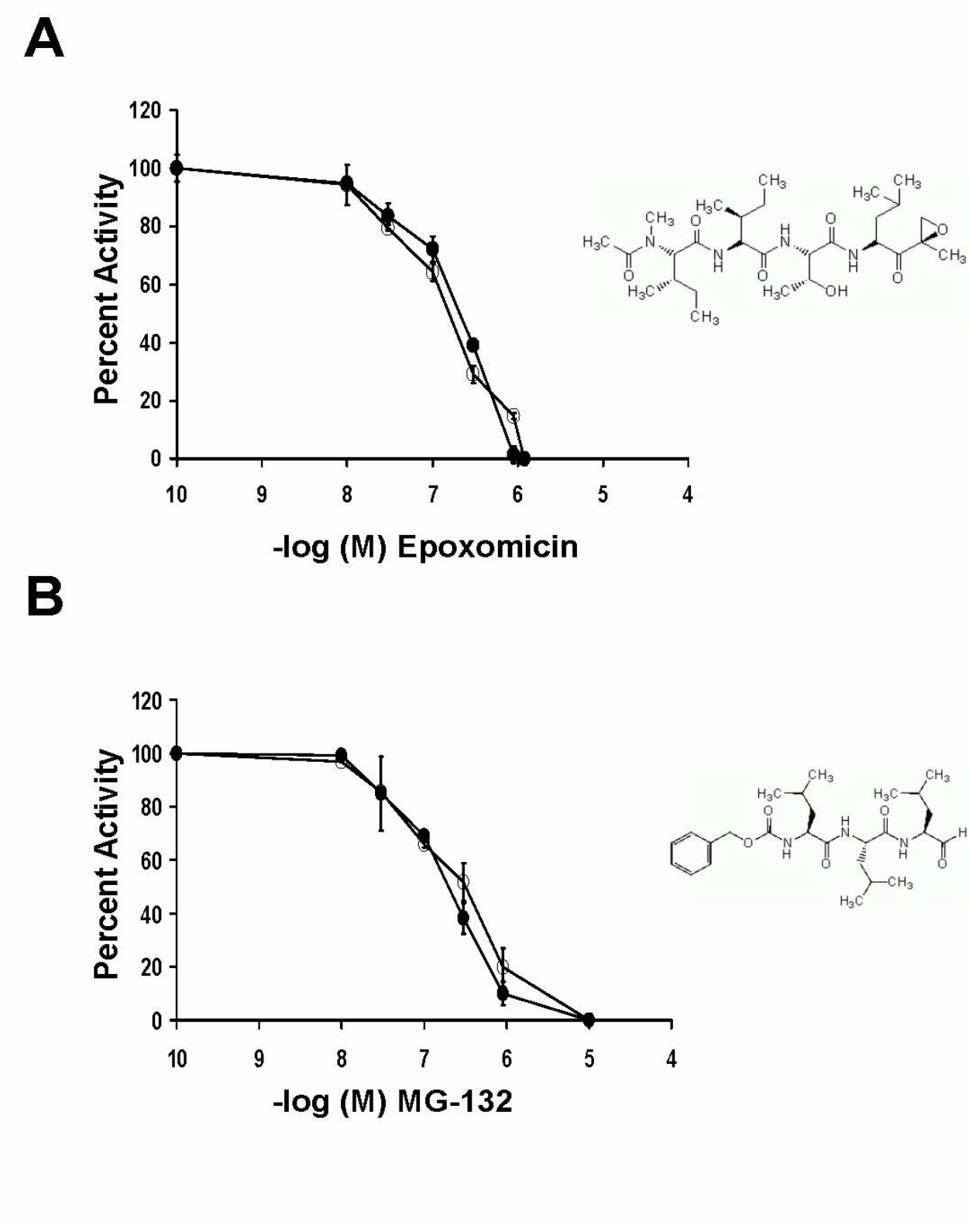

Figure 24. The relative affinities of the subunits that mediate the CTL activity for specific inhibitors are not altered in extracts prepared from *add66Δ* yeast

(Ramos *et al.*, 1998). Thus, it was possible that Add66p participates in proteasome subunit maturation and/or assembly. Moreover, I found that *ADD66* is 20% identical to proteasome assembly chaperone "2" (PAC2; Figure 25. This region of similarity between *ADD66* and PAC2 has been identified by other research groups (Hirano *et al.*, 2005; Li *et al.*, 2007). PAC2 was shown to facilitate the assembly of the 26S proteasome in mammals (Hirano *et al.*, 2005). PAC2 is also known as CLAST3 and HCCA3; a gene that is up-regulated in hepatic cancers (Wang *et al.*, 2001; Bahar *et al.*, 2002). Based on these published observations and my data presented above, I examined whether 20S proteasome assembly intermediates accumulate in yeast lacking Add66p.

Extracts derived from the *ADD66* or the *add66Δ* strains transformed with a control plasmid or with the Add66-*myc* expression plasmid were fractionated on a glycerol density gradient. A low percentage (4-25%) glycerol gradient was used in this experiment to better resolve early proteasome intermediates. This technique was previously employed to note assembly intermediates in mammalian cells when PAC2 expression was silenced (Hirano *et al.*, 2005). I first observed that the majority of 20S subunits and a component of the 19S cap resolved at fractions in the gradient that corresponded to particles with a molecular mass of ~2.5 MDa (Figure 26). This value is in good agreement with the native size of the 26S proteasome. Second, I observed a 20S immuno-reactive protein in a distinct, lighter fraction when extracts from the *add66Δ* strain were examined (see downward arrow, *add66Δ*, "α–20S"). This species, which migrated at ~300 kDa, was absent when extracts from wild type cells or from *add66Δ* yeast expressing endogenous levels of Add66p-*myc* were examined. Third, I found that the same 20S immuno-reactive species was present when extracts were resolved from yeast lacking

Figure 25. Sequence alignment of human PAC2 and yeast Add66p.

Single letter amino acid alignment of the full length sequence from human PAC2 (Accession number: CR457181) and yeast Add6p (Accession number Z28206 Y13137). Sequence identities are shown in black. Sequence alignment was performed by EMBOSS (needle) pairwise alignment algorithms (Blousum62: Gap open 10: Gap extend 0.5) (http://www.ebi.ac.uk/emboss/align/)..

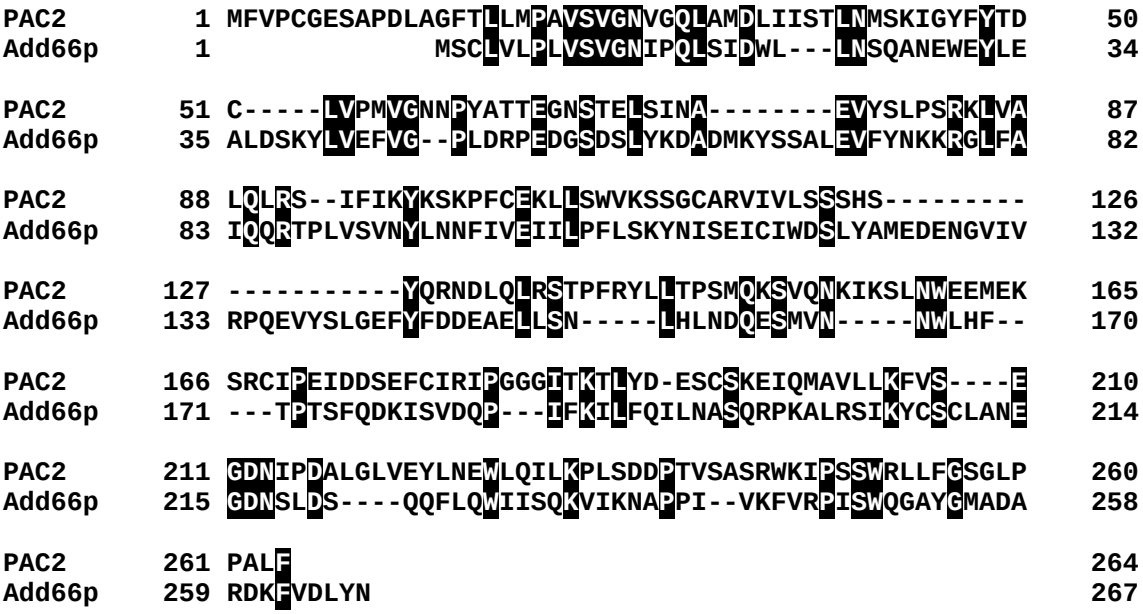

Figure 25. Sequence alignment of human PAC2 and yeast Add66p

Figure 26. Yeast deleted for *ADD66* accumulate a 20S intermediate and unprocessed 20S subunits.

Cell extracts were prepared from an *ADD66* and *add66Δ* strain containing either a control plasmid or a plasmid engineered for the endogenous expression of Add66p-*myc,* and from a *UMP1* (JD133) and *ump1Δ* (JD134) strain. A total of 5 mg of protein was then resolved on a linear glycerol gradient (4-25%) and fractions were collected. Proteins in every other fraction were examined for the presence of 20S subunits, a component of the 19S subunit (Cim5p), and Add66p-*myc* by western blot analysis. The migrations of molecular mass markers, which were analyzed in parallel, are indicated below the gel, the black downward bracket indicates fractions containing immature 20S subunits (a slower migrating doublet), and the black downward arrow indicates the migration of a 20S assembly intermediate. Note that the later two were observed only in extracts prepared from *add66Δ* and *ump1Δ* cells. The immuno-reactive HA species in the *UMP1* and *ump1Δ* gradients represents Pre2p (see Table 2 located in Appendix A).

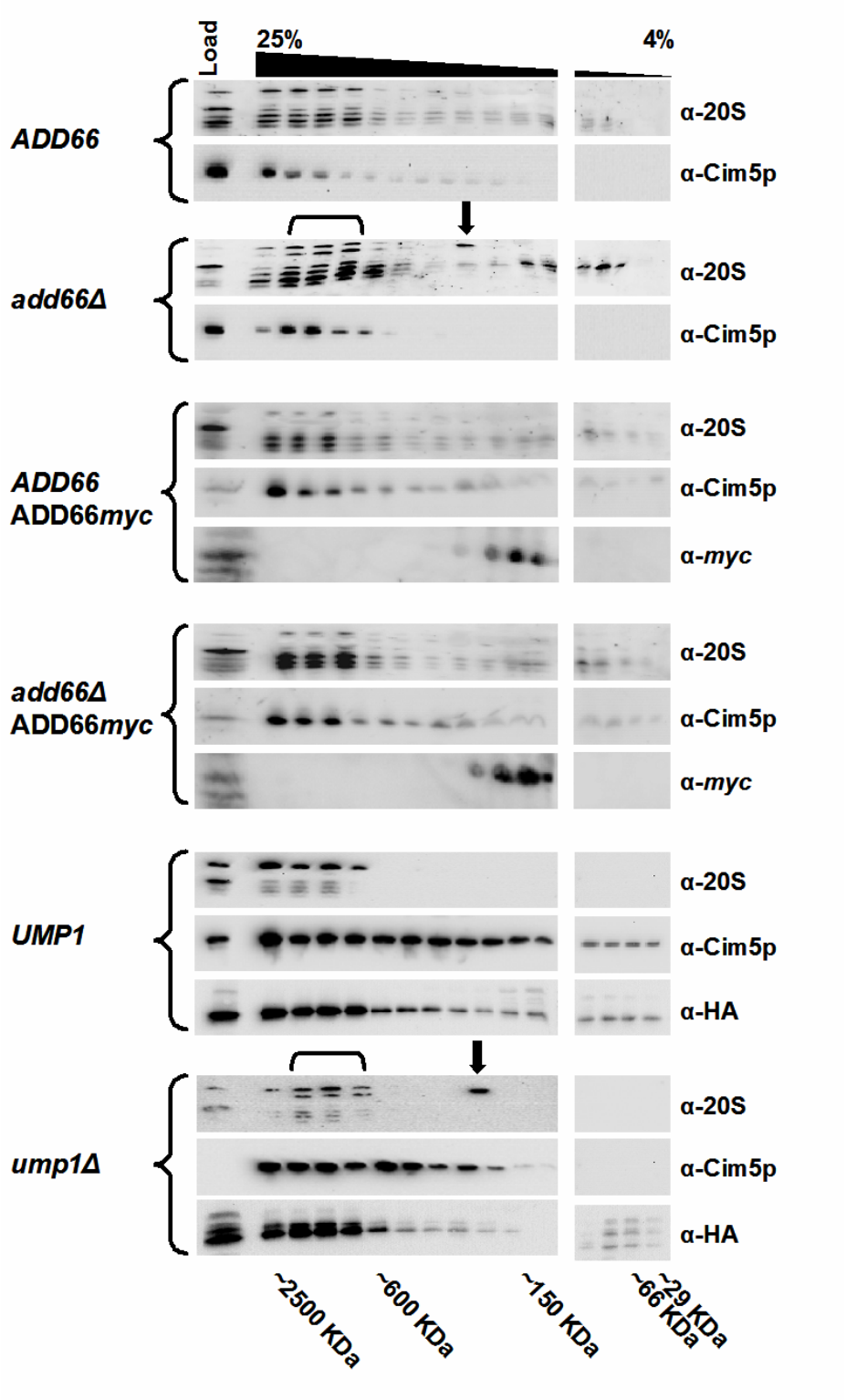

Figure 26. Yeast deleted for *ADD66* accumulate a 20S intermediate and unprocessed 20S subunits

Ump1p (*ump1Δ*, "α–20S"), a factor required for 20S maturation (Ramos *et al.*, 1998). Fourth, when extracts were examined from *add66Δ* or *ump1Δ* yeast, a 20S, slower-migrating doublet was observed that fractionated at the native size for 26S proteasomes (see downward bracket). Previous work demonstrated that one of the species in the doublet represents an unprocessed beta subunit in the 20S proteasome (Ramos *et al.*, 1998). This result suggests some overlap in the defects during 20S subunit processing in the *add66Δ* and *ump1Δ* strains. And fifth, I found that Add66p resided at a position consistent with a molecular mass of ~150-300 kDa, suggesting that Add66p, an ~30 kDa protein, is a component of a multi-protein complex and/or forms higher-order oligomers (see Chapter 4, below, and Li *et al*., 2007). Over-expression of Add66p-*myc* was also able to decrease the amount of the immature 20S doublet and of the ~300 kDa assembly intermediate (Figure 27), although the Add66p-*myc* instead resolved in fractions corresponding to a molecular mass of ~66-150 kDa. This suggests that over-expression of Add66p-*myc* rescues the *add66Δ* 20S maturation defect, but also results in improper association with itself and/or other proteins. Together, these data indicate that yeast deleted for *ADD66* accumulate an intermediate in the 20S assembly pathway, similar to what was observed in *ump1Δ* and *nob1Δ* strains (Ramos *et al.*, 1998; Tone *et al.*, 2000).

2.3.8 The stability of the 26S proteasome is not reduced in the *add66Δ* strain

Another explanation for these findings is that the overall stability of the 20S proteasome is compromised in the *add66Δ* strain and that the particle is labile in extracts derived from the *add66Δ* strain and breaks-down during gradient centrifugation. To test this possibility, I treated wild type and *add66Δ* extracts with two concentrations of detergent, which I predicted to either

Figure 27. Fractionation of proteasomes in lysates prepared after Add66p-*myc* over-expression in wild type and *add66Δ* yeast.

Cell extracts were prepared from an *ADD66* and *add66Δ* strain containing a plasmid engineered for the constitutive, strong over-expression of Add66p-*myc*. A total of 5 mg of protein were then resolved on a linear glycerol gradient (4-25%) and fractions were collected. Proteins in every other fraction were examined for the presence of 20S subunits, a component of the 19S subunit (Cim5p), and Add66p-*myc* by western blot analysis. The migrations of molecular mass markers, which were analyzed in parallel, are indicated below the gel.

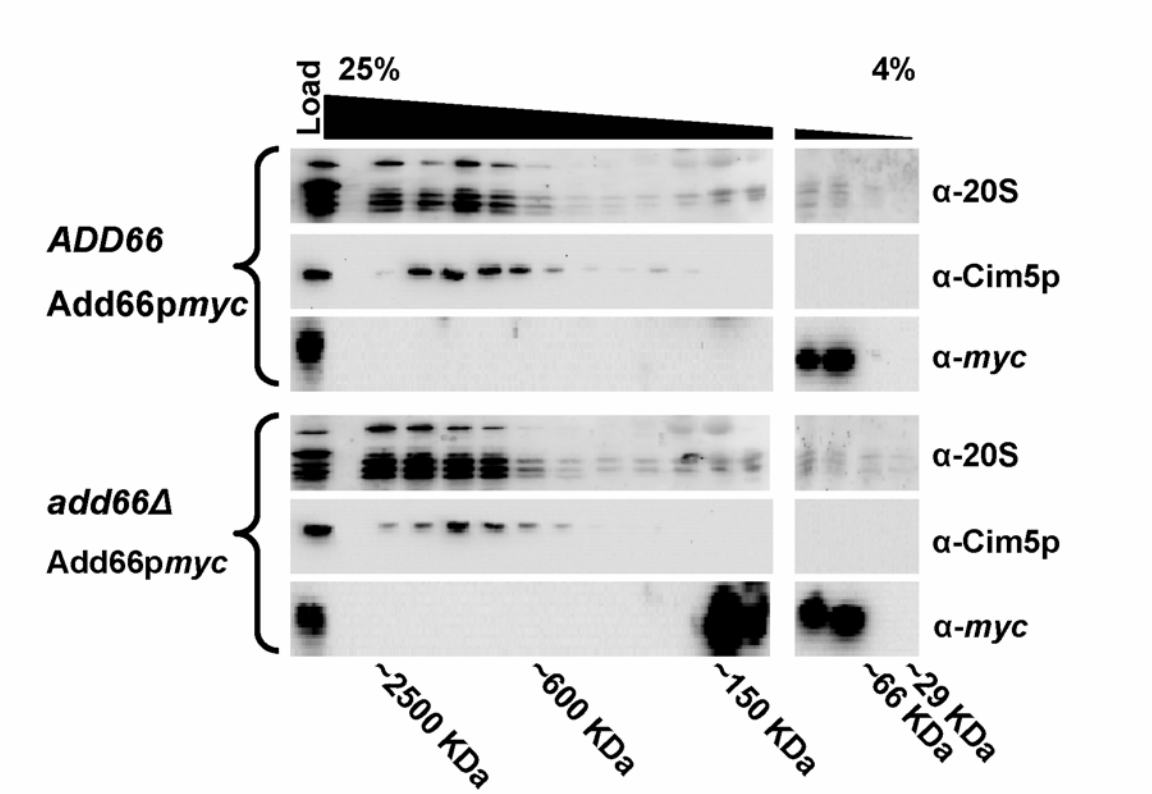

Figure 27. Fractionation of proteasomes in lysates prepared after Add66p-*myc* over-expression in wild type and *add66Δ* yeast

modestly or vigorously disrupt the integrity of the particle. The proteins in these treated extracts, as well as untreated samples, were fractionated on a 10-40% glycerol density gradient to resolve various proteasome complexes. As shown in Figure 28, all of the 20S immuno-reactive species fractionated at ~2.5 MDa—a size that corresponds to the native 26S particle—when extracts were examined from wild type or *ADD66*-deleted cells. In contrast, when extracts from *ADD66* and *add66Δ* cells were treated with 0.02% SDS the 20S subunits eluted in fractions consistent in size with a half proteasome complex at ~400 KDa. Treatment of cell extracts with 0.05% SDS further disrupted the 20S proteasomal subunits into smaller complexes that migrated at ~200-300 KDa. In each case, no significant differences were observed between gradients that employed extracts from *ADD66* and *add66Δ* cells, suggesting that the 26S particles, once assembled, are equally stable in wild type and *add66Δ* yeast.

2.3.9 Add66p is degraded by the 26S proteasome

A number of proteasome chaperones interact transiently with early proteasome assembly intermediates, and in some cases are then degraded by the proteasome (Ramos *et al.*, 1998; Tone *et al.*, 2000; Tone and Toh, 2002; Hirano *et al.*, 2005). I therefore incubated a *pdr5Δ* Add66p-*myc* expressing strain with either DMSO or MG-132. The *pdr5Δ* strain was employed based on the fact that this mutation, like other similarly employed mutations, disables a plasma membrane drug efflux pump; therefore, the effect of proteasome inhibitors is magnified (Balzi *et al.*, 1994; Lee and Goldberg, 1996). As shown in Figure 29A, Add66p-*myc* shifts to fractions containing complexes of greater molecular masses, which contain 20S subunits, when extracts were prepared from cells treated with MG-132. Treatment with MG-132 also results in the accumulation of the slower-migrating, 20S "doublets", as seen when extracts were examined

Figure 28. The stability of the 26S proteasome is not reduced in the *add66Δ* strain.

Extracts were prepared from *ADD66* or *add66Δ* strains and 5mg of protein were resolved on a linear glycerol gradient (10-40%). Gradients contained 0%, 0.02% or 0.05% SDS, which were analyzed in parallel. Proteins in every other fraction were immunoblotted for the indicated proteins or epitope tags. Size markers are indicated below the figure.

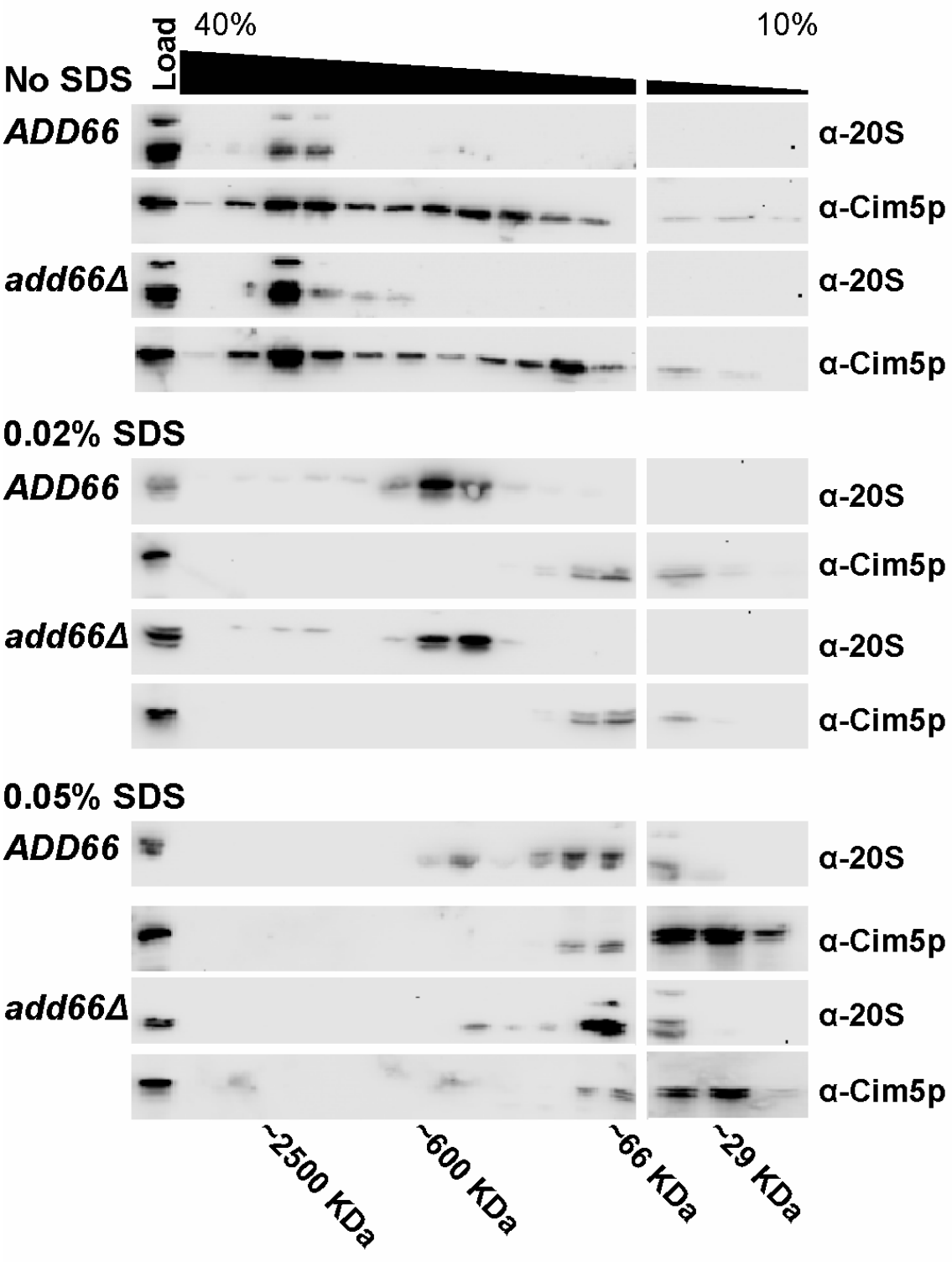

Figure 28. The stability of the 26S proteasome is not reduced in the add66Δ strain

Figure 29. Add66p is degraded by the 26S proteasome.

A *pdr5Δ* strained transformed with a plasmid designed for the constitutive expression of *ADD66myc* was incubated either with 100 μM MG-132 or the equivalent volume of DMSO for 1 h at 30°C. (A) Cell extracts from each strain were prepared and 5 mg of protein were resolved on a linear glycerol gradient (4-25%) and fractions were collected. Proteins in every other fraction were immunoblotted for 20S subunits, a component of the 19S subunit (Cim5p), and Add66p-*myc*. Molecular mass markers, which were analyzed in parallel, are indicated below the gel. Note that these blots were purposely over-exposed (compared to those in Figure 26). (B) The strains described in part A were harvested at the indicated time points after the addition of cycloheximide, and cell extracts were prepared and subjected to SDS-PAGE and immunoblotted for Add66p-*myc* and Sec61p (as a loading control). The amount of Add66p-*myc* at the start of the chase in each strain, after standardization to the amount of Sec61p at each time point, was set to 100%: (O), MG-132; (●), DMSO control. The data represent three independent experiments, +/- SD, with p values of 0.0812 (30 min), 0.0323 (60 min), and 0.0065 (90 min) when comparing the strain with and without MG132 treatment.

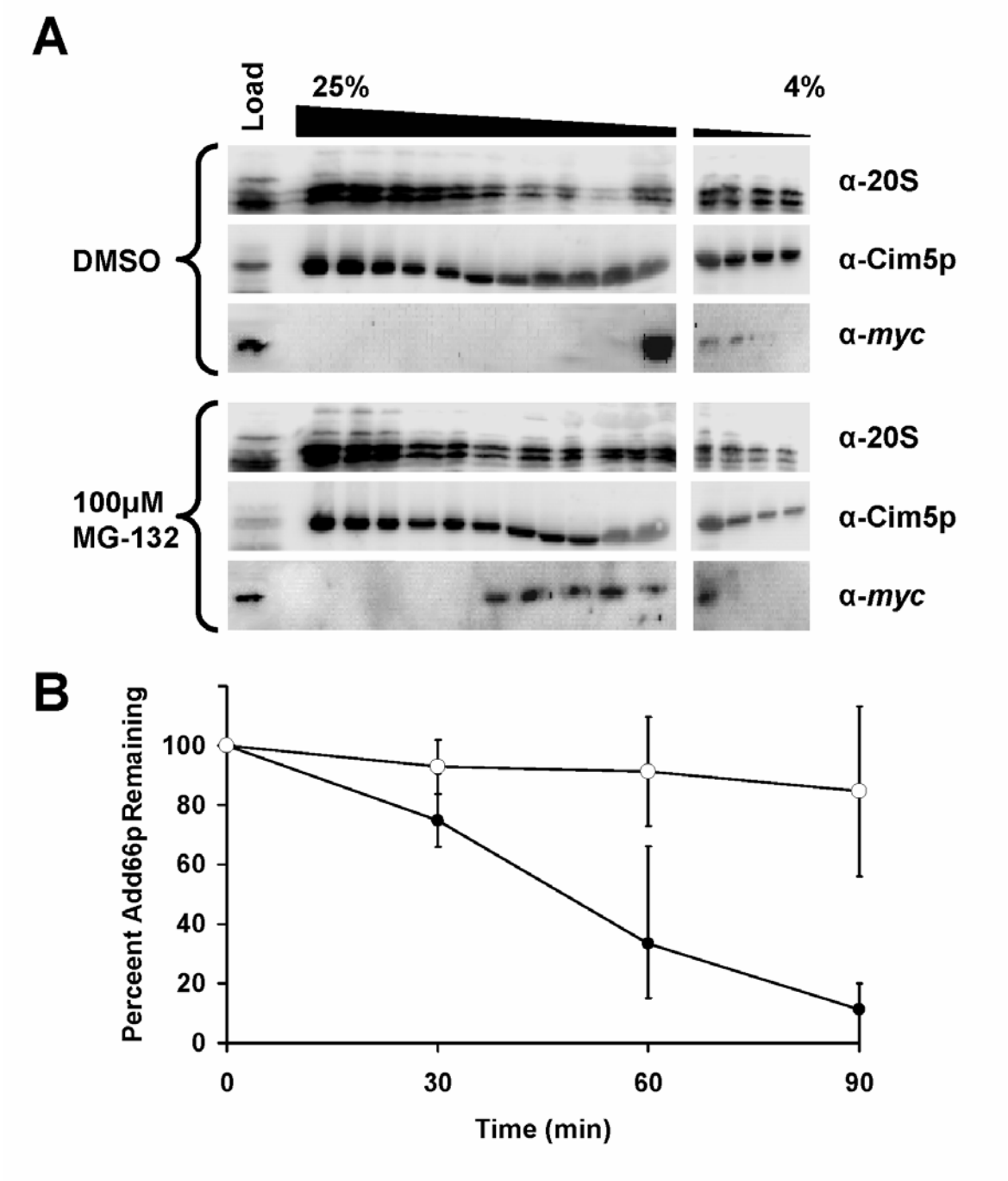

Figure 29. Add66p is degraded by the 26S proteasome

from *add66Δ* and *ump1Δ* strains (Figure 26) when the blots were over-exposed (data not shown).

Next, to examine whether Add66p, like several other proteasome chaperones, is degraded by the proteasome, a cycloheximide chase was performed in the presence or absence of MG-132. Once again, the *pdr5Δ* strain was transformed with a plasmid engineered for the constitutive expression of Add66p-*myc* and the cells were incubated with either DMSO or MG-132 for 1 hour prior to the chase (Figure 29B). Although Add66p was rapidly degraded in cells treated with DMSO, I discovered that the addition of MG-132 to wild type yeast cells resulted in a profound, reproducible stabilization of the protein, indicating that Add66p is a proteasome substrate.

2.3.10 A1PiZ expression in the *add66Δ* yeast strain

Even though the *add66Δ* strain displayed no visible phenotype when incubated on media supplemented with various carbohydrates or chemicals and incubated at elevated temperatures (Table 1), I observed a significant growth defect in ~15% of A1PiZ-expressing *add66Δ* cells (see Figure 30 for one example). Furthermore, these *add66Δ* cells had not obtained secondary mutations in the gene required for galactose utilization (Figure 30 last panel); i.e. a gal- phenotype might have given rise to this observation. This was shown by rescuing the A1PiZ-expression vector from *add66Δ* strains that were either inviable or viable on galactose-containing media, and then retransforming them with the expression vector. I found that this phenomenon most commonly arose stochastically since in any given transformation ~15% of the transformants containing the pGAL A1PiZ expression vector failed to grown on galactose (data not shown).

Figure 30. Over expression of A1PiZ in *add66Δ* yeast can result in lethality.

Ten-fold serial dilutions of *ADD66* and *add66Δ* transformed with either control plasmids or plasmids expressing A1PiM or A1PiZ (all of which were *URA*-marked) under the transcriptional control of a galactose inducible promoter were grown at 30°C for 48 h on YPD, SC-URA+GLC, or SC-URA+GAL (left half of figure). The growth defect in the *add66Δ* strain expressing A1PiZ in the presence of galactose was seen in ~15% of transformants after 50 individual transformants were examined (one transformant in which this phenomenon was observed is denoted by an asterisk, and a transformant in which growth was unaffected is denoted by a double-dagger). To establish that the lethal phenotype was not because the cells had become auxotrophic for galactose utilization (i.e., Gal-), the following protocol was followed: *add66Δ* strains transformed with either a control plasmid or a plasmid containing A1PiM or A1PiZ under the transcriptional control of a galactose inducible promoter were re-plated three times in the presence of 5FOA (in order to select for cells lacking the expression vector). Next, the resulting cultures (right half of figure) were serial diluted on 5FOA (to confirm selection for yeast lacking vector), SC-URA+GAL (to confirm that the yeast did indeed lack the *URA*-marked vector), or SC-URA+GAL (to confirm the Gal+ phenotype).

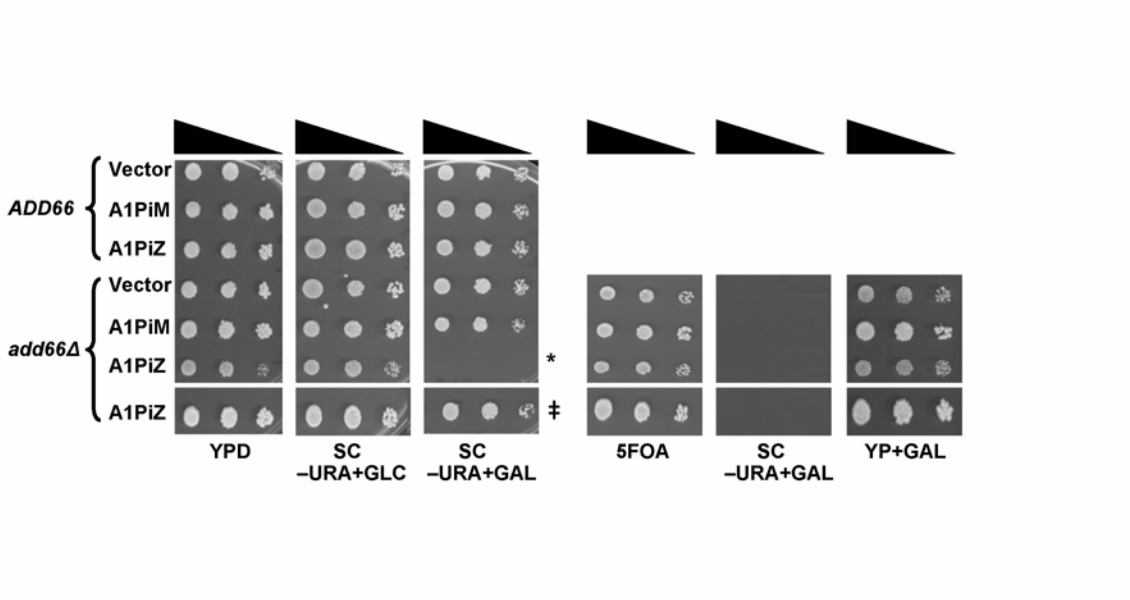

Figure 30. Over expression of A1PiZ in *add66Δ* yeast can result in lethality

Because it has been proposed that generic variations and/or stochastically elevated expression levels might modify the degradation efficiency and/or solubility of proteins associated with conformational diseases (Perlmutter, 2002; Kamimoto *et al.*, 2006), I reasoned that this phenomenon might have been recapitulated in A1PiZ-expressing yeast. One possibility is that the protein is expressed at different levels in each yeast cell, and that only *add66* mutants expressing the highest levels of A1PiZ were inviable. To test this hypothesis, I measured the A1PiZ expression levels by immunoprecipitation of radiolabeled A1PiZ at early time points after A1PiZ expression was induced in *add66Δ* cells that either succumbed (GD) or survived (ND). Examination of A1PiZ expression within 4 hours of A1PiZ induction showed that cells that succumbed to a growth defect did so within 2 hours of induction (i.e., a switch from glucose to galactose containing media (data not shown)). However, the level of A1PiZ expression within 2 hours of induction was identical in both strains (Figure 31).

Because the *add66Δ* growth defect shown in Figure 30 represents the stationary phase of growth, a series of growth curves were calculated from dividing *ADD66* and *add66Δ* strains on selectable media containing various carbon sources that affect A1PiZ expression system (Figure 32). Very little growth was observed over the time course in the wild type and *add66Δ* strains transformed with an expression vector inserted with A1Pi in selectable media containing 2.0% galactose (data not shown). In an effort to regulate the levels of the galactose inducible promoter, media containing 0.2% glucose and 2.0% galactose was utilized to limit the expression of AT. *ADD66* strains showed no defect in the doubling time when containing an empty

Figure 31. Expression of A1PiZ in different *add66Δ* strains

Representative image from a radiolabeled immunoprecipitation of A1PiZ expression in various yeast strains. Equivalent levels of cells from *add66Δ* strains that eventually either succumbed (GD) or survived (ND) induction of A1PiZ or an *add66Δ* strain containing an empty vector (V) were radiolabeled for 2 hours. Cells were lysed and immunoprecipitated for BiP (as a loading control) and A1PiZ. Cells that eventually succumbed to A1PiZ expression were still viable at this time point.

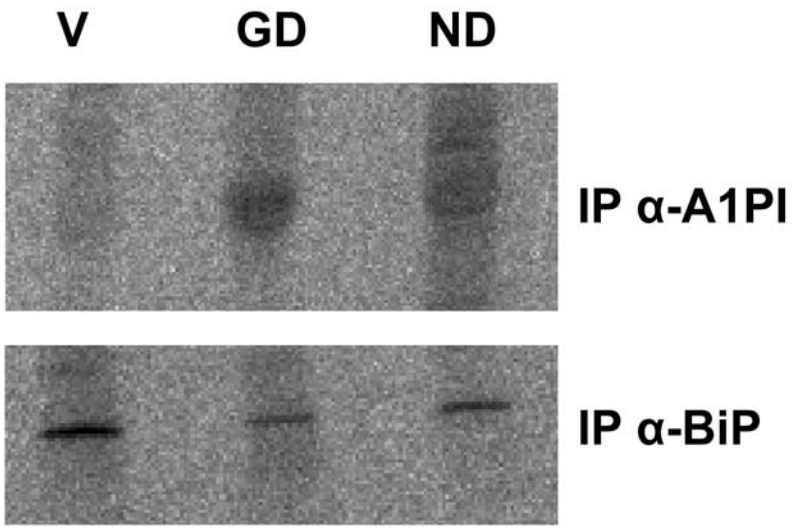

Figure 31. Expression of A1PiZ in different *add66Δ* strains

Figure 32. *add66Δ* yeast that succumb to A1PiZ expression stop growing at relatively early times when A1PiZ is induced.

Wild-type and *add66Δ* strains were transformed with expression plasmids containing A1PiM or A1PiZ under the control of a galactose inducible promoter or with the expression vector lacking an insert (pYes2). Equivalent numbers of transformed cells were grown for 18 h in selectable medium containing 2.0% raffinose and then switched to selectable media containing 2.0% glucose (Glc), or 2.0% galactose and 0.2% glucose for a 12 h time course at 30° C. Every 2 h the optical density (OD at 600 nm) of the culture was determined by a spectrophotometer and charted on a log scale.

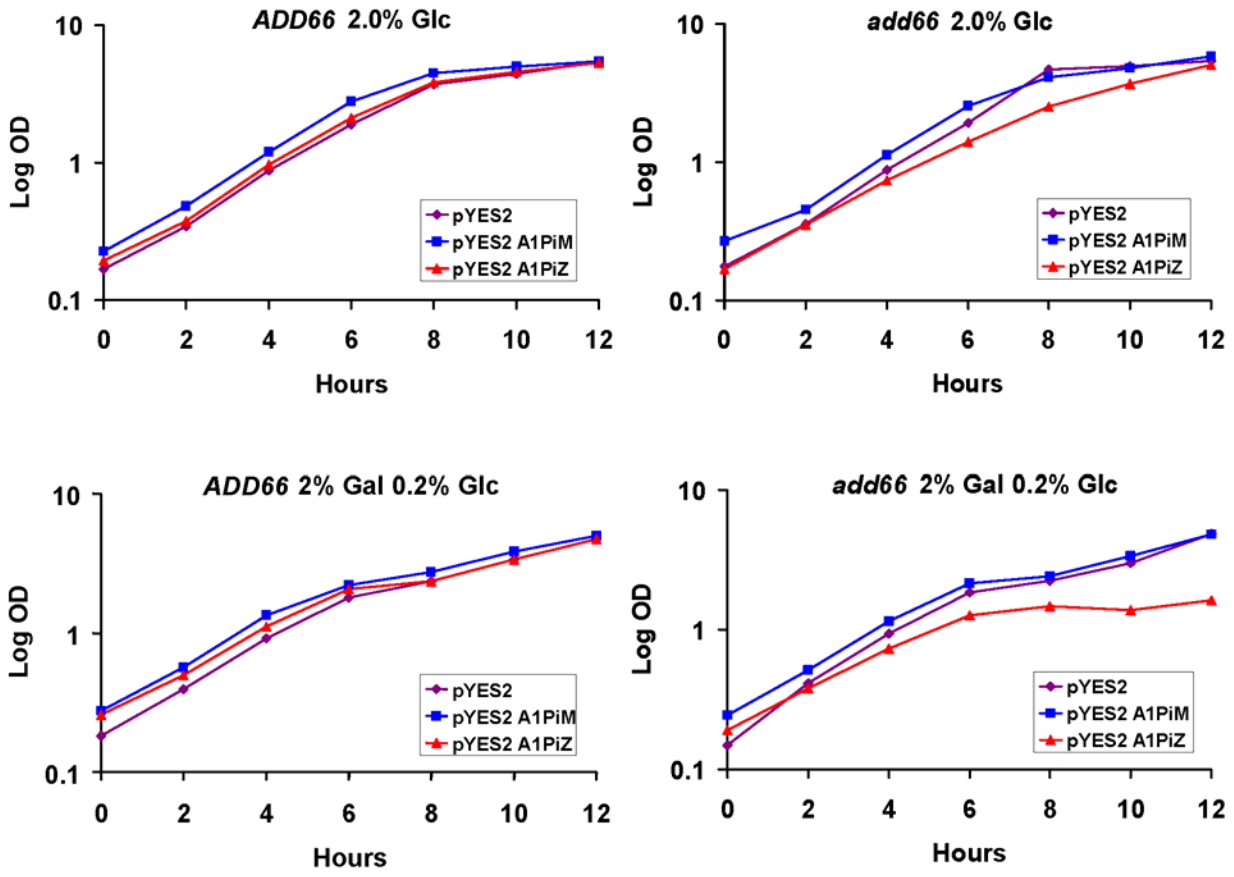

Figure 32. ***add66Δ*** **yeast that succumb to A1PiZ expression stop growing at relatively early times when A1PiZ is induced**

expression vector or a vector expressing wild type (A1PiM) or the Z mutant. In contrast, a significant defect in the doubling time was observed in *add66Δ* pYes2A1PiZ yeast (that succumbed to A1PiZ expression) after 8 hours, which is most likely due to the accumulation of high levels of the toxic A1PiZ polymer in the cells (Kruse *et al.*, 2006). Furthermore, *add66Δ* strains that do not succumb to A1PiZ expression did not show a similar defect (data not shown). Overall, the nature of this growth defect in A1PiZ expressing yeast is not clear.

2.3.11 PAC2 over-expression enhances A1PiZ degradation HELA cells.

As shown in Figure 25, Dr. Jeffrey Brodsky noted that a region in a mammalian protein exhibits low sequence identity with Add66p; during the course of my studies, a similar finding was reported by the Murata lab and the mammalian protein was characterized as PAC2, proteasome assembly chaperone-2 (Hirano *et al.*, 2005). PAC2 was also recently noted by the Hochstrasser lab to share 19% identity with *ADD66*, which they called *PBA2* for proteasome biogenesis associated polypeptide (Li *et al.*, 2007). Because PAC2 is expressed in hepatocytes (Wang *et al.*, 2001), the tissue in which A1Pi is synthesized, and because PAC2 over-expression accelerates proteasome biogenesis (Hirano *et al*., 2005), I hypothesized that PAC2 over-expression might help clear A1PiZ in mammalian cells. In collaboration with the Perlmutter lab, I cloned PAC2 into a mammalian expression vector (See section 2.2.3). Subsequently, Béla Schmidt of the Perlmutter lab utilized a HeLa cell line that stably expresses A1PiZ (Teckman *et al.*, 2001) and these cells were transiently transfected with vectors to drive the expression of PAC2 or GFP. We found that the HeLa cells over-expressing PAC2 showed a concentration-dependent reduction in the amount of A1PiZ, whereas the levels of A1PiZ were unaffected in cells transfected with equal amounts of the GFP-encoding DNA (Figure 33). These data suggest

Figure 33. PAC2 over expression enhances A1PiZ clearance in HeLa cells**.**

HeLa cells stably expressing A1PiZ were transiently transfected with pcDNA3.0 containing either the PAC2 or GFP coding sequences in the amounts indicated. Cells were harvested, and cell extracts were prepared and subjected to SDS-PAGE. Western blots for A1PiZ, GFP, and GADPH (as a loading control) were then performed.

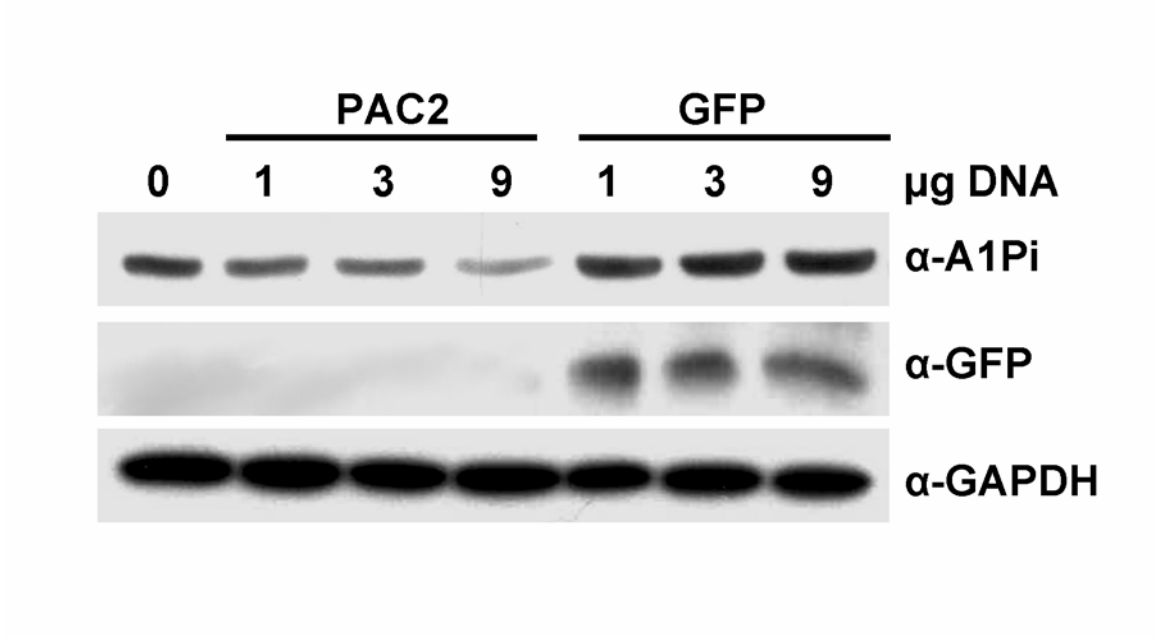

Figure 33. PAC2 over expression enhances A1PiZ clearance in HeLa cells

that PAC2 plays a role in the clearance of A1PiZ, perhaps similar to the role that Add66p plays during the degradation of A1PiZ in yeast (Palmer *et al.*, 2003).

3.0 THE REGULATION OF *ADD66* DURING THE UNFOLDED PROTEIN RESPONSE

3.1 INTRODUCTION

The accumulation of unfolded proteins in the endoplasmic reticulum (ER) activates a transcriptional induction process termed the unfolded protein response (UPR) (Kaufman, 1999; Patil and Walter, 2001). In *Saccharomyces cerevisiae*, the basic leucine zipper containing transcription factor Hac1p is responsible for transcriptional induction of a relatively small number of the approximately 380 UPR-target genes that have been identified (Cox and Walter, 1996; Mori *et al.*, 1996; Travers *et al.*, 2000). The transcription of many other UPR targets appear to be activated by the Gcn4p transcription factor, which is not sufficient to bind UPR targets during permissive conditions; however up-regulation of the gene, as seen during ER stress, does cause an induction of the UPR (Patil *et al.*, 2004). In any event, targets of the UPR include ER localized molecular chaperones, components of the ER-associated degradation machinery, and numerous proteins involved in various aspects of the secretory pathway. These proteins alleviate the accumulation of unfolded proteins residing within the ER. Induction of these UPR targets is crucial for ER homeostasis under stress conditions and cells unable to induce the UPR are highly sensitive to ER stress (Kaufman, 1999; Patil and Walter, 2001).

The expression and activity of Hac1p are tightly regulated at the level of mRNA splicing.

HAC1 mRNA is constitutively synthesized but contains an un-spliced intron under non-stress conditions (Cox and Walter, 1996; Kawahara *et al.*, 1997). Splicing of *HAC1* precursor mRNA is initiated by Ire1p-mediated processing, and is the result of ER stress (Sidrauski and Walter, 1997). Ire1p is a transmembrane protein kinase with endoribonuclease activity, and is activated by ER stress-induced homodimerization and subsequent autophosphorylation (Cox *et al.*, 1993; Mori *et al.*, 1993; Shamu and Walter, 1996; Welihinda and Kaufman, 1996). It is not yet clear how unfolded ER proteins activate the cytosolic nuclease activity of Ire1p.

Splicing regulates the activity of Hac1p in two ways. First, Hac1p is synthesized only after splicing occurs, since the *HAC1* intron inhibits translation (Kawahara *et al.*, 1997). Second, activity of Hac1p artificially translated from spliced mRNA is much stronger than that of Hac1p translated from un-spliced mRNA. This is the result of the DNA-binding domain being encoded by the first exon, whereas the activation domain is encoded by the second exon (Mori *et al.*, 2000). Regardless, the subsequent activation of Hac1p target genes in the nucleus occurs via direct binding to a *cis*-acting UPR element (UPRE) (Mori *et al.*, 1992; Mori *et al.*, 1998). The UPRE was originally defined as a 22-bp sequence that up-regulates the transcription of *KAR2*, the gene that encodes yeast BiP (ER lumenal Hsp70p) (Mori *et al.*, 1992). The necessity of the 22-bp sequence has since been simplified to a 10-bp core sequence and has subsequently been reduced to an essential seven nucleotide E-box-like palindrome (CAGNGTG) (Mori *et al.*, 1998).

In this chapter, I report on the characterization of a nucleotide sequence up-stream of the coding region of *ADD66*, which is likely involved in its transcriptional regulation during times of ER stress. The *ADD66* gene is known to be up-regulated during ER stress via the UPR and strains lacking *ADD66* initiate the UPR (Travers *et al.*, 2000; Palmer *et al.*, 2003). Furthermore,

the nucleotide sequence that I identified upstream of *ADD66* shows similarity to the consensus sequence recognized by Hac1p, suggesting that Hac1p may regulate *ADD66*. Interestingly, the putative UPRE resides in the gene upstream of *ADD66*, which is known as *LOS1*.

3.2 MATERIALS AND METHODS

3.2.1 Strains and growth conditions

An *add66Δ* disruption cassette was obtained by amplifying pRS400 (Brachmann *et al.*, 1998) with the following oligonucleotides: 5' ACT TCA GGA AAG AAT AGC ACA AAA CCC AAA GGA ACA TAC GCT GTG CGG TAT TTC ACA CCG 3' and 5' ATA TAT GCA CTT GTA TAG AAA ACA GAT ATA CTT CTC GGT TAG ATT GTA CTG AGA GTG CAC. An *los1Δ* disruption cassette was obtained by amplifying pRS400 (Brachmann *et al.*, 1998) with insertion of a *KanMX* gene utilizing the following oligonucleotides: 5' AAG CAA CCT ATA GAA CAA GTG TTT CCA GTC AAA TCG AGG ACT GTG CGG TAT TTC ACA CCG 3' and 5' TAT TCT TAT TTA CGG AGG TGG CTG TGA CTG CAG TGT CTA TAG ATT GTA CTG AGA GTG CAC 3'. *ADD66* and *LOS1* mutants were then isolated on G418-containing medium as previously described (Brachmann *et al.*, 1998).

All yeast strains used in this study are detailed in Table 2 (located in Appendix A) and were grown on yeast extract-peptone (YP)-dextrose (YPD (2%)) medium. Yeast were grown at the indicated temperatures and all genetic and molecular manipulations followed standard published protocols (Adams *et al.*, 1997).

3.2.2 mRNA isolation and analysis

A single yeast colony was inoculated into 2 ml of YPD incubated over night at 30° C with vigorous shaking. The culture was diluted into 10 ml of YPD (pH 5.4) to an OD (optical density measured at 600 nm) of 0.25 and grown for 4 h at 30°C with vigorous shaking to obtain mid-log phase cells. Ten ODs of cells were harvested and resuspended in YPD adjusted to pH 5.4 and supplemented either with or without 2 mM DTT and incubated at 30° C with vigorous shaking for 2 h. A total of 5 ODs of cells were harvested by centrifugation at 3000 rpm for 5 min in a clinical centrifuge. Cells were then resuspended in 0.2 ml of RNA buffer ((0.5 M NaCl, 0.2 M Tris-HCL (pH 7.6), 1.0% SDS). A total of 0.2 g of glass beads were added, and lystates were prepared by vigorous agitation on a Vortex mixer five times for one min with a one min incubation in an ice bath between each treatment. Total RNA was isolated utilizing the RNeasy Mini kit (Qiagen) in conjunction with the standard protocol provided by the manufacturer. RNA concentration and purity were determined spectrophotometrically by measuring the A_{260} and A_{280}. Only samples with a ratio of A_{260}/A_{280} higher than 1.8 were used. Aliquots of all RNA samples were frozen and stored at -20°C.

Reverse transcription (RT) was conducted by utilizing random primers (Hexanucleotide Mix (Roche)), dNTP mix (Applied Biosystems), and the company-supplied protocol for the Super Script II Reverse Transcriptase (Invitrogen) kit with the following thermacyclic protocol: 1 cycle of 25 C° for 10 min, 37 C° for 1 hr, 72 C° for 10 min, 23 C° for 10 min and finally stored at 4 C°. Subsequent PCR reactions were performed to examine actin and *ADD66* mRNA levels in accordance with the GoTaq PCR Kit (Promega) protocol. *ADD66* mRNA was amplified with 5’ CGC TAT ATA AAG ACG CTG 3’ and 5’ GAA TAT ACC TCC TGT GGA CG 3’ primers

and actin was amplified with 5' TGT CAC CAA CTG CGA CGA TA 3' and 5' GGC TTG GAT GGA AAC GTA GA3' primers with the following PCR protocol: 1cycle of 94 C° for 2 min, 30 cycles of 94 C° for 1 min, 45 C° for 1 min, 72 C° for 1 min, 1 cycle of 72 C° for 10 min, and finally store at 4 C°. PCR products were resolved on a 1.0% agarose gel, stained with 2 μg/ml ethidium bromide, and images were obtained on a Kodak 440CF Image Station, and the results were quantified using Kodak 1D (version 3.6) imaging software.

3.3 RESULTS

3.3.1 Identification of a UPRE like sequence within the promoter of *ADD66*

Examining targets of the unfolded protein response as well as their induction level revealed a robust increase in the level of *ADD66* mRNA when cells were treated with ER stress inducing compounds (Casagrande *et al.*, 2000; Travers *et al.*, 2000). Specifically, there was a 9.8 fold increase in *ADD66* mRNA levels in cells treated with tunicamycin to inhibit *N*-linked glycosylation (Travers *et al.*, 2000). Expression of mouse major histocompatability complex class I heavy chain (H-2K^b), an ERAD substrate when unassembled but stable when the UPR is compromised, increased *ADD66* mRNA 2.5-fold (Casagrande *et al.*, 2000). Taken together, *ADD66* apears to be a *bona fide* UPR target, although examination of the 5' UTR of *ADD66* failed to detect a UPRE (Travers *et al.*, 2000). One caveat of that initial search was that only previously described UPRE sequences (as observed in *KAR2)* were sought. The original 22-bp UPRE sequence has subsequently been reduced to an essential seven nucleotide E-box-like palindrome (CAGNGTG) (Mori *et al.*, 1992; Mori *et al.*, 1998), which again was not detected

upstream of *ADD66*, at least in the region between *ADD66* and *LOS1* (Figure 34A). However, expansion of the search criteria yielded a putative *ADD66* UPRE 284 bps upstream of the coding region of *ADD66* and residing in the correct orientation to induce *ADD66* expression. Interestingly, this putative UPRE is located within the coding region of the neighboring gene, *LOS1*. *LOS1* is a nonessential tRNA alternate splicing enzyme located 249 base pairs upstream of *ADD66* (Yoshihisa *et al.*, 2003). The putative *ADD66* UPRE maintains 6 of the 7 essential nucleotides described as the E-box-like palindrome (Figure 34B). Furthermore, comparisons of this region of DNA in three other yeast strains show a conservation of these nucleotides, suggesting an important function for this sequence (Figure 34B).

3.3.2 The *ADD66* UPRE is necessary for *ADD66* mRNA induction during ER stress

Given the similarity of the *ADD66* UPRE to the *KAR2* UPRE, and given that this sequence is conserved within different yeast specieis, I predict that this putative UPRE sequence would be required to provide maximal induction of *ADD66* during the unfolded protein response. In order to examine this hypothesis, a series of yeast strains were constructed or obtained from other sources (Figure 35). The *add66Δ* and *los1Δ* strains in the BY4742 background were constructed by disrupting the desired gene with a *KANMX* cassette (Brachmann *et al.*, 1998). The final two isogenic strains, in the W303-1A strain background, were obtained from the Endo lab, which included a wild type as well as a second *los1Δ* strain. The second *los1Δ* strain had the majority of the *LOS1* gene disrupted, by an *ADE2* cassette, but retained the region that contained the putative *ADD66* UPRE (Figure 35A MT3) (Yoshihisa *et al.*, 2003).

Figure 34. The *ADD66* promoter contains a UPRE-like sequence and is conserved in four different *Saccharomyces* species

(A) A simple diagram of the chromosomal locations of the putative *ADD66* UPRE (red) in relation to the coding regions of the *ADD66* (blue) and *LOS1* (green) genes. Arrows indicate the direction of transcription from *ADD66* (Crick stand) and *LOS1* (Watson strand). (B) Nucleotide sequence alignment of the putative UPRE for *ADD66* in four different yeast species compared to the *KAR2* UPRE. Sequences were obtained from the *Saccharomyces* Genome Database (http://www.yeastgenome.org/). Bold type face shows identity with the *KAR2* UPRE, which is 153-bp upstream of the *KAR2* start site. The putative *ADD66* UPRE is 284-bp upstream of the start site and is in the correct orientation to induce *ADD66* expression. Red type face indicates the E-box-like palindrome. Underline shows the core 10 base pair element.

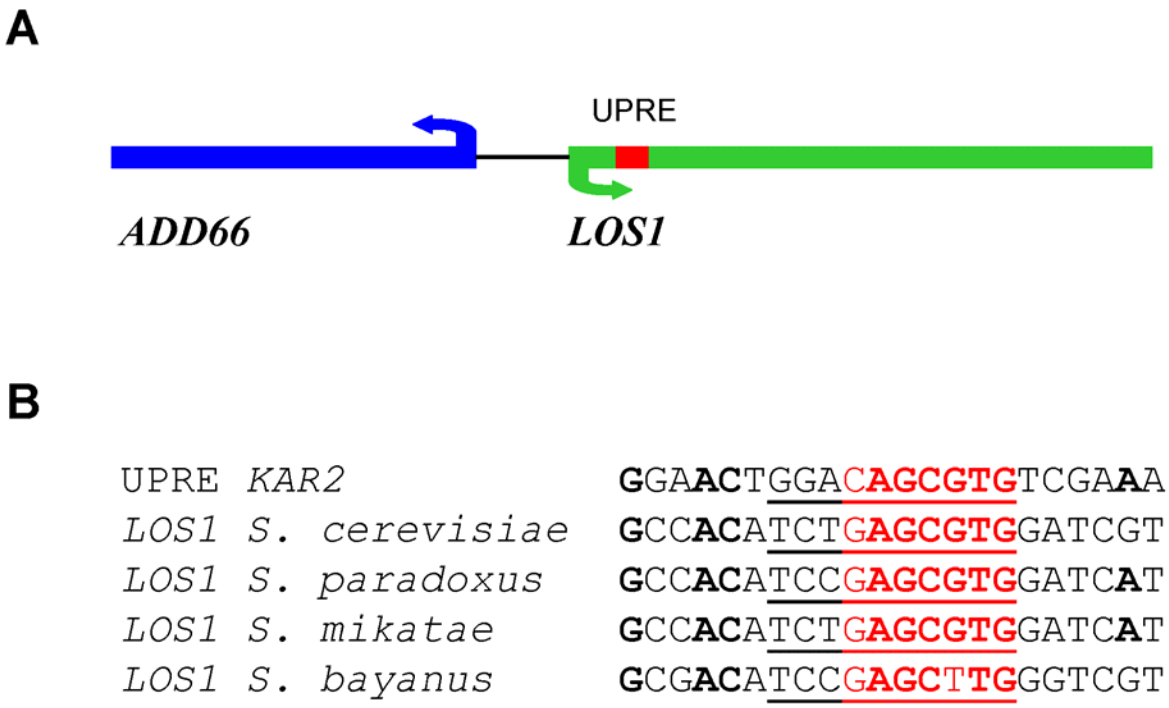

Figure 34. The *ADD66* promoter contains a UPRE-like sequence and is conserved in four different Saccharomyces species

Figure 35. *ADD66* strains used to examine UPR regulation

(A) A diagram of the chromosomal locations of the putative *ADD66* UPRE (red) in relation to the coding regions of the genomic *ADD66* (blue) and *LOS1* (green) genes. The *ADD66* (WT1; BY4742) strain is isogenic to *add66Δ* (MT1) and *los1Δ* (MT2) strains. MT1 and MT2 are disruptions with the insertion of a *KANMX* gene (black). The other *ADD66* wild type (WT2; W303-1A) strain is isogenic to *los1Δ* (MT3) in which *LOS1* is replaced with *ADE2* (grey) while still maintaining the putative *ADD66* UPRE. All strains are described in Section 3.2.1 and in Table 2, located in Appendix A. The *ADD66*, *LOS1*, *KanMX*, and *ADE2* genes are presented in relative size to each other. Asterisks denote the locations of primers utilized for the RT-PCR of *ADD66,* as presented in Figure 36. (B) PCR products corresponding to the regions of the *ADD66* (left panel) and *LOS1* (right panel) genes in the five strains indicated above. Primers utilized for this PCR are detailed in section 3.2.1. The sizes of the PCR products are shown to the left of the figure.

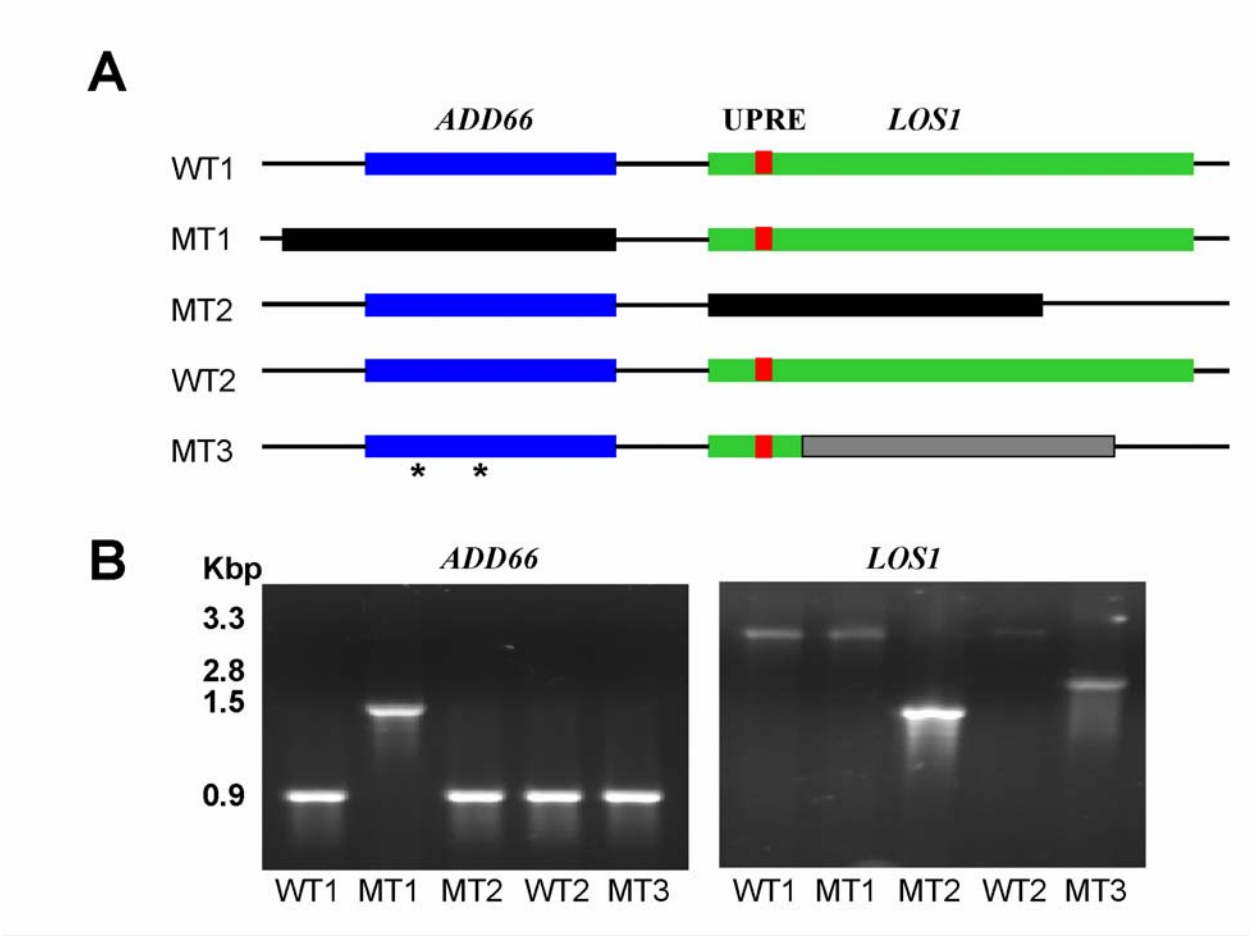

Figure 35. ***ADD66*** **strains used to examine UPR regulation**

To examine *ADD66* mRNA induction during ER stress, mid-log phase yeast cells were subjected to 2 mM DTT to increase the propensity of misfolded proteins within the ER (Travers *et al.*, 2000). Cells under identical conditions were also mock-treated. Cells treated with DTT that contained the putative *ADD66* UPRE showed an increase in the levels of *ADD66* expression (Figure 36A, WT1, WT2, and MT3). As predicted, strains that did not contain putative *ADD66* UPRE maintained basal levels of mRNA induction when treated with DTT (Figure 36A, MT2). Furthermore, there was a significant difference between the level of *ADD66* mRNA induction when comparing the two different yeast genotypes. The BY4742 *ADD66* strain incubated with DTT showed a 2.3 fold increase in expression of *ADD66* mRNA compared to non-treated cells, whereas the W303-1A strain exhibited a 7.9 fold increase. Taken together, these very preliminary data suggest that the region containing the putative *ADD66* UPRE is necessary for transcriptional induction during the unfolded protein response.

Figure 36. The *ADD66* UPRE facilitates *ADD66* mRNA induction during ER stress

RT-PCR was performed on the *ADD66* (BY4742; WT1), *add66Δ* (BY4742; MT1), *los1Δ* (BY4742; MT2), *ADD66* (W303-1A; WT2), and *los1Δ* (W303-1A; MT3) strains. (A) Relative fold increase of *ADD66* mRNA expression when cells were incubated with 2mM DTT (black bars) or the equivalent volume of water (white bars) for 2 hours at 30° C. The RT-PCR product was obtained by amplifying an internal region of the *ADD66* gene (Figure 35, asterisks). Quantification of each PCR product was determined by measuring the intensities of the various products, and then normalizing these values to the levels measured for the actin RT-PCR product. The relative fold increase was subsequently determined by normalizing each RT-PCR product to the product from the untreated isogenic WT strain, which was set to 1. (B) The agarose gels used to amass the data for part A are presented. Each strain was treated with (+) or without (-) DTT as indicated. It is important to note that these data represent one experiment utilizing one set of PCR parameters. In addition, the mRNA might not be within the linear range for the assay.

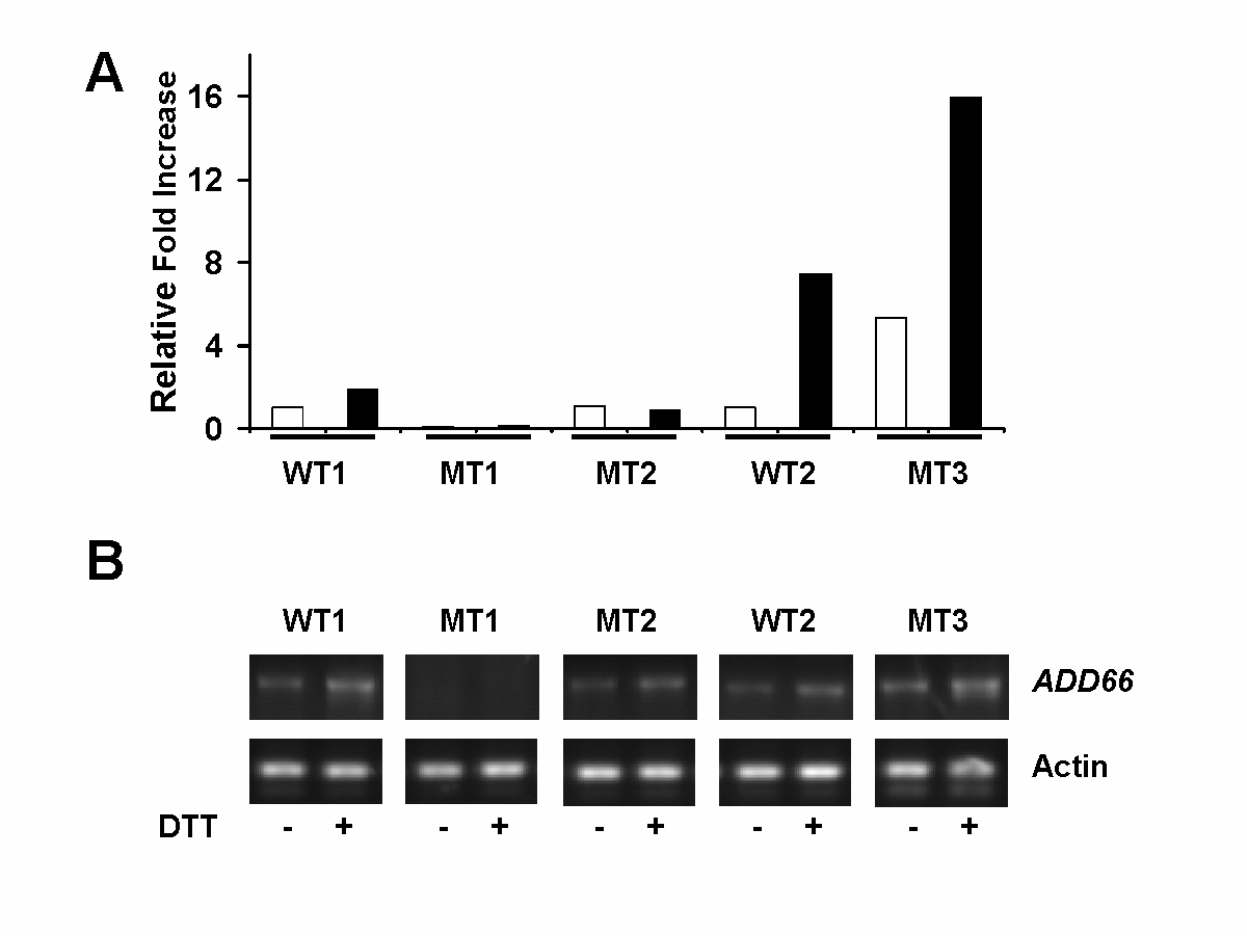

Figure 36. The *ADD66* UPRE facilitates *ADD66* mRNA induction during ER stress

4.0 DISCUSSION

4.1 INTRODUCTION

In this chapter I will revisit the data presented in this dissertation from chapters two and three and discuss the significance and relevance of these findings. Furthermore, I will present these findings in the context of what is currently known about proteasome assembly, maturation, and activity and the regulation of *ADD66* during the unfolded protein response.

4.2 *ADD66* IS REQUIRED FOR MAXIMAL CHYMOTRYPSIN-LIKE ACTIVITY OF THE 26S PROTEASOME

In this dissertation I presented the characterization of Add66p (Chapter 2), a protein previously implicated in the ERAD of A1PiZ in yeast (Palmer *et al.*, 2003). I found that strains deleted for *ADD66* accumulate polyubiquitinated proteins and grow poorly when they are unable to mount a UPR upon being challenged with a UPR-inducing agent. These data can be explained by my discovery that the CTL activity of the proteasome is compromised in *add66Δ* yeast. Yeast deleted for *ADD66* also accumulate the similar proteasome assembly intermediates as those observed when the gene encoding the Ump1p proteasome assembly factor is disabled. My observations are consistent with the fact that Add66p is found in a multi-protein complex that

includes Pre1p and Pre5p—proteins embedded within the 20S core particle—as well as Ump1p itself (Ho *et al.*, 2002; Krogan *et al.*, 2006). Based on these data, I propose that Add66p is a yeast proteasome assembly chaperone (PAC, discussed below) and is vital for maximal proteasome function.

A surprising aspect of this research was that deletion of *ADD66* appeared to affect the CTL activity of the 26S proteasome, whereas there were no obvious defects in the TL and PGPH activities. This is in contrast to the fact that all three activities are decreased in an *ump1Δ* strain (Ramos *et al.*, 1998). I propose two explanations for this phenomenon. First, Ump1p may have a global effect on proteasome activity due to its role as an assembly checkpoint during the dimerization of half proteasomes (Li *et al.*, 2007). Thus, deletion of *UMP1* may result in a significant accumulation of defective dimers or other intermediates, thus reducing the level of functional 26S proteasomes. In contrast, the Add66p-dependence during proteasome maturation may give rise to subtle changes in proteasome assembly or even in the conformations of individual, catalytic subunits or associated subunits. Consistent with this model, more severe proteasome assembly defects were noted in *ump1Δ* versus *add66Δ* mutants when intermediates were resolved by gel filtration chromatography (Ramos et al., 1998; Li et al., 2007). Second, more trivially, I note that neither the TL nor PGPH activities was measured when the activities of specific proteasome assembly factors were ablated (Tone and Toh, 2002; Hirano *et al.*, 2005; Hirano *et al.*, 2006). Therefore, it remains possible that unique effects on proteolytic activities do exist when related PACs are disabled, at least in some cell types or under specific conditions.

4.3 ADD66P FACILITATES EFFICIENT PROTEASOME ASSEMBLY

The recent characterization of PACs in both yeast and mammals have yielded new insights into the previously described pathway of proteasome biogenesis (Chen and Hochstrasser, 1995, 1996; Heinemeyer *et al.*, 1997; Ramos *et al.*, 1998; Arendt and Hochstrasser, 1999; Burri *et al.*, 2000; Griffin *et al.*, 2000; Tone *et al.*, 2000; Witt *et al.*, 2000; Tone and Toh, 2002; Ramos *et al.*, 2004; Hirano *et al.*, 2005; Hirano *et al.*, 2006; Li *et al.*, 2007). The symmetrical, 20S barrel-shaped core particle (CP) of the proteasome is comprised of two half-proteasome (15S) complexes (Nandi *et al.*, 1997). These half-proteasomes contain a ring of alpha subunits and a ring of beta subunits, three of which are responsible for the CP's proteolytic activity and must be processed (Figure 3). In mammals, after the two 15S complexes combine, the "pro" regions in the beta subunits are cleaved and a cohort of PACs—including hUmp1 (also known as POMP or Proteassemblin), PAC1, PAC2, and PAC3—participate in complex formation. PAC1 and PAC2 have been proposed to maintain the assembly-competence of the alpha ring and are degraded after the assembly of the two half proteasomes; in contrast, PAC3 assists in the assembly of the beta ring before dissociating from the complex. PAC3 also recruits hUmp1, which later catalyzes the dimerization of the two half-proteasomes; in yeast Nob1p helps glue the 19S particle to the CP (Tone and Toh, 2002; Hirano *et al.*, 2005; Hirano *et al.*, 2006). Based on my results and data derived from studies of PAC2 function in mammalian cells (Hirano *et al.*, 2005; Hirano *et al.*, 2006), I propose that Add66p is the *S. cerevisiae* homologue of PAC2: [1] The proteins are ~20% identical throughout their sequence; [2] Both factors are proteasome substrates; [3] Lowering protein levels (by RNAi in mammalian cells) or completely ablating the gene (in yeast) leads to the accumulation of CP precursors, increases the concentration of

polyubiquitinated proteins, and decreases the proteasome's CTL activity; and [4] MG-132 treatment in each cell-type results in the accumulation of the protein in heavier (larger complexes) fractions after glycerol gradient centrifugation.

Very recent work from Hochstrasser and colleagues reported that Add66p (which they named Pba2p, for proteasome biogenesis associated polypeptide) associates with another protein (Pba1p) to form a stable complex (Li *et al.*, 2007); the Add66p-Pba1p complex resolves with distinct proteasome assembly intermediates and it was found that deletion of *ADD66* restores the growth of an *ump1Δ* mutant, which is consistent with antagonistic action between Ump1 and the PACs. They also reported that the concentration of a pro-β5 assembly intermediate increased in the *add66Δ* mutant, which is consistent with the intermediate I observe in *add66Δ* yeast (Figure 26 and Figure 27). Combined with the results reported here and with studies in mammalian cells (Hirano *et al.*, 2005; Hirano *et al.*, 2006), these data provide support that Pba1p and Add66p have similar functions as PAC1 and PAC2, respectively.

4.4 ADD66P IS INVOLVED IN THE DEGRADATION OF A DISCRETE SET OF PROTEINS

In contrast to other studies of PAC function in mammalian cells and yeast, I have determined the importance of Add66p on the degradation of a distinct class of proteins. More specifically, I have discovered a link between PAC function and ERAD. In previous work, the Brodsky and McCracken laboratories noted that Add66p facilitates the degradation of some ERAD substrates (A1PiZ and the cystic fibrosis transmembrane conductance regulator, CFTR) but not others (CPY* and pro-α factor) (Palmer *et al.*, 2003). At first glance, these data and the results

presented in this dissertation may seem at odds. If the proteasome is partially disabled in *add66* mutants, why isn't the turn-over of all ERAD substrates affected similarly, especially since any one of the proteasome's three activities may be sufficient to remove an ERAD substrate (Oberdorf *et al.*, 2001)? Consistent with data from other laboratories, I suggest two possible answers to this question:

First, I propose that the rate-limiting step during ERAD differs for unique classes of substrates. Notably, ERAD can be envisaged as a five-step temporal and—for some substrates—spatial process, consisting of substrate identification, retro-translocation, polyubiquitination, deubiquitination, and degradation (Figure 5). In reality, each of these steps is likely further delineated into multiple, discrete kinetic events. Regardless, the overall rate of substrate degradation, as for any multi-step process, is established by the rate-limiting step. For the degradation of some substrates, it has been shown that de-ubiquitination is the rate-limiting step (Yao and Cohen, 2002; Guterman and Glickman, 2004; Hanna *et al.*, 2006). At present, the identity of the DUB that acts on A1PiZ and whether it is proteasome associated are unknown. During ERAD, the removal of a specific substrate class (proteins in the "ERAD-L" family) takes significantly longer than the removal of other substrates (proteins in the "ERAD-C" family). This may be because only ERAD-L substrates can transit to the Golgi apparatus prior to ER-retrieval and degradation (Vashist *et al.*, 2001). Thus, effects arising from impaired proteasome function (Figure 19-22) might be masked by earlier steps in the ERAD process when they are acting as an alternative, rate-limiting step.

Second, it has been proposed that proteasome isoforms exist within cells: those that are stable and those that recycle (Fujimuro *et al.*, 1998; Tone and Toh, 2002). In fact it was later reported that the proteasome disassembles after ATP hydrolysis and substrate degradation

(Babbitt *et al.*, 2005). Combined with the concept that specific proteasome sub-populations may recognize distinct classes of substrates (Fujimuro *et al.*, 1998), it is possible that A1PiZ is degraded by only one of these "classes". Formally then, the deletion of *ADD66* might compromise the assembly of a unique proteasome sub-set, which is required for the degradation of some but not all substrates. Alternatively, the absence of Add66p might alter the proteasome's interaction with the ER membrane. Different ERAD substrates might be delivered from the ER in different conformations, only some of which may require close apposition of the proteasome with the ER and possibly Sec61p, which is the translocation and possibly the retro-translocation channel (Kalies *et al.*, 2005).

4.5 RELATIONSHIP OF *ADD66Δ* YEAST EXPRESSING A1PIZ

One of the long-term goals of my studies is to identify conserved yeast genes that impact the ERAD of distinct substrates. This undertaking is particularly relevant for A1PiZ, given that only a small percentage of *A1PiZ* homozygotes develop severe liver disease (Sveger, 1988). It is believed that both environmental and genetic modifiers play a role in determining the onset and severity of liver disease (Wu *et al.*, 1994; Perlmutter, 2002). Therefore, it is critical that genetic polymorphisms or secondary mutations that alter A1PiZ quality control are identified. Intriguingly, I found that ~15% of *add66Δ* cells expressing A1PiZ are inviable (data not shown, Figure 30 for one example). In principle, one might be able to co-opt this phenotype to screen for second-site or suppressor mutations. It is also possible that the observed genetic penetrance arises from stochastic variability in some cells relative to others: Recent insights into phenotypic variation have led to a greater understanding of the "noise" that accounts for the stochastic nature

of protein production and phenotypic variation, especially in single-cell organisms (Raser and O'Shea, 2004; Newman *et al.*, 2006; Samoilov *et al.*, 2006).

Another explanation for why a sub-population of cells exhibit growth defects (and why a sub-population of individuals with ATD develop liver disease) is that alternate mechanisms exist to clear the ER of A1PiZ. Indeed, it is now established that the autophagic pathway can degrade A1PiZ in mammalian cells (Teckman and Perlmutter, 2000; Kamimoto *et al.*, 2006) and in yeast (Kruse *et al.*, 2006) when the protein is over-expressed. However, I found that the autophagic pathway is active in *add66Δ* cells (Figure 15), suggesting that variations in this alternate mode of protein quality control do not contribute to the toxic effects of A1PiZ, at least in yeast. In the future, it will be important to measure how variations in the efficiency of autophagy, as well as variations in the relative steady-state levels of A1PiZ, impact A1PiZ clearance and liver disease in individuals afflicted with ATD.

4.6 ROLE OF PAC2 IN A1PIZ CLEARANCE

In Chapter 2, I showed that expression of Add66p is required for maximal proteasome activity in yeast, and previous studies have shown that Add66p facilitates the efficient degradation of A1PiZ (Palmer *et al.*, 2003). As noted above, I also propose that Add66p functions similarly to mammalian PAC2 (Hirano *et al.*, 2005; Hirano *et al.*, 2006; Li *et al.*, 2007). Neverless, these data do not address the fundamental question of whether PAC2 plays a role in the regulation of the mutant form of AT in mammalian tissues. In collaboration with the Perlmutter lab, we observed that PAC2 over-expression enhances A1PiZ clearance in HeLa cells (Figure 33).

While these data are extremely encouraging, they are preliminary and difficult to interpret with a high level of confidence. Thus, further investigations will be necessary to determine if PAC2 plays a significant role in the clearance of A1PiZ. Specifically, all three proteolytic activities of the 26S proteasome in cells over-expressing PAC2 must be quantified and compared to control HeLa cells to determine if the over-expression of PAC2 induces higher rates of proteolytic activity. Next, PAC2 knock-down, performed by RNAi as previously published (Hirano *et al.*, 2005), will need to be undertaken to examine the effects on A1PiZ solubility and stability. Finally, it would be interesting to determine if PAC2 decreases the accumulation of A1PiZ observed in the *add66Δ* yeast strain. If the results from the experiments described above are positive, then we can conclude that PAC2 plays a role in the clearance of A1PiZ, perhaps in a manner similar to the one that Add66p plays during the degradation of A1PiZ in yeast (Palmer *et al.*, 2003).

4.7 REGULATION OF *ADD66* DURING THE UNFOLDED PROTEIN RESPONSE

It has been previously shown that *ADD66* mRNA is induced robustly during to the unfolded protein response (Casagrande *et al.*, 2000; Travers *et al.*, 2000). To begin characterizing the regulation of *ADD66* during the UPR, two questions needed to be addressed: First is *ADD66* expression transcriptionally regulated by the transcription factor Hac1p, which is one of the two known transcription factors that up-regulates the 380 genes targeted by the UPR (Mori *et al.*, 1992; Cox and Walter, 1996; Sidrauski *et al.*, 1996; Mori *et al.*, 1998; Travers *et al.*, 2000)? Second, does the *ADD66* promoter contain a *bona fide* UPRE, which is a conserved sequence recognized by Hac1p (Mori *et al.*, 1992; Mori *et al.*, 1998)?

A previous examination of the 5' UTR of *ADD66* did not reveal a UPRE (Mori *et al.*, 1992; Mori *et al.*, 1998; Travers *et al.*, 2000). However, I have expanded the search and identified a putative *ADD66* UPRE, which is located in the correct orientation for proper transcriptional regulation of *ADD66* (Figure 34A). The putative *ADD66* UPRE maintains 6 of the 7 essential nucleotides described as the E-box-like palindrome (Figure 34B). Furthermore, preliminary data suggest that the region containing the putative *ADD66* UPRE is required for maximal induction of *ADD66* mRNA during the UPR (Figure 36).

As stated, these data are preliminary and require further investigations, because only one assay was performed. Replicates should be carried out to determine the significance of the data. Next, it was shown previously that yeast cells treated with 2mM DTT produced a 9-fold induction of *ADD66* mRNA expression (Travers *et al.*, 2000), while I observed only 2- or 5-fold induction (Figure 36A, BY4724 or W303-1A yeast strains respectively). While the parameters to induce ER stress in the yeast cells were similar to previously published methods, the detection of mRNA induction was different. While I performed RT-PCR, the previous study utilized microarray analysis, which could possibly account for the variability I observed (Travers *et al.*, 2000). Finally, it is unknown whether the RT-PCR assay I performed was within the linear range of the assay, which is essential to accurately measure mRNA induction. Thus, the decreased mRNA induction I observed in my initial assay may be masking a true, higher level of induction. It should be noted that in parallel with the *ADD66* induction studies, *KAR2*, a known UPR target, induction was also examined, and no significant increase of expression was observed (data not shown) (Mori *et al.*, 1992; Cox *et al.*, 1993; Mori *et al.*, 1998; Patil *et al.*, 2004). I hypothesize that the lack of *KAR2* induction, which is basally produced at abundant levels (13.6 copies of *KAR2* mRNA per cell versus 0.8 copies of *ADD66* mRNA per cell

(http://web.wi.mit.edu/young/expression/transcriptome2.html), was not detectable via RT-PCR during ER stress, because the substrate was already saturating the system. Thus, further assays will need to be conducted, varying the RT-PCR conditions. Furthermore, real time PCR can be employed to complement this assay. Finally, the deletion of *ADD66* caused sufficient ER stress to induce the UPR, as detected by an *in vitro* β-Galactosidase reporter assay (Palmer *et al.*, 2003). Therefore, I predict that the putative *ADD66* UPRE, cloned as a UAS into the reporter plasmid, would be sufficient to report ER stress. These experiments will be performed in the future.

To induce the UPR, Hac1p binds to the target gene's UPRE (Patil and Walter, 2001; Schroder and Kaufman, 2005). Currently, it is unclear if transcriptional regulation of *ADD66* is conducted by Hac1p. However, the idea of *ADD66* transcriptional regulation by Hac1p is supported by the identification of a putative UPRE. To examine if Hac1p binds upstream of *ADD66*, electrophoretic mobility shift assays (EMSA) will need to be conducted on DNA isolated from yeast strains, under conditions that promote ER stress, containing or lacking the *ADD66* UPRE. It is predicted that the sequence containing the putative *ADD66* UPRE is sufficient to bind Hac1p when these strains are grown in conditions that induce the UPR. The EMSA assay results will be complimented with a chromatin immunoprecipitation (CHIP) assay to verify Hac1p association with the putative *ADD66* UPRE *in vivo*. These two assays will be performed in the future.

4.8 POSSIBLE FUTURE DIRECTIONS OF RESEARCH CONCERNING ADD66P

Beyond the experiments detailed above concerning the regulation of *ADD66* during UPR

induction, future work should be conducted concerning Add66p's role in proteasome assembly and activity. The eukaryotic proteasome is one of the most complex ring shaped macromolecules, and future efforts must focus on the resolution of pre-half proteasome complexes. The isolation of these initial proteasome assembly intermediates and subsequent analysis with tandem mass spectrometry will allow better insights how the proteasome subunits associate with the various PACs, i.e. Add66p, as well as the order of events regarding of subunit assembly. Furthermore, this line of investigation may also isolate yet unidentified PACs.

.

APPENDIX A

YEAST STRAINS USED IN THIS STUDY

Table 2. Yeast strains used in this study

Strain	Relevant Genotype	Reference
ADD66 (BY4742)	MATα *his3Δ1 leu2Δ0 lys2Δ0 ura3Δ0*	Invitrogen
add66Δ	MATα *add66::kanMX his3Δ1 leu2Δ0 lys2Δ0 ura3Δ0*	Invitrogen
ire1Δ	MATα *ire1::kanMX his3Δ1 leu2Δ0 lys2Δ0 ura3Δ0*	Invitrogen
ire1Δ add66Δ	MATα *ire1::kanMX add66::HIS3 his3Δ1 leu2Δ0 lys2Δ0 ura3Δ0*	this study
ADD66 (W303)	MAT**a** *ade2-1 can1-100 his3-11,15 leu2-3,112 trp1-1, urs3-1*	
add66Δ	MAT**a** *add66::kanMX ade2-1 can1-100 his3-11,15 leu2-3,112 trp1-1, ura3-1*	this study
CIM5	MATα *ura3-52 lys2-801 ade2-101 his3Δ200 leu2- Δ1*	Ghislain *et al*, 1993
cim5-1	MAT**a** *cim5-1 ura3-52 his3Δ0200 leu2- Δ1*	Ghislain *et al*, 1993
atg14Δ	MATα *atg14::kanMX his3Δ1 leu2Δ0 lys2Δ0 ura3Δ0*	Invitrogen

pdr5Δ	MAT**a** *pdr5::kanMX his3Δ1 leu2Δ0 ura3Δ0 lys2Δ0 met15Δ0*	this study
JD133	MAT**a** *his3-Δ200 leu2-3,112 lys2-801 trp1-Δ63 ura3-52 UMP1*-ha::YIplac128 *PRE2*-HA::YIplac211	Ramos *et al*., 1998
JD134	MAT**a** *his3-Δ200 leu2-3,112 lys2-801 trp1-Δ63 ura3-52 ump1-Δ1*::*HIS*3 *PRE2*-HA::YIplac211	Ramos *et al*., 1998
add66Δ	MATα *add66::kanMX his3Δ1 leu2Δ0 lys2Δ0 ura3Δ0*	Invitrogen
add37Δ	MATα *add37::kanMX his3Δ1 leu2Δ0 lys2Δ0 ura3Δ0*	Invitrogen
add67Δ	MATα *add67::kanMX his3Δ1 leu2Δ0 lys2Δ0 ura3Δ0*	Invitrogen
add68Δ	MATα *add68::kanMX his3Δ1 leu2Δ0 lys2Δ0 ura3Δ0*	Invitrogen
add66Δ	MATα *add66::kanMX his3Δ1 leu2Δ0 lys2Δ0 ura3Δ0*	Invitrogen
los1Δ	MATα *los1::kanMX his3Δ1 leu2Δ0 lys2Δ0 ura3Δ0*	Invitrogen
RJD1144	MAT**a** *his3Δ200 leu2-3,112 lys2-801 trp1Δ63 ura3-52 PRE1-Flag-HIS6::Ylpac211 (URA3)*	Vera *et al*., 2000
W303-1A	MAT**a** *ura3-1, leu2-1, trp 1-1, his3-11, can1-100 ADE2*	Yoshihisa, 2003
TYSC188	MAT**a** *ura3-1, leu2-1, trp 1-1, his3-11, can1-100 ADE2 los1::URA3* (W303-1A)	Yoshihisa, 2003

APPENDIX B

HEAT SHOCK PROTEIN (HSP101) EXPRESSION IN *ARABIDOPSIS THALIANA* UNDER CONTROLLED THERMAL CONDITIONS

B.1 INTRODUCTION

Global warming as well as climate shifts have presented a unique ecological situation in regards to plant tolerance and fitness. The ability or the inability to adapt to various and sudden temperature shifts can result in a decrease in an individual's or species' fitness as well as biodiversity in a natural community of plants. Previous examination of plant thermal tolerance, specifically crop plants, demonstrated a decrease in corn crop yield when the plants experienced a temperature increase during the growing seasons (Lobell and Asner, 2003). High temperature affects organisms by causing membrane integrity loss, protein inactivation and denaturation, and metabolic and cellular disequilibrium, which may ultimately lead to cellular death (Quinn, 1988; Lindquist, 1992; Los and Murata, 2000). However, most plant species have an innate capacity to survive high temperature stress and can sense and acclimate to high temperatures with metabolic and cellular adjustments. This allows some level of tolerance to heat extremes that would otherwise be lethal. This process is known as acquired thermal tolerance (Vierling, 1991).

Heat shock proteins (HSPs) are a type of molecular chaperone that reduces protein

denaturation and aggregation, targets denatured proteins for proteasome degradation, and facilitates protein folding necessary for proper maturation (Johnson and Craig, 1997; Lee and Vierling, 2000; Frydman, 2001). Plant HSPs lessen high temperature stress by allowing some level of thermal protein protection (Vierling, 1991).

The Tonsor lab wished to examine the naturally occurring genetic variation in expression of heat shock protein 101 (HSP101), in *Arabidopsis thaliana.* *Arabidopsis thaliana*, commonly called arabidopsis, thale or mouse-ear cress, is a small flowering plant related to cabbage and mustard. HSP101 has been shown previously to be a component of acquired thermal tolerance in *Arabidopsis thaliana* (Queitsch *et al.*, 2000). In other eukaryotes, members of this class of proteins are involved in thermal tolerance and repairing aggregated proteins (Sanchez and Lindquist, 1990; Sanchez *et al.*, 1992; Parsell *et al.*, 1994; Lindquist *et al.*, 1995; Glover and Lindquist, 1998). Over the past decade, there has been significant research in the role of HSPs as capacitors of variation (Queitsch *et al.*, 2002; Maresca and Schwartz, 2006), but there is little known about variations of HSP101 expression and the effects of these variations. Therefore, in collaboration with the Tonsor lab, I examined nine different *Arabidopsis thaliana* ecotypes to quantify their HSP101 expression levels grown at various temperatures.

B.2 MATERIALS AND METHODS

B.2.1 HSP101 Isolation, expression, and quantification

The experiment consisted of four replicate arrays, and the following protocols were performed by Imene Boumaza, Toby Liss, and Steve Tonsor. Each array contained three replicate plants of each genotype. Labeling was blind and location within an array was random. Plants were grown in Ray Leach SC10 "Supercell Conetainer" 164 ml. plastic pots (http://www.stuewe.com/products/rayleach.html) filled with Turface (www.turface.com) growth medium. After five days at 4 ºC (to break dormancy) , racks of 21 Supercell Conetainers were placed in fiberglass trays and watered with an automatic ebb-and-flood system in which nutrients were supplied with Dosatron apportioners at a rate that maximized plant growth (Tonsor, unpublished). Plants were grown in two Conviron PGW36 chambers retrofitted with automatic mist and watering controls. Light was supplied at 270 µMoles photons $m^{-2}s^{-1}$ for 16 hrs/24 hour period. Temperatures cycled between 15 and 22 ºC night/day. Two thermal treatments were imposed. The control treatment was maintained as described above. An HSP induction treatment was imposed by moving one array containing three replicates of each genotype from each of the control chambers to a third chamber for 2-3 hours every Monday, Wednesday and Friday between 11:00 and 15:00. This third chamber had identical conditions to the control

chambers, except that temperature was maintained at 38 ºC. After the ~2-hour induction treatment, all plants were returned to the control treatment chambers. Locations of the control and induction replicate trays were switched within control chambers following each induction treatment to minimize location effects within the control chamber. However, individual plants were consistently given either the control treatment or the periodic HSP induction treatment.

At day 21, a single leaf was removed from each plant and total protein extract was obtained and clarified utilizing a previously established protocol (Hong and Vierling 2001). I then assayed Hsp101 content was by western blot analysis. In brief, 5 μg of total protein of each sample was resolved by SDS-PAGE and transferred onto nitrocellulose. Hsp101 and GAPDH (glyceraldehyde-3-phosphate dehydrogenase), a component of the glycolytic pathway, were identified by western blotting using anti-Hsp101 and anti-GAPDH. Western blots were developed using Enhanced Chemiluminescence (Pierce) according to the manufacturer's instructions. Images were obtained on a Kodak 440CF Image Station. The results were quantified using Kodak 1D (version 3.6) imaging software, normalizing the level of Hsp101 expression to the background as well as to GAPDH levels.

B.3 RESULTS

B.3.1 Temperature-response curve slopes differ genetically among natural populations across an induction temperature gradient

A previous study demonstrated that HSP101 is a component of acquired thermal tolerance in *Arabidopsis thaliana* (Queitsch *et al.*, 2000). However, this study did not account for genetic variation of the *Arabidopsis* ecotypes located throughout the world, which could affect HSP101 expression as a result of evolutionary pressures, such as acquired thermal tolerance. Therefore, the Tonsor lab collected nine representative *Arabidopsis* species and subjected them to brief and various temperatures. Next, leaves were collected from these plants (Table 3). The Tonsor lab isolated cellular extracts from the different ecotypes, which I subsequently used to examine and quantify the level of HSP101 expression by immunoblotting techniques (Figure 37). The HSP101 levels of these various ecotypes showed very little variation of protein expression at lower temperatures (22-34° C). However, HSP101 protein levels showed significant variability in the different ecotypes when grown at 40° C. Particularly, PHW-24 and Loch Ness, the two ecotypes examined in this study that resided at the most northern latitude, showed the greatest induction of HSP101 when heat shocked to 40° C.

Table 3. ***Arabidopsis thaliana*** **species utilized in this study**

Northern latitude (lat) and longitude (lon) (negative sign indicates West, positive East) are given. "Accession" names are those used in the www.arabidopsis.org stock list.

Accession	Common Name	Country	Town/Source	Lat	Lon	Altitude (m)
Col	Columbia	Poland	Landsberg/Warthe	53	16	100
Sha	Shakdara	Tadjikistan	Pamiro-Alay	38	68	3400
Mt	Martuba	Libya	Martuba/Cyrenaika	33	23	312
Ct	Catania	Italy	Catania, Sicily	37	15	100
Lc	Loch Ness	Scotland	Loch Ness	58	-5	100
Bay	Bayreuth	Germany	Bayreuth	49	16.5	150
Est	Estland	Russia	Estland	59	28	200
Co	Coimbra	Portugal	Coimbra	41	-9	100
PHW-24	N/A	United Kingdom	Sidmouth	51	-3	10

Figure 37. HSP101 induction due to temperature variation in nine different *Arabidopsis thaliana* ecotypes.

Leaves from nine different wild type *Arabidopsis thaliana* ecotypes ((Bayreuth ; Bay, Columbia ; Col, Coimbra ; Co, Estland ; Est, Loch Ness ; LC, Martuba; Mt, No common name; PHW-24, Shakdara ; Sha, Catania ; Ct) see Table 3) were collected after heat induction at various temperatures (22, 28, 34, and 40°C). Proteins in the leaf cellular extracts were resolved by SDS-PAGE and quantitative western blots were performed to detect the protein levels of HSP101 and GAPDH (as a loading control). (A) Relative protein levels were determined by quantifying the intensities of HSP101 expression, and then normalizing these values to the levels GAPDH expression. Data represents the means of 9 independent experiments. (B) A representative western blot used to amass the data in part A. The samples resolved in the three lanes for each temperature are three random ecotypes assayed in this study.

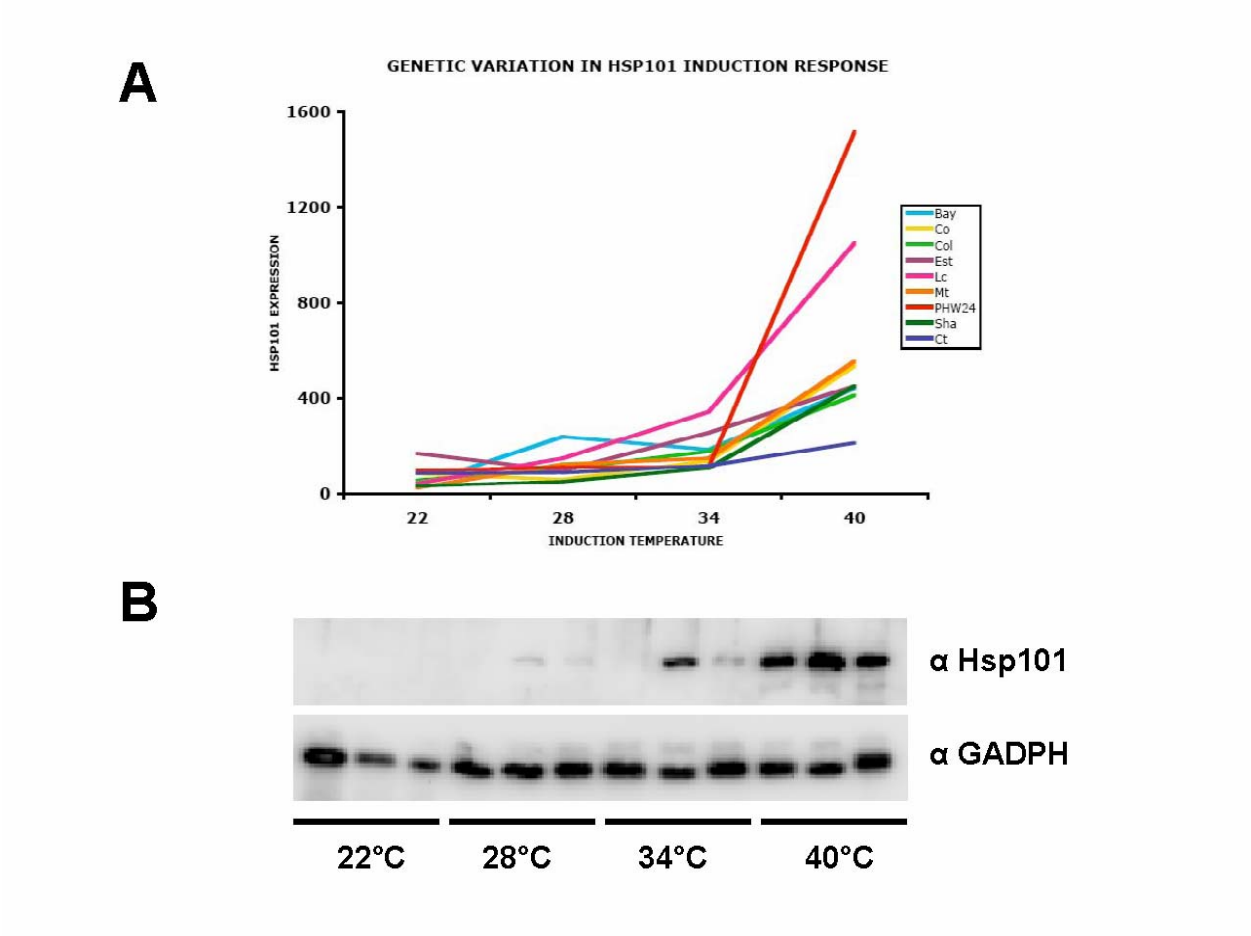

Figure 37. HSP101 induction due to temperature variation in nine different *Arabidopsis thaliana* ecotypes

B.4 DISCUSSION

During cellular stress, such as seen during growth at relatively non-permissive temperatures, for a given species there is an increased propensity of proteins to denature, misfold, or aggregate (Johnson and Craig, 1997; Brodsky and McCracken, 1999; Fewell *et al.*, 2001; Frydman, 2001; Cristofari and Darlix, 2002; Nishikawa *et al.*, 2005; Schroder and Kaufman, 2005). Furthermore, prolonged exposure to these stress-inducing conditions may ultimately lead to cell death. Thus one must have a series of adaptive processes to prevent an untimely demise. One of these processes is HSP induction, which is a significant response to alleviate the negative results of thermal stress (Johnson and Craig, 1997; Lee and Vierling, 2000; Frydman, 2001). As noted earlier, HSP101 is a component of acquired thermal tolerance in *Arabidopsis thaliana* (Queitsch *et al.*, 2000). If HSP101 expression is beneficial, it suggests that this protein, as well as other proteins in the HSP family, would be s trongly and constitutively expressed regardless of the thermal conditions the plant might encounter. However, examination of the nine ecotypes of *Arabidopsis* shows that the induction response varies widely in this species, both in the maximum amount of HSP101 expression in this experiment, as well as in the sensitivity to various temperature triggers (Figure 37). These observations lead to two questions; why is HSP101 induced during times of thermal stress and not as strongly at other times, and why is there variation of HSP101 expression in the different ecotypes of *Arabidopsis*?

To address the first question, there has been evidence suggesting that HSP expression is costly in both terms of energy and nitrogen use (Feder and Hofmann, 1999). While the Tonsor lab demonstrated that the expression of the HSPs improves the amount of fruit in plants and thus

fitness when HSP is expressed (unpublished data), long-term expression of these molecular chaperones would ultimately reduce the fitness of the individual. Thus, HSP101 is rapidly induced during times of thermal stress, but is not maintained for prolonged periods.

To address the second question, we must consider the wide variations among the nine ecotypes of *Arabidopsis* in regards to the induction response at different temperatures. The results suggest evolutionary adaptation. Ecotypes such as PW-24 and Loch Ness, whose natural habitat is at the most northern latitude of those examined, exhibited the greatest induction of HSP101 at temperature greater than 38°C (Figure 37 and Table 3). In contrast, ecotypes located closer to the equator, such as Catania and Martuba, showed a modest temperature-dependant increase in the level of HSP101 expression (Figure 37 and Table 3). This suggests that the various ecotypes have adapted to their respective environments, at least with regard to thermal stress. Northern ecotypes, which would have a lower mean temperature than those latitudes closer to the equator, would require a rapid response to sudden and dramatic tempature increases. Expression of HSP101 could accommodate the infrequent increase levels of denature, misfold, or aggregated proteins. Indeed data from studies on plant HSP101 homologues support this view. It is unclear at this time what other adaptations these ecotypes might have acquired over time.

These observations suggest further studies in the evolutionary adaptation of thermal tolerance and its variation in natural populations. This will be invaluable in understanding the evolution of complex cellular stress responses and the cost-benefits of these responses in a varying environment. Since agriculture output is strongly affected by thermal conditions, understanding the consequences of adapted thermal tolerance can be of considerable value for agriculture and man kind as a whole.

BIBLIOGRAPHY

Abeliovich, H., and Klionsky, D.J. (2001). Autophagy in yeast: mechanistic insights and physiological function. Microbiol Mol Biol Rev *65*, 463-479, table of contents.

Abeliovich, H., Zhang, C., Dunn, W.A., Jr., Shokat, K.M., and Klionsky, D.J. (2003). Chemical genetic analysis of Apg1 reveals a non-kinase role in the induction of autophagy. Mol Biol Cell *14*, 477-490.

Adams, A., Gottschling, D.E., Kaiser, C.A., and Stearns, T. (1997). Methods in Yeast Genetics. Cold Spring Harbor Laboratory Press: Plainview, New York.

Ahner, A., and Brodsky, J.L. (2004). Checkpoints in ER-associated degradation: excuse me, which way to the proteasome? Trends Cell Biol *14*, 474-478.

Arendt, C.S., and Hochstrasser, M. (1999). Eukaryotic 20S proteasome catalytic subunit propeptides prevent active site inactivation by N-terminal acetylation and promote particle assembly. Embo J *18*, 3575-3585.

Aridor, M., and Hannan, L.A. (2000). Traffic jam: a compendium of human diseases that affect intracellular transport processes. Traffic *1*, 836-851.

Aridor, M., and Hannan, L.A. (2002). Traffic jams II: an update of diseases of intracellular transport. Traffic *3*, 781-790.

Asher, G., Reuven, N., and Shaul, Y. (2006). 20S proteasomes and protein degradation "by default". Bioessays *28*, 844-849.

Ashford, T.P., and Porter, K.R. (1962). Cytoplasmic components in hepatic cell lysosomes. J Cell Biol *12*, 198-202.

Baba, M., Osumi, M., Scott, S.V., Klionsky, D.J., and Ohsumi, Y. (1997). Two distinct pathways for targeting proteins from the cytoplasm to the vacuole/lysosome. J Cell Biol *139*, 1687-1695.

Babbitt, S.E., Kiss, A., Deffenbaugh, A.E., Chang, Y.H., Bailly, E., Erdjument-Bromage, H., Tempst, P., Buranda, T., Sklar, L.A., Baumler, J., Gogol, E., and Skowyra, D. (2005).

ATP hydrolysis-dependent disassembly of the 26S proteasome is part of the catalytic cycle. Cell *121*, 553-565.

Bahar, R., J, O.W., Kawamura, K., Seimiya, M., Wang, Y., Hatano, M., Okada, S., Tokuhisa, T., Watanabe, T., and Tagawa, M. (2002). Growth retardation, polyploidy, and multinucleation induced by Clast3, a novel cell cycle-regulated protein. J Biol Chem *277*, 40012-40019.

Balzi, E., Wang, M., Leterme, S., Van Dyck, L., and Goffeau, A. (1994). PDR5, a novel yeast multidrug resistance conferring transporter controlled by the transcription regulator PDR1. J Biol Chem *269*, 2206-2214.

Barlowe, C., Orci, L., Yeung, T., Hosobuchi, M., Hamamoto, S., Salama, N., Rexach, M.F., Ravazzola, M., Amherdt, M., and Schekman, R. (1994). COPII: a membrane coat formed by Sec proteins that drive vesicle budding from the endoplasmic reticulum. Cell *77*, 895-907.

Bays, N.W., Gardner, R.G., Seelig, L.P., Joazeiro, C.A., and Hampton, R.Y. (2001). Hrd1p/Der3p is a membrane-anchored ubiquitin ligase required for ER-associated degradation. Nat Cell Biol *3*, 24-29.

Bernales, S., McDonald, K.L., and Walter, P. (2006). Autophagy Counterbalances Endoplasmic Reticulum Expansion during the Unfolded Protein Response. PLoS Biol *4*, e423.

Bochtler, M., Ditzel, L., Groll, M., Hartmann, C., and Huber, R. (1999). The proteasome. Annu Rev Biophys Biomol Struct *28*, 295-317.

Bonifacino, J.S., and Glick, B.S. (2004). The mechanisms of vesicle budding and fusion. Cell *116*, 153-166.

Brachmann, C.B., Davies, A., Cost, G.J., Caputo, E., Li, J., Hieter, P., and Boeke, J.D. (1998). Designer deletion strains derived from Saccharomyces cerevisiae S288C: a useful set of strains and plasmids for PCR-mediated gene disruption and other applications. Yeast *14*, 115-132.

Brantly, M., Courtney, M., and Crystal, R.G. (1988). Repair of the secretion defect in the Z form of alpha 1-antitrypsin by addition of a second mutation. Science *242*, 1700-1702.

Braun, S., Matuschewski, K., Rape, M., Thoms, S., and Jentsch, S. (2002). Role of the ubiquitin-selective CDC48(UFD1/NPL4)chaperone (segregase) in ERAD of OLE1 and other substrates. Embo J *21*, 615-621.

Brodsky, J.L., Lawrence, J.G., and Caplan, A.J. (1998). Mutations in the cytosolic DnaJ homologue, YDJ1, delay and compromise the efficient translation of heterologous proteins in yeast. Biochemistry *37*, 18045-18055.

Brodsky, J.L., and McCracken, A.A. (1999). ER protein quality control and proteasome-mediated protein degradation. Semin Cell Dev Biol *10*, 507-513.

Brodsky, J.L., Werner, E.D., Dubas, M.E., Goeckeler, J.L., Kruse, K.B., and McCracken, A.A. (1999). The requirement for molecular chaperones during endoplasmic reticulum-associated protein degradation demonstrates that protein export and import are mechanistically distinct. J Biol Chem *274*, 3453-3460.

Bryant, N.J., and Stevens, T.H. (1998). Vacuole biogenesis in Saccharomyces cerevisiae: protein transport pathways to the yeast vacuole. Microbiol Mol Biol Rev *62*, 230-247.

Burri, L., Hockendorff, J., Boehm, U., Klamp, T., Dohmen, R.J., and Levy, F. (2000). Identification and characterization of a mammalian protein interacting with 20S proteasome precursors. Proc Natl Acad Sci U S A *97*, 10348-10353.

Cabral, C.M., Liu, Y., Moremen, K.W., and Sifers, R.N. (2002). Organizational diversity among distinct glycoprotein endoplasmic reticulum-associated degradation programs. Mol Biol Cell *13*, 2639-2650.

Cadwell, K., and Coscoy, L. (2005). Ubiquitination on nonlysine residues by a viral E3 ubiquitin ligase. Science *309*, 127-130.

Campra, J.L., Craig, J.R., Peters, R.L., and Reynolds, T.B. (1973). Cirrhosis associated with partial deficiency of alpha-1 antitrypsin in an adult. Ann Intern Med *78*, 233-238.

Carlson, J.A., Rogers, B.B., Sifers, R.N., Finegold, M.J., Clift, S.M., DeMayo, F.J., Bullock, D.W., and Woo, S.L. (1989). Accumulation of PiZ alpha 1-antitrypsin causes liver damage in transgenic mice. J Clin Invest *83*, 1183-1190.

Carrell, R.W., and Lomas, D.A. (1997). Conformational disease. Lancet *350*, 134-138.

Carrell, R.W., and Lomas, D.A. (2002). Alpha1-antitrypsin deficiency--a model for conformational diseases. N Engl J Med *346*, 45-53.

Casagrande, R., Stern, P., Diehn, M., Shamu, C., Osario, M., Zuniga, M., Brown, P.O., and Ploegh, H. (2000). Degradation of proteins from the ER of S. cerevisiae requires an intact unfolded protein response pathway. Mol Cell *5*, 729-735.

Chen, P., and Hochstrasser, M. (1995). Biogenesis, structure and function of the yeast 20S proteasome. Embo J *14*, 2620-2630.

Chen, P., and Hochstrasser, M. (1996). Autocatalytic subunit processing couples active site formation in the 20S proteasome to completion of assembly. Cell *86*, 961-972.

Ciechanover, A., and Ben-Saadon, R. (2004). N-terminal ubiquitination: more protein substrates join in. Trends Cell Biol *14*, 103-106.

Ciechanover, A., Elias, S., Heller, H., and Hershko, A. (1982). "Covalent affinity" purification of ubiquitin-activating enzyme. J Biol Chem *257*, 2537-2542.

Clague, M.J. (1998). Molecular aspects of the endocytic pathway. Biochem J *336 (Pt 2)*, 271-

282.

Clairmont, C.A., De Maio, A., and Hirschberg, C.B. (1992). Translocation of ATP into the lumen of rough endoplasmic reticulum-derived vesicles and its binding to luminal proteins including BiP (GRP 78) and GRP 94. J Biol Chem *267*, 3983-3990.

Clark, S.L., Jr. (1957). Cellular differentiation in the kidneys of newborn mice studies with the electron microscope. J Biophys Biochem Cytol *3*, 349-362.

Colp, C., Pappas, J., Moran, D., and Lieberman, J. (1993). Variants of alpha 1-antitrypsin in Puerto Rican children with asthma. Chest *103*, 812-815.

Coughlan, C.M., and Brodsky, J.L. (2003). Yeast as a model system to investigate protein conformational diseases. Methods Mol Biol *232*, 77-90.

Coughlan, C.M., and Brodsky, J.L. (2005). Use of yeast as a model system to investigate protein conformational diseases. Mol Biotechnol *30*, 171-180.

Coughlan, C.M., Walker, J.L., Cochran, J.C., Wittrup, K.D., and Brodsky, J.L. (2004). Degradation of mutated bovine pancreatic trypsin inhibitor in the yeast vacuole suggests post-endoplasmic reticulum protein quality control. J Biol Chem *279*, 15289-15297.

Cox, J.S., Shamu, C.E., and Walter, P. (1993). Transcriptional induction of genes encoding endoplasmic reticulum resident proteins requires a transmembrane protein kinase. Cell *73*, 1197-1206.

Cox, J.S., and Walter, P. (1996). A novel mechanism for regulating activity of a transcription factor that controls the unfolded protein response. Cell *87*, 391-404.

Credle, J.J., Finer-Moore, J.S., Papa, F.R., Stroud, R.M., and Walter, P. (2005). On the mechanism of sensing unfolded protein in the endoplasmic reticulum. Proc Natl Acad Sci U S A *102*, 18773-18784.

Cristofari, G., and Darlix, J.L. (2002). The ubiquitous nature of RNA chaperone proteins. Prog Nucleic Acid Res Mol Biol *72*, 223-268.

Cruz, M., Molina, J.A., Pedrola, D., and Munoz-Lopez, F. (1976). Cirrhosis and heterozygous alpha1-antitrypsin deficiency in a 4-year-old girl. Helv Paediatr Acta *30*, 501-507.

Deter, R.L., Baudhuin, P., and De Duve, C. (1967). Participation of lysosomes in cellular autophagy induced in rat liver by glucagon. J Cell Biol *35*, C11-16.

Deter, R.L., and De Duve, C. (1967). Influence of glucagon, an inducer of cellular autophagy, on some physical properties of rat liver lysosomes. J Cell Biol *33*, 437-449.

Deveraux, Q., Ustrell, V., Pickart, C., and Rechsteiner, M. (1994). A 26 S protease subunit that binds ubiquitin conjugates. J Biol Chem *269*, 7059-7061.

Dimcheff, D.E., Askovic, S., Baker, A.H., Johnson-Fowler, C., and Portis, J.L. (2003). Endoplasmic reticulum stress is a determinant of retrovirus-induced spongiform neurodegeneration. J Virol *77*, 12617-12629.

Ecker, D.J., Khan, M.I., Marsh, J., Butt, T.R., and Crooke, S.T. (1987). Chemical synthesis and expression of a cassette adapted ubiquitin gene. J Biol Chem *262*, 3524-3527.

Eden, E., Mitchell, D., Mehlman, B., Khouli, H., Nejat, M., Grieco, M.H., and Turino, G.M. (1997). Atopy, asthma, and emphysema in patients with severe alpha-1-antitrypysin deficiency. Am J Respir Crit Care Med *156*, 68-74.

Ellgaard, L., and Helenius, A. (2003). Quality control in the endoplasmic reticulum. Nat Rev Mol Cell Biol *4*, 181-191.

Enenkel, C., Lehmann, A., and Kloetzel, P.M. (1998). Subcellular distribution of proteasomes implicates a major location of protein degradation in the nuclear envelope-ER network in yeast. Embo J *17*, 6144-6154.

Evan, G.I., Lewis, G.K., Ramsay, G., and Bishop, J.M. (1985). Isolation of monoclonal antibodies specific for human c-myc proto-oncogene product. Mol Cell Biol *5*, 3610-3616.

Feder, M.E., and Hofmann, G.E. (1999). Heat-shock proteins, molecular chaperones, and the stress response: evolutionary and ecological physiology. Annu Rev Physiol *61*, 243-282.

Fewell, S.W., Travers, K.J., Weissman, J.S., and Brodsky, J.L. (2001). The action of molecular chaperones in the early secretory pathway. Annu Rev Genet *35*, 149-191.

Foreman, R.C., Judah, J.D., and Colman, A. (1984). Xenopus oocytes can synthesise but do not secrete the Z variant of human alpha 1-antitrypsin. FEBS Lett *168*, 84-88.

Frand, A.R., and Kaiser, C.A. (1998). The ERO1 gene of yeast is required for oxidation of protein dithiols in the endoplasmic reticulum. Mol Cell *1*, 161-170.

Frentzel, S., Pesold-Hurt, B., Seelig, A., and Kloetzel, P.M. (1994). 20 S proteasomes are assembled via distinct precursor complexes. Processing of LMP2 and LMP7 proproteins takes place in 13-16 S preproteasome complexes. J Mol Biol *236*, 975-981.

Frydman, J. (2001). Folding of newly translated proteins in vivo: the role of molecular chaperones. Annu Rev Biochem *70*, 603-647.

Fujimuro, M., Tanaka, K., Yokosawa, H., and Toh-e, A. (1998). Son1p is a component of the 26S proteasome of the yeast Saccharomyces cerevisiae. FEBS Lett *423*, 149-154.

Gaczynska, M., and Osmulski, P.A. (2005). Small-molecule inhibitors of proteasome activity. Methods Mol Biol *301*, 3-22.

Gerards, W.L., de Jong, W.W., Bloemendal, H., and Boelens, W. (1998). The human

proteasomal subunit HsC8 induces ring formation of other alpha-type subunits. J Mol Biol *275*, 113-121.

Gerards, W.L., Enzlin, J., Haner, M., Hendriks, I.L., Aebi, U., Bloemendal, H., and Boelens, W. (1997). The human alpha-type proteasomal subunit HsC8 forms a double ringlike structure, but does not assemble into proteasome-like particles with the beta-type subunits HsDelta or HsBPROS26. J Biol Chem *272*, 10080-10086.

Ghislain, M., Udvardy, A., and Mann, C. (1993). S. cerevisiae 26S protease mutants arrest cell division in G2/metaphase. Nature *366*, 358-362.

Glickman, M.H., and Ciechanover, A. (2002). The ubiquitin-proteasome proteolytic pathway: destruction for the sake of construction. Physiol Rev *82*, 373-428.

Glickman, M.H., Rubin, D.M., Fried, V.A., and Finley, D. (1998). The regulatory particle of the Saccharomyces cerevisiae proteasome. Mol Cell Biol *18*, 3149-3162.

Glover, J.R., and Lindquist, S. (1998). Hsp104, Hsp70, and Hsp40: a novel chaperone system that rescues previously aggregated proteins. Cell *94*, 73-82.

Goeckeler, J.L., Stephens, A., Lee, P., Caplan, A.J., and Brodsky, J.L. (2002). Overexpression of yeast Hsp110 homolog Sse1p suppresses ydj1-151 thermosensitivity and restores Hsp90-dependent activity. Mol Biol Cell *13*, 2760-2770.

Goll, D.E., Thompson, V.F., Li, H., Wei, W., and Cong, J. (2003). The calpain system. Physiol Rev *83*, 731-801.

Gorbea, C., Taillandier, D., and Rechsteiner, M. (1999). Assembly of the regulatory complex of the 26S proteasome. Mol Biol Rep *26*, 15-19.

Gorlach, A., Klappa, P., and Kietzmann, T. (2006). The endoplasmic reticulum: folding, calcium homeostasis, signaling, and redox control. Antioxid Redox Signal *8*, 1391-1418.

Griffin, T.A., Slack, J.P., McCluskey, T.S., Monaco, J.J., and Colbert, R.A. (2000). Identification of proteassemblin, a mammalian homologue of the yeast protein, Ump1p, that is required for normal proteasome assembly. Mol Cell Biol Res Commun *3*, 212-217.

Groll, M., Bajorek, M., Kohler, A., Moroder, L., Rubin, D.M., Huber, R., Glickman, M.H., and Finley, D. (2000). A gated channel into the proteasome core particle. Nat Struct Biol *7*, 1062-1067.

Guterman, A., and Glickman, M.H. (2004). Complementary roles for Rpn11 and Ubp6 in deubiquitination and proteolysis by the proteasome. J Biol Chem *279*, 1729-1738.

Hampsey, M. (1997). A review of phenotypes in Saccharomyces cerevisiae. Yeast *13*, 1099-1133.

Hampton, R.Y., Gardner, R.G., and Rine, J. (1996). Role of 26S proteasome and HRD genes in

the degradation of 3-hydroxy-3-methylglutaryl-CoA reductase, an integral endoplasmic reticulum membrane protein. Mol Biol Cell *7*, 2029-2044.

Hanna, J., Hathaway, N.A., Tone, Y., Crosas, B., Elsasser, S., Kirkpatrick, D.S., Leggett, D.S., Gygi, S.P., King, R.W., and Finley, D. (2006). Deubiquitinating enzyme Ubp6 functions noncatalytically to delay proteasomal degradation. Cell *127*, 99-111.

He, C., Song, H., Yorimitsu, T., Monastyrska, I., Yen, W.L., Legakis, J.E., and Klionsky, D.J. (2006). Recruitment of Atg9 to the preautophagosomal structure by Atg11 is essential for selective autophagy in budding yeast. J Cell Biol *175*, 925-935.

Heinemeyer, W., Fischer, M., Krimmer, T., Stachon, U., and Wolf, D.H. (1997). The active sites of the eukaryotic 20 S proteasome and their involvement in subunit precursor processing. J Biol Chem *272*, 25200-25209.

Heinemeyer, W., Kleinschmidt, J.A., Saidowsky, J., Escher, C., and Wolf, D.H. (1991). Proteinase yscE, the yeast proteasome/multicatalytic-multifunctional proteinase: mutants unravel its function in stress induced proteolysis and uncover its necessity for cell survival. Embo J *10*, 555-562.

Heinemeyer, W., Ramos, P.C., and Dohmen, R.J. (2004). The ultimate nanoscale mincer: assembly, structure and active sites of the 20S proteasome core. Cell Mol Life Sci *61*, 1562-1578.

Heinemeyer, W., Trondle, N., Albrecht, G., and Wolf, D.H. (1994). PRE5 and PRE6, the last missing genes encoding 20S proteasome subunits from yeast? Indication for a set of 14 different subunits in the eukaryotic proteasome core. Biochemistry *33*, 12229-12237.

Hilt, W., Enenkel, C., Gruhler, A., Singer, T., and Wolf, D.H. (1993). The PRE4 gene codes for a subunit of the yeast proteasome necessary for peptidylglutamyl-peptide-hydrolyzing activity. Mutations link the proteasome to stress- and ubiquitin-dependent proteolysis. J Biol Chem *268*, 3479-3486.

Hirano, Y., Hayashi, H., Iemura, S., Hendil, K.B., Niwa, S., Kishimoto, T., Kasahara, M., Natsume, T., Tanaka, K., and Murata, S. (2006). Cooperation of Multiple Chaperones Required for the Assembly of Mammalian 20S Proteasomes. Mol Cell *24*, 977-984.

Hirano, Y., Hendil, K.B., Yashiroda, H., Iemura, S., Nagane, R., Hioki, Y., Natsume, T., Tanaka, K., and Murata, S. (2005). A heterodimeric complex that promotes the assembly of mammalian 20S proteasomes. Nature *437*, 1381-1385.

Ho, Y., Gruhler, A., Heilbut, A., Bader, G.D., Moore, L., Adams, S.L., Millar, A., Taylor, P., Bennett, K., Boutilier, K., Yang, L., Wolting, C., Donaldson, I., Schandorff, S., Shewnarane, J., Vo, M., Taggart, J., Goudreault, M., Muskat, B., Alfarano, C., Dewar, D., Lin, Z., Michalickova, K., Willems, A.R., Sassi, H., Nielsen, P.A., Rasmussen, K.J., Andersen, J.R., Johansen, L.E., Hansen, L.H., Jespersen, H., Podtelejnikov, A., Nielsen, E., Crawford, J., Poulsen, V., Sorensen, B.D., Matthiesen, J., Hendrickson, R.C., Gleeson, F., Pawson, T., Moran, M.F., Durocher, D., Mann, M., Hogue, C.W., Figeys,

D., and Tyers, M. (2002). Systematic identification of protein complexes in Saccharomyces cerevisiae by mass spectrometry. Nature *415*, 180-183.

Hoppe, T. (2005). Multiubiquitylation by E4 enzymes: 'one size' doesn't fit all. Trends Biochem Sci *30*, 183-187.

Huang, L., Shen, M., Chernushevich, I., Burlingame, A.L., Wang, C.C., and Robertson, C.D. (1999). Identification and isolation of three proteasome subunits and their encoding genes from Trypanosoma brucei. Mol Biochem Parasitol *102*, 211-223.

Huang, W.P., and Klionsky, D.J. (2002). Autophagy in yeast: a review of the molecular machinery. Cell Struct Funct *27*, 409-420.

Hurley, J.H., Lee, S., and Prag, G. (2006). Ubiquitin-binding domains. Biochem J *399*, 361-372.

Huyer, G., Longsworth, G.L., Mason, D.L., Mallampalli, M.P., McCaffery, J.M., Wright, R.L., and Michaelis, S. (2004). A striking quality control subcompartment in Saccharomyces cerevisiae: the endoplasmic reticulum-associated compartment. Mol Biol Cell *15*, 908-921.

Hwang, C., Sinskey, A.J., and Lodish, H.F. (1992). Oxidized redox state of glutathione in the endoplasmic reticulum. Science *257*, 1496-1502.

Jackson, P.K., Eldridge, A.G., Freed, E., Furstenthal, L., Hsu, J.Y., Kaiser, B.K., and Reimann, J.D. (2000). The lore of the RINGs: substrate recognition and catalysis by ubiquitin ligases. Trends Cell Biol *10*, 429-439.

Jackson, R.C., and Blobel, G. (1977). Post-translational cleavage of presecretory proteins with an extract of rough microsomes from dog pancreas containing signal peptidase activity. Proc Natl Acad Sci U S A *74*, 5598-5602.

Janoff, A. (1985). Elastase in tissue injury. Annu Rev Med *36*, 207-216.

Joazeiro, C.A., and Weissman, A.M. (2000). RING finger proteins: mediators of ubiquitin ligase activity. Cell *102*, 549-552.

Johnson, A.E., and van Waes, M.A. (1999). The translocon: a dynamic gateway at the ER membrane. Annu Rev Cell Dev Biol *15*, 799-842.

Johnson, E.S., Ma, P.C., Ota, I.M., and Varshavsky, A. (1995). A proteolytic pathway that recognizes ubiquitin as a degradation signal. J Biol Chem *270*, 17442-17456.

Johnson, J.L., and Craig, E.A. (1997). Protein folding in vivo: unraveling complex pathways. Cell *90*, 201-204.

Kabani, M., Beckerich, J.M., and Brodsky, J.L. (2002). Nucleotide exchange factor for the yeast Hsp70 molecular chaperone Ssa1p. Mol Cell Biol *22*, 4677-4689.

Kabani, M., Kelley, S.S., Morrow, M.W., Montgomery, D.L., Sivendran, R., Rose, M.D., Gierasch, L.M., and Brodsky, J.L. (2003). Dependence of endoplasmic reticulum-associated degradation on the peptide binding domain and concentration of BiP. Mol Biol Cell *14*, 3437-3448.

Kalies, K.U., Allan, S., Sergeyenko, T., Kroger, H., and Romisch, K. (2005). The protein translocation channel binds proteasomes to the endoplasmic reticulum membrane. Embo J *24*, 2284-2293.

Kamada, Y., Funakoshi, T., Shintani, T., Nagano, K., Ohsumi, M., and Ohsumi, Y. (2000). Tor-mediated induction of autophagy via an Apg1 protein kinase complex. J Cell Biol *150*, 1507-1513.

Kametaka, S., Okano, T., Ohsumi, M., and Ohsumi, Y. (1998). Apg14p and Apg6/Vps30p form a protein complex essential for autophagy in the yeast, Saccharomyces cerevisiae. J Biol Chem *273*, 22284-22291.

Kamimoto, T., Shoji, S., Hidvegi, T., Mizushima, N., Umebayashi, K., Perlmutter, D.H., and Yoshimori, T. (2006). Intracellular inclusions containing mutant alpha1-antitrypsin Z are propagated in the absence of autophagic activity. J Biol Chem *281*, 4467-4476.

Kaufman, R.J. (1999). Stress signaling from the lumen of the endoplasmic reticulum: coordination of gene transcriptional and translational controls. Genes Dev *13*, 1211-1233.

Kawahara, T., Yanagi, H., Yura, T., and Mori, K. (1997). Endoplasmic reticulum stress-induced mRNA splicing permits synthesis of transcription factor Hac1p/Ern4p that activates the unfolded protein response. Mol Biol Cell *8*, 1845-1862.

Keenan, R.J., Freymann, D.M., Stroud, R.M., and Walter, P. (2001). The signal recognition particle. Annu Rev Biochem *70*, 755-775.

Kim, J., and Klionsky, D.J. (2000). Autophagy, cytoplasm-to-vacuole targeting pathway, and pexophagy in yeast and mammalian cells. Annu Rev Biochem *69*, 303-342.

Kim, J., Lee, K.N., Yi, G.S., and Yu, M.H. (1995). A thermostable mutation located at the hydrophobic core of alpha 1-antitrypsin suppresses the folding defect of the Z-type variant. J Biol Chem *270*, 8597-8601.

King, M.A., Stone, J.A., Diaz, P.T., Mueller, C.F., Becker, W.J., and Gadek, J.E. (1996). Alpha 1-antitrypsin deficiency: evaluation of bronchiectasis with CT. Radiology *199*, 137-141.

Kisselev, A.F., Akopian, T.N., Woo, K.M., and Goldberg, A.L. (1999). The sizes of peptides generated from protein by mammalian 26 and 20 S proteasomes. Implications for understanding the degradative mechanism and antigen presentation. J Biol Chem *274*, 3363-3371.

Klionsky, D.J., Cueva, R., and Yaver, D.S. (1992). Aminopeptidase I of Saccharomyces cerevisiae is localized to the vacuole independent of the secretory pathway. J Cell Biol

119, 287-299.

Knop, M., Hauser, N., and Wolf, D.H. (1996). N-Glycosylation affects endoplasmic reticulum degradation of a mutated derivative of carboxypeptidase yscY in yeast. Yeast *12*, 1229-1238.

Kostova, Z., and Wolf, D.H. (2003). For whom the bell tolls: protein quality control of the endoplasmic reticulum and the ubiquitin-proteasome connection. Embo J *22*, 2309-2317.

Krogan, N.J., Cagney, G., Yu, H., Zhong, G., Guo, X., Ignatchenko, A., Li, J., Pu, S., Datta, N., Tikuisis, A.P., Punna, T., Peregrin-Alvarez, J.M., Shales, M., Zhang, X., Davey, M., Robinson, M.D., Paccanaro, A., Bray, J.E., Sheung, A., Beattie, B., Richards, D.P., Canadien, V., Lalev, A., Mena, F., Wong, P., Starostine, A., Canete, M.M., Vlasblom, J., Wu, S., Orsi, C., Collins, S.R., Chandran, S., Haw, R., Rilstone, J.J., Gandi, K., Thompson, N.J., Musso, G., St Onge, P., Ghanny, S., Lam, M.H., Butland, G., Altaf-Ul, A.M., Kanaya, S., Shilatifard, A., O'Shea, E., Weissman, J.S., Ingles, C.J., Hughes, T.R., Parkinson, J., Gerstein, M., Wodak, S.J., Emili, A., and Greenblatt, J.F. (2006). Global landscape of protein complexes in the yeast Saccharomyces cerevisiae. Nature *440*, 637-643.

Kruse, K.B., Brodsky, J.L., and McCracken, A.A. (2006). Characterization of an ERAD gene as VPS30/ATG6 reveals two alternative and functionally distinct protein quality control pathways: one for soluble Z variant of human alpha-1 proteinase inhibitor (A1PiZ) and another for aggregates of A1PiZ. Mol Biol Cell *17*, 203-212.

Kuhlbrodt, K., Mouysset, J., and Hoppe, T. (2005). Orchestra for assembly and fate of polyubiquitin chains. Essays Biochem *41*, 1-14.

Kuhn, K.M., DeRisi, J.L., Brown, P.O., and Sarnow, P. (2001). Global and specific translational regulation in the genomic response of Saccharomyces cerevisiae to a rapid transfer from a fermentable to a nonfermentable carbon source. Mol Cell Biol *21*, 916-927.

Lam, Y.A., Lawson, T.G., Velayutham, M., Zweier, J.L., and Pickart, C.M. (2002). A proteasomal ATPase subunit recognizes the polyubiquitin degradation signal. Nature *416*, 763-767.

Lander, E.S., Linton, L.M., Birren, B., Nusbaum, C., Zody, M.C., Baldwin, J., Devon, K., Dewar, K., Doyle, M., FitzHugh, W., Funke, R., Gage, D., Harris, K., Heaford, A., Howland, J., Kann, L., Lehoczky, J., LeVine, R., McEwan, P., McKernan, K., Meldrim, J., Mesirov, J.P., Miranda, C., Morris, W., Naylor, J., Raymond, C., Rosetti, M., Santos, R., Sheridan, A., Sougnez, C., Stange-Thomann, N., Stojanovic, N., Subramanian, A., Wyman, D., Rogers, J., Sulston, J., Ainscough, R., Beck, S., Bentley, D., Burton, J., Clee, C., Carter, N., Coulson, A., Deadman, R., Deloukas, P., Dunham, A., Dunham, I., Durbin, R., French, L., Grafham, D., Gregory, S., Hubbard, T., Humphray, S., Hunt, A., Jones, M., Lloyd, C., McMurray, A., Matthews, L., Mercer, S., Milne, S., Mullikin, J.C., Mungall, A., Plumb, R., Ross, M., Shownkeen, R., Sims, S., Waterston, R.H., Wilson, R.K., Hillier, L.W., McPherson, J.D., Marra, M.A., Mardis, E.R., Fulton, L.A., Chinwalla, A.T., Pepin, K.H., Gish, W.R., Chissoe, S.L., Wendl, M.C., Delehaunty,

K.D., Miner, T.L., Delehaunty, A., Kramer, J.B., Cook, L.L., Fulton, R.S., Johnson, D.L., Minx, P.J., Clifton, S.W., Hawkins, T., Branscomb, E., Predki, P., Richardson, P., Wenning, S., Slezak, T., Doggett, N., Cheng, J.F., Olsen, A., Lucas, S., Elkin, C., Uberbacher, E., Frazier, M., Gibbs, R.A., Muzny, D.M., Scherer, S.E., Bouck, J.B., Sodergren, E.J., Worley, K.C., Rives, C.M., Gorrell, J.H., Metzker, M.L., Naylor, S.L., Kucherlapati, R.S., Nelson, D.L., Weinstock, G.M., Sakaki, Y., Fujiyama, A., Hattori, M., Yada, T., Toyoda, A., Itoh, T., Kawagoe, C., Watanabe, H., Totoki, Y., Taylor, T., Weissenbach, J., Heilig, R., Saurin, W., Artiguenave, F., Brottier, P., Bruls, T., Pelletier, E., Robert, C., Wincker, P., Smith, D.R., Doucette-Stamm, L., Rubenfield, M., Weinstock, K., Lee, H.M., Dubois, J., Rosenthal, A., Platzer, M., Nyakatura, G., Taudien, S., Rump, A., Yang, H., Yu, J., Wang, J., Huang, G., Gu, J., Hood, L., Rowen, L., Madan, A., Qin, S., Davis, R.W., Federspiel, N.A., Abola, A.P., Proctor, M.J., Myers, R.M., Schmutz, J., Dickson, M., Grimwood, J., Cox, D.R., Olson, M.V., Kaul, R., Raymond, C., Shimizu, N., Kawasaki, K., Minoshima, S., Evans, G.A., Athanasiou, M., Schultz, R., Roe, B.A., Chen, F., Pan, H., Ramser, J., Lehrach, H., Reinhardt, R., McCombie, W.R., de la Bastide, M., Dedhia, N., Blocker, H., Hornischer, K., Nordsiek, G., Agarwala, R., Aravind, L., Bailey, J.A., Bateman, A., Batzoglou, S., Birney, E., Bork, P., Brown, D.G., Burge, C.B., Cerutti, L., Chen, H.C., Church, D., Clamp, M., Copley, R.R., Doerks, T., Eddy, S.R., Eichler, E.E., Furey, T.S., Galagan, J., Gilbert, J.G., Harmon, C., Hayashizaki, Y., Haussler, D., Hermjakob, H., Hokamp, K., Jang, W., Johnson, L.S., Jones, T.A., Kasif, S., Kaspryzk, A., Kennedy, S., Kent, W.J., Kitts, P., Koonin, E.V., Korf, I., Kulp, D., Lancet, D., Lowe, T.M., McLysaght, A., Mikkelsen, T., Moran, J.V., Mulder, N., Pollara, V.J., Ponting, C.P., Schuler, G., Schultz, J., Slater, G., Smit, A.F., Stupka, E., Szustakowski, J., Thierry-Mieg, D., Thierry-Mieg, J., Wagner, L., Wallis, J., Wheeler, R., Williams, A., Wolf, Y.I., Wolfe, K.H., Yang, S.P., Yeh, R.F., Collins, F., Guyer, M.S., Peterson, J., Felsenfeld, A., Wetterstrand, K.A., Patrinos, A., Morgan, M.J., de Jong, P., Catanese, J.J., Osoegawa, K., Shizuya, H., Choi, S., and Chen, Y.J. (2001). Initial sequencing and analysis of the human genome. Nature *409*, 860-921.

Larsson, C. (1978). Natural history and life expectancy in severe alpha1-antitrypsin deficiency, Pi Z. Acta Med Scand *204*, 345-351.

Laskey, R.A., Honda, B.M., Mills, A.D., and Finch, J.T. (1978). Nucleosomes are assembled by an acidic protein which binds histones and transfers them to DNA. Nature *275*, 416-420.

Law, R.H., Zhang, Q., McGowan, S., Buckle, A.M., Silverman, G.A., Wong, W., Rosado, C.J., Langendorf, C.G., Pike, R.N., Bird, P.I., and Whisstock, J.C. (2006). An overview of the serpin superfamily. Genome Biol *7*, 216.

Lecker, S.H., Goldberg, A.L., and Mitch, W.E. (2006). Protein degradation by the ubiquitin-proteasome pathway in normal and disease states. J Am Soc Nephrol *17*, 1807-1819.

Lee, D.H., and Goldberg, A.L. (1996). Selective inhibitors of the proteasome-dependent and vacuolar pathways of protein degradation in Saccharomyces cerevisiae. J Biol Chem *271*, 27280-27284.

Lee, G.J., and Vierling, E. (2000). A small heat shock protein cooperates with heat shock protein

70 systems to reactivate a heat-denatured protein. Plant Physiol *122*, 189-198.

Leggett, D.S., Hanna, J., Borodovsky, A., Crosas, B., Schmidt, M., Baker, R.T., Walz, T., Ploegh, H., and Finley, D. (2002). Multiple associated proteins regulate proteasome structure and function. Mol Cell *10*, 495-507.

Letourneur, F., Gaynor, E.C., Hennecke, S., Demolliere, C., Duden, R., Emr, S.D., Riezman, H., and Cosson, P. (1994). Coatomer is essential for retrieval of dilysine-tagged proteins to the endoplasmic reticulum. Cell *79*, 1199-1207.

Li, X., Kusmierczyk, A.R., Wong, P., Emili, A., and Hochstrasser, M. (2007). beta-Subunit appendages promote 20S proteasome assembly by overcoming an Ump1-dependent checkpoint. Embo J *26*, 2339-2349.

Lilley, B.N., and Ploegh, H.L. (2004). A membrane protein required for dislocation of misfolded proteins from the ER. Nature *429*, 834-840.

Lindquist, S. (1992). Heat-shock proteins and stress tolerance in microorganisms. Curr Opin Genet Dev *2*, 748-755.

Lindquist, S., Patino, M.M., Chernoff, Y.O., Kowal, A.S., Singer, M.A., Liebman, S.W., Lee, K.H., and Blake, T. (1995). The role of Hsp104 in stress tolerance and [PSI+] propagation in Saccharomyces cerevisiae. Cold Spring Harb Symp Quant Biol *60*, 451-460.

Lobell, D.B., and Asner, G.P. (2003). Climate and management contributions to recent trends in U.S. agricultural yields. Science *299*, 1032.

Lomas, D.A., Evans, D.L., Finch, J.T., and Carrell, R.W. (1992). The mechanism of Z alpha 1-antitrypsin accumulation in the liver. Nature *357*, 605-607.

Lomas, D.A., and Parfrey, H. (2004). Alpha1-antitrypsin deficiency. 4: Molecular pathophysiology. Thorax *59*, 529-535.

Los, D.A., and Murata, N. (2000). Regulation of enzymatic activity and gene expression by membrane fluidity. Sci STKE *2000*, PE1.

Mahadeva, R., Chang, W.S., Dafforn, T.R., Oakley, D.J., Foreman, R.C., Calvin, J., Wight, D.G., and Lomas, D.A. (1999). Heteropolymerization of S, I, and Z alpha1-antitrypsin and liver cirrhosis. J Clin Invest *103*, 999-1006.

Maresca, B., and Schwartz, J.H. (2006). Sudden origins: a general mechanism of evolution based on stress protein concentration and rapid environmental change. Anat Rec B New Anat *289*, 38-46.

Mast, A.E., Enghild, J.J., and Salvesen, G. (1992). Conformation of the reactive site loop of alpha 1-proteinase inhibitor probed by limited proteolysis. Biochemistry *31*, 2720-2728.

McCracken, A.A., and Brodsky, J.L. (2003). Evolving questions and paradigm shifts in endoplasmic-reticulum-associated degradation (ERAD). Bioessays *25*, 868-877.

McCracken, A.A., Karpichev, I.V., Ernaga, J.E., Werner, E.D., Dillin, A.G., and Courchesne, W.E. (1996). Yeast mutants deficient in ER-associated degradation of the Z variant of alpha-1-protease inhibitor. Genetics *144*, 1355-1362.

McCracken, A.A., and Kruse, K.B. (1993). Selective protein degradation in the yeast exocytic pathway. Mol Biol Cell *4*, 729-736.

McCracken, A.A., Kruse, K.B., and Brown, J.L. (1989). Molecular basis for defective secretion of the Z variant of human alpha-1-proteinase inhibitor: secretion of variants having altered potential for salt bridge formation between amino acids 290 and 342. Mol Cell Biol *9*, 1406-1414.

Meusser, B., Hirsch, C., Jarosch, E., and Sommer, T. (2005). ERAD: the long road to destruction. Nat Cell Biol *7*, 766-772.

Michalak, M., Robert Parker, J.M., and Opas, M. (2002). Ca2+ signaling and calcium binding chaperones of the endoplasmic reticulum. Cell Calcium *32*, 269-278.

Mitch, W.E., and Goldberg, A.L. (1996). Mechanisms of muscle wasting. The role of the ubiquitin-proteasome pathway. N Engl J Med *335*, 1897-1905.

Mori, K., Kawahara, T., Yoshida, H., Yanagi, H., and Yura, T. (1996). Signalling from endoplasmic reticulum to nucleus: transcription factor with a basic-leucine zipper motif is required for the unfolded protein-response pathway. Genes Cells *1*, 803-817.

Mori, K., Ma, W., Gething, M.J., and Sambrook, J. (1993). A transmembrane protein with a cdc2+/CDC28-related kinase activity is required for signaling from the ER to the nucleus. Cell *74*, 743-756.

Mori, K., Ogawa, N., Kawahara, T., Yanagi, H., and Yura, T. (1998). Palindrome with spacer of one nucleotide is characteristic of the cis-acting unfolded protein response element in Saccharomyces cerevisiae. J Biol Chem *273*, 9912-9920.

Mori, K., Ogawa, N., Kawahara, T., Yanagi, H., and Yura, T. (2000). mRNA splicing-mediated C-terminal replacement of transcription factor Hac1p is required for efficient activation of the unfolded protein response. Proc Natl Acad Sci U S A *97*, 4660-4665.

Mori, K., Sant, A., Kohno, K., Normington, K., Gething, M.J., and Sambrook, J.F. (1992). A 22 bp cis-acting element is necessary and sufficient for the induction of the yeast KAR2 (BiP) gene by unfolded proteins. Embo J *11*, 2583-2593.

Mornex, J.F., Chytil-Weir, A., Martinet, Y., Courtney, M., LeCocq, J.P., and Crystal, R.G. (1986). Expression of the alpha-1-antitrypsin gene in mononuclear phagocytes of normal and alpha-1-antitrypsin-deficient individuals. J Clin Invest *77*, 1952-1961.

Mumberg, D., Muller, R., and Funk, M. (1995). Yeast vectors for the controlled expression of heterologous proteins in different genetic backgrounds. Gene *156*, 119-122.

Myerowitz, R.L., Handzel, Z.T., and Robbins, J.B. (1972). Human serum 1 -antitrypsin: isolation and demonstration of electrophoretic and immunologic heterogeneity. Clin Chim Acta *39*, 307-317.

Nakagawa, T., Zhu, H., Morishima, N., Li, E., Xu, J., Yankner, B.A., and Yuan, J. (2000). Caspase-12 mediates endoplasmic-reticulum-specific apoptosis and cytotoxicity by amyloid-beta. Nature *403*, 98-103.

Nandi, D., Tahiliani, P., Kumar, A., and Chandu, D. (2006). The ubiquitin-proteasome system. J Biosci *31*, 137-155.

Nandi, D., Woodward, E., Ginsburg, D.B., and Monaco, J.J. (1997). Intermediates in the formation of mouse 20S proteasomes: implications for the assembly of precursor beta subunits. Embo J *16*, 5363-5375.

Newman, J.R., Ghaemmaghami, S., Ihmels, J., Breslow, D.K., Noble, M., DeRisi, J.L., and Weissman, J.S. (2006). Single-cell proteomic analysis of S. cerevisiae reveals the architecture of biological noise. Nature *441*, 840-846.

Ng, D.T., Spear, E.D., and Walter, P. (2000). The unfolded protein response regulates multiple aspects of secretory and membrane protein biogenesis and endoplasmic reticulum quality control. J Cell Biol *150*, 77-88.

Nishikawa, S., Brodsky, J.L., and Nakatsukasa, K. (2005). Roles of molecular chaperones in endoplasmic reticulum (ER) quality control and ER-associated degradation (ERAD). J Biochem (Tokyo) *137*, 551-555.

Nishikawa, S., Hirata, A., and Nakano, A. (1994). Inhibition of endoplasmic reticulum (ER)-to-Golgi transport induces relocalization of binding protein (BiP) within the ER to form the BiP bodies. Mol Biol Cell *5*, 1129-1143.

Nishikawa, S.I., Fewell, S.W., Kato, Y., Brodsky, J.L., and Endo, T. (2001). Molecular chaperones in the yeast endoplasmic reticulum maintain the solubility of proteins for retrotranslocation and degradation. J Cell Biol *153*, 1061-1070.

Noda, T., Suzuki, K., and Ohsumi, Y. (2002). Yeast autophagosomes: de novo formation of a membrane structure. Trends Cell Biol *12*, 231-235.

Oberdorf, J., Carlson, E.J., and Skach, W.R. (2001). Redundancy of mammalian proteasome beta subunit function during endoplasmic reticulum associated degradation. Biochemistry *40*, 13397-13405.

Ogata, M., Hino, S., Saito, A., Morikawa, K., Kondo, S., Kanemoto, S., Murakami, T., Taniguchi, M., Tanii, I., Yoshinaga, K., Shiosaka, S., Hammarback, J.A., Urano, F., and Imaizumi, K. (2006). Autophagy is activated for cell survival after endoplasmic reticulum

stress. Mol Cell Biol *26*, 9220-9231.

Okamura, K., Kimata, Y., Higashio, H., Tsuru, A., and Kohno, K. (2000). Dissociation of Kar2p/BiP from an ER sensory molecule, Ire1p, triggers the unfolded protein response in yeast. Biochem Biophys Res Commun *279*, 445-450.

Orlowski, M., and Wilk, S. (2000). Catalytic activities of the 20 S proteasome, a multicatalytic proteinase complex. Arch Biochem Biophys *383*, 1-16.

Ostergaard, S., Olsson, L., and Nielsen, J. (2000). Metabolic engineering of Saccharomyces cerevisiae. Microbiol Mol Biol Rev *64*, 34-50.

Palmer, E.A., Kruse, K.B., Fewell, S.W., Buchanan, S.M., Brodsky, J.L., and McCracken, A.A. (2003). Differential requirements of novel A1PiZ degradation deficient (ADD) genes in ER-associated protein degradation. J Cell Sci *116*, 2361-2373.

Parfrey, H., Mahadeva, R., and Lomas, D.A. (2003). Alpha(1)-antitrypsin deficiency, liver disease and emphysema. Int J Biochem Cell Biol *35*, 1009-1014.

Parsell, D.A., Kowal, A.S., Singer, M.A., and Lindquist, S. (1994). Protein disaggregation mediated by heat-shock protein Hsp104. Nature *372*, 475-478.

Patil, C., and Walter, P. (2001). Intracellular signaling from the endoplasmic reticulum to the nucleus: the unfolded protein response in yeast and mammals. Curr Opin Cell Biol *13*, 349-355.

Patil, C.K., Li, H., and Walter, P. (2004). Gcn4p and novel upstream activating sequences regulate targets of the unfolded protein response. PLoS Biol *2*, E246.

Perlmutter, D.H. (2002). Liver injury in alpha1-antitrypsin deficiency: an aggregated protein induces mitochondrial injury. J Clin Invest *110*, 1579-1583.

Perlmutter, D.H., Kay, R.M., Cole, F.S., Rossing, T.H., Van Thiel, D., and Colten, H.R. (1985). The cellular defect in alpha 1-proteinase inhibitor (alpha 1-PI) deficiency is expressed in human monocytes and in Xenopus oocytes injected with human liver mRNA. Proc Natl Acad Sci U S A *82*, 6918-6921.

Peters, J.M., Franke, W.W., and Kleinschmidt, J.A. (1994). Distinct 19 S and 20 S subcomplexes of the 26 S proteasome and their distribution in the nucleus and the cytoplasm. J Biol Chem *269*, 7709-7718.

Piitulainen, E., and Eriksson, S. (1999). Decline in FEV1 related to smoking status in individuals with severe alpha1-antitrypsin deficiency (PiZZ). Eur Respir J *13*, 247-251.

Plemper, R.K., Bohmler, S., Bordallo, J., Sommer, T., and Wolf, D.H. (1997). Mutant analysis links the translocon and BiP to retrograde protein transport for ER degradation. Nature *388*, 891-895.

Pollard, M.G., Travers, K.J., and Weissman, J.S. (1998). Ero1p: a novel and ubiquitous protein with an essential role in oxidative protein folding in the endoplasmic reticulum. Mol Cell *1*, 171-182.

Qu, D., Teckman, J.H., Omura, S., and Perlmutter, D.H. (1996). Degradation of a mutant secretory protein, alpha1-antitrypsin Z, in the endoplasmic reticulum requires proteasome activity. J Biol Chem *271*, 22791-22795.

Queitsch, C., Hong, S.W., Vierling, E., and Lindquist, S. (2000). Heat shock protein 101 plays a crucial role in thermotolerance in Arabidopsis. Plant Cell *12*, 479-492.

Queitsch, C., Sangster, T.A., and Lindquist, S. (2002). Hsp90 as a capacitor of phenotypic variation. Nature *417*, 618-624.

Quinn, P.J. (1988). Effects of temperature on cell membranes. Symp Soc Exp Biol *42*, 237-258.

Ramos, P.C., Hockendorff, J., Johnson, E.S., Varshavsky, A., and Dohmen, R.J. (1998). Ump1p is required for proper maturation of the 20S proteasome and becomes its substrate upon completion of the assembly. Cell *92*, 489-499.

Ramos, P.C., Marques, A.J., London, M.K., and Dohmen, R.J. (2004). Role of C-terminal extensions of subunits beta2 and beta7 in assembly and activity of eukaryotic proteasomes. J Biol Chem *279*, 14323-14330.

Rapoport, T.A., Matlack, K.E., Plath, K., Misselwitz, B., and Staeck, O. (1999). Posttranslational protein translocation across the membrane of the endoplasmic reticulum. Biol Chem *380*, 1143-1150.

Raser, J.M., and O'Shea, E.K. (2004). Control of stochasticity in eukaryotic gene expression. Science *304*, 1811-1814.

Raught, B., Gingras, A.C., and Sonenberg, N. (2001). The target of rapamycin (TOR) proteins. Proc Natl Acad Sci U S A *98*, 7037-7044.

Reed, S.I. (2006). The ubiquitin-proteasome pathway in cell cycle control. Results Probl Cell Differ *42*, 147-181.

Richmond, R.J., and Zellner, K.M. (2005). Alpha1-antitrypsin deficiency: incidence and implications. Dimens Crit Care Nurs *24*, 255-260; quiz 261-252.

Rock, K.L., Gramm, C., Rothstein, L., Clark, K., Stein, R., Dick, L., Hwang, D., and Goldberg, A.L. (1994). Inhibitors of the proteasome block the degradation of most cell proteins and the generation of peptides presented on MHC class I molecules. Cell *78*, 761-771.

Rohde, J., Heitman, J., and Cardenas, M.E. (2001). The TOR kinases link nutrient sensing to cell growth. J Biol Chem *276*, 9583-9586.

Romisch, K. (2005). Endoplasmic reticulum-associated degradation. Annu Rev Cell Dev Biol

21, 435-456.

Rubin, D.M., Glickman, M.H., Larsen, C.N., Dhruvakumar, S., and Finley, D. (1998). Active site mutants in the six regulatory particle ATPases reveal multiple roles for ATP in the proteasome. Embo J *17*, 4909-4919.

Rudnick, D.A., and Perlmutter, D.H. (2005). Alpha-1-antitrypsin deficiency: a new paradigm for hepatocellular carcinoma in genetic liver disease. Hepatology *42*, 514-521.

Saeki, Y., Isono, E., and Toh, E.A. (2005). Preparation of ubiquitinated substrates by the PY motif-insertion method for monitoring 26S proteasome activity. Methods Enzymol *399*, 215-227.

Salvesen, G.S., and Dixit, V.M. (1997). Caspases: intracellular signaling by proteolysis. Cell *91*, 443-446.

Samoilov, M.S., Price, G., and Arkin, A.P. (2006). From fluctuations to phenotypes: the physiology of noise. Sci STKE *2006*, re17.

Sanchez, Y., and Lindquist, S.L. (1990). HSP104 required for induced thermotolerance. Science *248*, 1112-1115.

Sanchez, Y., Taulien, J., Borkovich, K.A., and Lindquist, S. (1992). Hsp104 is required for tolerance to many forms of stress. Embo J *11*, 2357-2364.

Savory, P.J., and Rivett, A.J. (1993). Leupeptin-binding site(s) in the mammalian multicatalytic proteinase complex. Biochem J *289 (Pt 1)*, 45-48.

Sayeed, A., and Ng, D.T. (2005). Search and destroy: ER quality control and ER-associated protein degradation. Crit Rev Biochem Mol Biol *40*, 75-91.

Schmidt, B.Z., and Perlmutter, D.H. (2005). Grp78, Grp94, and Grp170 interact with alpha1-antitrypsin mutants that are retained in the endoplasmic reticulum. Am J Physiol Gastrointest Liver Physiol *289*, G444-455.

Schmidtke, G., Schmidt, M., and Kloetzel, P.M. (1997). Maturation of mammalian 20 S proteasome: purification and characterization of 13 S and 16 S proteasome precursor complexes. J Mol Biol *268*, 95-106.

Schroder, M., Chang, J.S., and Kaufman, R.J. (2000). The unfolded protein response represses nitrogen-starvation induced developmental differentiation in yeast. Genes Dev *14*, 2962-2975.

Schroder, M., and Kaufman, R.J. (2005). The mammalian unfolded protein response. Annu Rev Biochem *74*, 739-789.

Schubert, U., Anton, L.C., Gibbs, J., Norbury, C.C., Yewdell, J.W., and Bennink, J.R. (2000). Rapid degradation of a large fraction of newly synthesized proteins by proteasomes.

Nature *404*, 770-774.

Seemuller, E., Lupas, A., Stock, D., Lowe, J., Huber, R., and Baumeister, W. (1995). Proteasome from Thermoplasma acidophilum: a threonine protease. Science *268*, 579-582.

Shamu, C.E., and Walter, P. (1996). Oligomerization and phosphorylation of the Ire1p kinase during intracellular signaling from the endoplasmic reticulum to the nucleus. Embo J *15*, 3028-3039.

Sharon, M., Taverner, T., Ambroggio, X.I., Deshaies, R.J., and Robinson, C.V. (2006). Structural organization of the 19S proteasome lid: insights from MS of intact complexes. PLoS Biol *4*, e267.

Sidhar, S.K., Lomas, D.A., Carrell, R.W., and Foreman, R.C. (1995). Mutations which impede loop/sheet polymerization enhance the secretion of human alpha 1-antitrypsin deficiency variants. J Biol Chem *270*, 8393-8396.

Sidrauski, C., Cox, J.S., and Walter, P. (1996). tRNA ligase is required for regulated mRNA splicing in the unfolded protein response. Cell *87*, 405-413.

Sidrauski, C., and Walter, P. (1997). The transmembrane kinase Ire1p is a site-specific endonuclease that initiates mRNA splicing in the unfolded protein response. Cell *90*, 1031-1039.

Sikorski, R.S., and Hieter, P. (1989). A system of shuttle vectors and yeast host strains designed for efficient manipulation of DNA in Saccharomyces cerevisiae. Genetics *122*, 19-27.

Soboleva, T.A., and Baker, R.T. (2004). Deubiquitinating enzymes: their functions and substrate specificity. Curr Protein Pept Sci *5*, 191-200.

Stirling, C.J., Rothblatt, J., Hosobuchi, M., Deshaies, R., and Schekman, R. (1992). Protein translocation mutants defective in the insertion of integral membrane proteins into the endoplasmic reticulum. Mol Biol Cell *3*, 129-142.

Suzuki, K., Kamada, Y., and Ohsumi, Y. (2002). Studies of cargo delivery to the vacuole mediated by autophagosomes in Saccharomyces cerevisiae. Dev Cell *3*, 815-824.

Suzuki, K., Kirisako, T., Kamada, Y., Mizushima, N., Noda, T., and Ohsumi, Y. (2001). The pre-autophagosomal structure organized by concerted functions of APG genes is essential for autophagosome formation. Embo J *20*, 5971-5981.

Sveger, T. (1988). The natural history of liver disease in alpha 1-antitrypsin deficient children. Acta Paediatr Scand *77*, 847-851.

Swanson, R., Locher, M., and Hochstrasser, M. (2001). A conserved ubiquitin ligase of the nuclear envelope/endoplasmic reticulum that functions in both ER-associated and Matalpha2 repressor degradation. Genes Dev *15*, 2660-2674.

Teckman, J.H., Burrows, J., Hidvegi, T., Schmidt, B., Hale, P.D., and Perlmutter, D.H. (2001). The proteasome participates in degradation of mutant alpha 1-antitrypsin Z in the endoplasmic reticulum of hepatoma-derived hepatocytes. J Biol Chem *276*, 44865-44872.

Teckman, J.H., Gilmore, R., and Perlmutter, D.H. (2000). Role of ubiquitin in proteasomal degradation of mutant alpha(1)-antitrypsin Z in the endoplasmic reticulum. Am J Physiol Gastrointest Liver Physiol *278*, G39-48.

Teckman, J.H., and Perlmutter, D.H. (2000). Retention of mutant alpha(1)-antitrypsin Z in endoplasmic reticulum is associated with an autophagic response. Am J Physiol Gastrointest Liver Physiol *279*, G961-974.

Tone, Y., Tanahashi, N., Tanaka, K., Fujimuro, M., Yokosawa, H., and Toh-e, A. (2000). Nob1p, a new essential protein, associates with the 26S proteasome of growing saccharomyces cerevisiae cells. Gene *243*, 37-45.

Tone, Y., and Toh, E.A. (2002). Nob1p is required for biogenesis of the 26S proteasome and degraded upon its maturation in Saccharomyces cerevisiae. Genes Dev *16*, 3142-3157.

Travers, K.J., Patil, C.K., Wodicka, L., Lockhart, D.J., Weissman, J.S., and Walter, P. (2000). Functional and genomic analyses reveal an essential coordination between the unfolded protein response and ER-associated degradation. Cell *101*, 249-258.

Tsai, B., Ye, Y., and Rapoport, T.A. (2002). Retro-translocation of proteins from the endoplasmic reticulum into the cytosol. Nat Rev Mol Cell Biol *3*, 246-255.

Tuttle, D.L., and Dunn, W.A., Jr. (1995). Divergent modes of autophagy in the methylotrophic yeast Pichia pastoris. J Cell Sci *108 (Pt 1)*, 25-35.

Van Molle, W., Libert, C., Fiers, W., and Brouckaert, P. (1997). Alpha 1-acid glycoprotein and alpha 1-antitrypsin inhibit TNF-induced but not anti-Fas-induced apoptosis of hepatocytes in mice. J Immunol *159*, 3555-3564.

Vashist, S., Kim, W., Belden, W.J., Spear, E.D., Barlowe, C., and Ng, D.T. (2001). Distinct retrieval and retention mechanisms are required for the quality control of endoplasmic reticulum protein folding. J Cell Biol *155*, 355-368.

Vashist, S., and Ng, D.T. (2004). Misfolded proteins are sorted by a sequential checkpoint mechanism of ER quality control. J Cell Biol *165*, 41-52.

Verbanac, K.M., and Heath, E.C. (1986). Biosynthesis, processing, and secretion of M and Z variant human alpha 1-antitrypsin. J Biol Chem *261*, 9979-9989.

Verma, R., Aravind, L., Oania, R., McDonald, W.H., Yates, J.R., 3rd, Koonin, E.V., and Deshaies, R.J. (2002). Role of Rpn11 metalloprotease in deubiquitination and degradation by the 26S proteasome. Science *298*, 611-615.

Verma, R., Chen, S., Feldman, R., Schieltz, D., Yates, J., Dohmen, J., and Deshaies, R.J. (2000).

Proteasomal proteomics: identification of nucleotide-sensitive proteasome-interacting proteins by mass spectrometric analysis of affinity-purified proteasomes. Mol Biol Cell *11*, 3425-3439.

Verma, R., and Deshaies, R.J. (2005). Assaying degradation and deubiquitination of a ubiquitinated substrate by purified 26S proteasomes. Methods Enzymol *398*, 391-399.

Vierling, E. (1991). The roles of heat shock proteins in plants. Annu Rev Plant Physiol Plant Mol Biol *42*, 570-620.

Voges, D., Zwickl, P., and Baumeister, W. (1999). The 26S proteasome: a molecular machine designed for controlled proteolysis. Annu Rev Biochem *68*, 1015-1068.

Wahlman, J., Demartino, G.N., Skach, W.R., Bulleid, N.J., Brodsky, J.L., and Johnson, A.E. (2007). Real-Time Fluorescence Detection of ERAD Substrate Retrotranslocation in a Mammalian In Vitro System. Cell *129*, 943-955.

Walz, J., Erdmann, A., Kania, M., Typke, D., Koster, A.J., and Baumeister, W. (1998). 26S proteasome structure revealed by three-dimensional electron microscopy. J Struct Biol *121*, 19-29.

Wang, X.Z., and Ron, D. (1996). Stress-induced phosphorylation and activation of the transcription factor CHOP (GADD153) by p38 MAP Kinase. Science *272*, 1347-1349.

Wang, Z.X., Hu, G.F., Wang, H.Y., and Wu, M.C. (2001). Expression of liver cancer associated gene HCCA3. World J Gastroenterol *7*, 821-825.

Welihinda, A.A., and Kaufman, R.J. (1996). The unfolded protein response pathway in Saccharomyces cerevisiae. Oligomerization and trans-phosphorylation of Ire1p (Ern1p) are required for kinase activation. J Biol Chem *271*, 18181-18187.

Werner, E.D., Brodsky, J.L., and McCracken, A.A. (1996). Proteasome-dependent endoplasmic reticulum-associated protein degradation: an unconventional route to a familiar fate. Proc Natl Acad Sci U S A *93*, 13797-13801.

Wiertz, E.J., Tortorella, D., Bogyo, M., Yu, J., Mothes, W., Jones, T.R., Rapoport, T.A., and Ploegh, H.L. (1996). Sec61-mediated transfer of a membrane protein from the endoplasmic reticulum to the proteasome for destruction. Nature *384*, 432-438.

Williams, N. (1996). Yeast genome sequence ferments new research. Science *272*, 481.

Witt, E., Zantopf, D., Schmidt, M., Kraft, R., Kloetzel, P.M., and Kruger, E. (2000). Characterisation of the newly identified human Ump1 homologue POMP and analysis of LMP7(beta 5i) incorporation into 20 S proteasomes. J Mol Biol *301*, 1-9.

Wu, Y., Whitman, I., Molmenti, E., Moore, K., Hippenmeyer, P., and Perlmutter, D.H. (1994). A lag in intracellular degradation of mutant alpha 1-antitrypsin correlates with the liver disease phenotype in homozygous PiZZ alpha 1-antitrypsin deficiency. Proc Natl Acad

Sci U S A *91*, 9014-9018.

Xu, P., and Peng, J. (2006). Dissecting the ubiquitin pathway by mass spectrometry. Biochim Biophys Acta *1764*, 1940-1947.

Yang, Y., Fruh, K., Ahn, K., and Peterson, P.A. (1995). In vivo assembly of the proteasomal complexes, implications for antigen processing. J Biol Chem *270*, 27687-27694.

Yao, T., and Cohen, R.E. (2002). A cryptic protease couples deubiquitination and degradation by the proteasome. Nature *419*, 403-407.

Yao, Y., Toth, C.R., Huang, L., Wong, M.L., Dias, P., Burlingame, A.L., Coffino, P., and Wang, C.C. (1999). alpha5 subunit in Trypanosoma brucei proteasome can self-assemble to form a cylinder of four stacked heptamer rings. Biochem J *344 Pt 2*, 349-358.

Ye, Y., Shibata, Y., Yun, C., Ron, D., and Rapoport, T.A. (2004). A membrane protein complex mediates retro-translocation from the ER lumen into the cytosol. Nature *429*, 841-847.

Yoneda, T., Imaizumi, K., Oono, K., Yui, D., Gomi, F., Katayama, T., and Tohyama, M. (2001). Activation of caspase-12, an endoplastic reticulum (ER) resident caspase, through tumor necrosis factor receptor-associated factor 2-dependent mechanism in response to the ER stress. J Biol Chem *276*, 13935-13940.

Yoshihisa, T., and Anraku, Y. (1990). A novel pathway of import of alpha-mannosidase, a marker enzyme of vacuolar membrane, in Saccharomyces cerevisiae. J Biol Chem *265*, 22418-22425.

Yoshihisa, T., Yunoki-Esaki, K., Ohshima, C., Tanaka, N., and Endo, T. (2003). Possibility of cytoplasmic pre-tRNA splicing: the yeast tRNA splicing endonuclease mainly localizes on the mitochondria. Mol Biol Cell *14*, 3266-3279.

Youker, R.T., Walsh, P., Beilharz, T., Lithgow, T., and Brodsky, J.L. (2004). Distinct roles for the Hsp40 and Hsp90 molecular chaperones during cystic fibrosis transmembrane conductance regulator degradation in yeast. Mol Biol Cell *15*, 4787-4797.

Yu, M.H., Lee, K.N., and Kim, J. (1995). The Z type variation of human alpha 1-antitrypsin causes a protein folding defect. Nat Struct Biol *2*, 363-367.

Yuan, W., Tuttle, D.L., Shi, Y.J., Ralph, G.S., and Dunn, W.A., Jr. (1997). Glucose-induced microautophagy in Pichia pastoris requires the alpha-subunit of phosphofructokinase. J Cell Sci *110 (Pt 16)*, 1935-1945.

Zhang, Y., Nijbroek, G., Sullivan, M.L., McCracken, A.A., Watkins, S.C., Michaelis, S., and Brodsky, J.L. (2001). Hsp70 molecular chaperone facilitates endoplasmic reticulum-associated protein degradation of cystic fibrosis transmembrane conductance regulator in yeast. Mol Biol Cell *12*, 1303-1314.

Zhou, J., Liu, C.Y., Back, S.H., Clark, R.L., Peisach, D., Xu, Z., and Kaufman, R.J. (2006). The

crystal structure of human IRE1 luminal domain reveals a conserved dimerization interface required for activation of the unfolded protein response. Proc Natl Acad Sci U S A *103*, 14343-14348.